Moisture design with regard to deterioration of materials and structures - with special reference to frost destruction

Fagerlund, Göran

2006

Citation for published version (APA):
Fagerlund, G. (2006). *Moisture design with regard to deterioration of materials and structures - with special reference to frost destruction*. (Report TVBM; Vol. 3130). Division of Building Materials, LTH, Lund University.

Total number of authors:
1

LUND INSTITUTE OF TECHNOLOGY
LUND UNIVERSITY

Division of Building Materials

MOISTURE DESIGN WITH REGARD TO DURABILITY

With special reference to frost destruction

Göran Fagerlund

Report TVBM-3130 Lund 2006

LUND INSTITUTE OF TECHNOLOGY
LUND UNIVERSITY

Division of Building Materials

MOISTURE DESIGN WITH REGARD TO DURABILITY

With special reference to frost destruction

Göran Fagerlund

Report TVBM-3130 Lund 2006

ISRN LUTVDG/TVBM--06/3130--SE(1-128)

ISSN 0348-7911 TVBM

Lund Institute of Technology
Division of Building Materials
Box 118
SE-221 00 Lund, Sweden

Telephone: 46-46-2227415
Telefax: 46-46-2224427
www.byggnadsmaterial.lth.se

PREFACE

This work was sponsored by *The Swedish Research Council for Environment, Agricultural Sciences and Spatial Planning* (FORMAS). The work was performed at the Division of Building Materials, Lund Institute of Technology at Lund University.

The work is composed of three parts:

- An overview of the concept *moisture design with regard to service life.*
  This report, Chapters 1-5.

- A practical application of *service life analysis applied to frost damage*, based on materials testing.
  This report, Chapter 6.

- A theoretical analysis of methods for service life design of concrete and concrete structures exposed to internal frost damage.
  Reported in, *A Service Life Model for Frost Damage in Concrete. Div. of Building Materials. Lund Institute of Technology. Report TVBM-3119, Lund 2004. Reference (Fagerlund 2004)*

The financial support given by FORMAS is gratefully acknowledged.

Lund, February 2006

Göran Fagerlund

CONTENTS

Page

Chapter 4 presents principles and methods for calculation of the *risk of moisture induced damage*. For well-defined critical moisture levels, the damage risk can be calculated according to the same stochastic principles as the risk of structural collapse; the critical moisture level corresponds to the fracture load, and the actually occurring moisture level corresponds to the actual structural load. In design, the risk of failure should be lower than a prescribed level, which can, however, be much lower for moisture damage than for structural collapse.

Estimation of the damage risk is more complex in cases where the critical moisture level is less well-defined, and where it is also a function of duration of the load. Ways of handling these cases are discussed briefly.

Chapter 5 discusses the concept *service life*. This can be estimated when the time functions of the critical and actually occurring moisture levels are known, or can be predicted for all crucial parts in the structure.

The most complex problem is to estimate the future moisture field in the structure. It is shown that the best solution is to define a *"representative environment"* that represents the real complex environment in as good manner as possible. In this way a *"representative service life"* can be obtained. Then the real environment is exchanged for a cyclic variation in outer moisture conditions. From the outer moisture variation the inner moisture variation in the material is calculated. Methods in traditional moisture mechanics are used. The method can be used for structures that have *moisture levels within ranges 1 and 2*.

For some structures and destruction types *moisture range 3* is decisive for service life. Then the concept *"equivalent capillary absorption time"* is used. An experimental long-term capillary absorption curve is extrapolated until the critical moisture level is reached. In this way a *"potential service life"* can be determined. The method is used for service life with regard to *frost damage*. The method is exemplified.

The principles of *service life design* are presented. A selected material is analyzed with regard to its critical and estimated future moisture level in practical use, during its intended service life. If it is likely that the critical moisture level will be transgressed a new material or material quality is selected. The analysis is repeated until a safe material is found.

Chapter 6 presents a number of *experimental applications* of the concept *potential service life* with regard to *internal frost damage*. 10 different materials were investigated experimentally with regard to the critical moisture level and the long-term water absorption. Materials from 5 different material families were investigated; 2 clay bricks, 1 sand-lime brick, 1 cellular concrete, 5 types of concrete/cement mortar, 1 natural stone.

A well-defined *critical moisture level* was easily detected for all materials by a freeze/thaw experiment on moisture sealed specimens. For all materials the critical moisture level was located to the over-capillary moisture range 3; i.e. frost damage can only occur if the material has been able to take up water for quite long time; days, months or years.

A *long-term water uptake experiment* was used for defining an expression for the long-term water absorption. The standard deviation in water uptake was normally found to be fairly small.

For each material the *frost damage risk* as function of water absorption time was analysed stochastically. The potential service life was found to be very different for different materials. If only 20% risk of damage is accepted, the service life was only a few hours for the sand-lime brick, less than a week for cellular concrete, sandstone and under-burnt clay brick, but almost 2 years for concrete with low water-cement ratio and high air content. The results are in fair accordance with what is known from practice.

A short discussion of the maximum and minimum possible critical moisture levels is performed. A quantitative application is made to concrete.

1 MOISTURE RANGES

Moisture in materials can be divided into three ranges, see Figure 1.1, which shows moisture equilibrium curves, i.e. the relation between relative humidity (RH), or the capillary pressure ("suction"), and the equilibrium moisture content.

Note: The shape of the curves will depend on whether the actual water content has been reached by *absorption* from a drier condition or by *drying* from a more moist condition. This hysteresis between absorption and drying, which is sometimes considerable, is not shown in the figure.

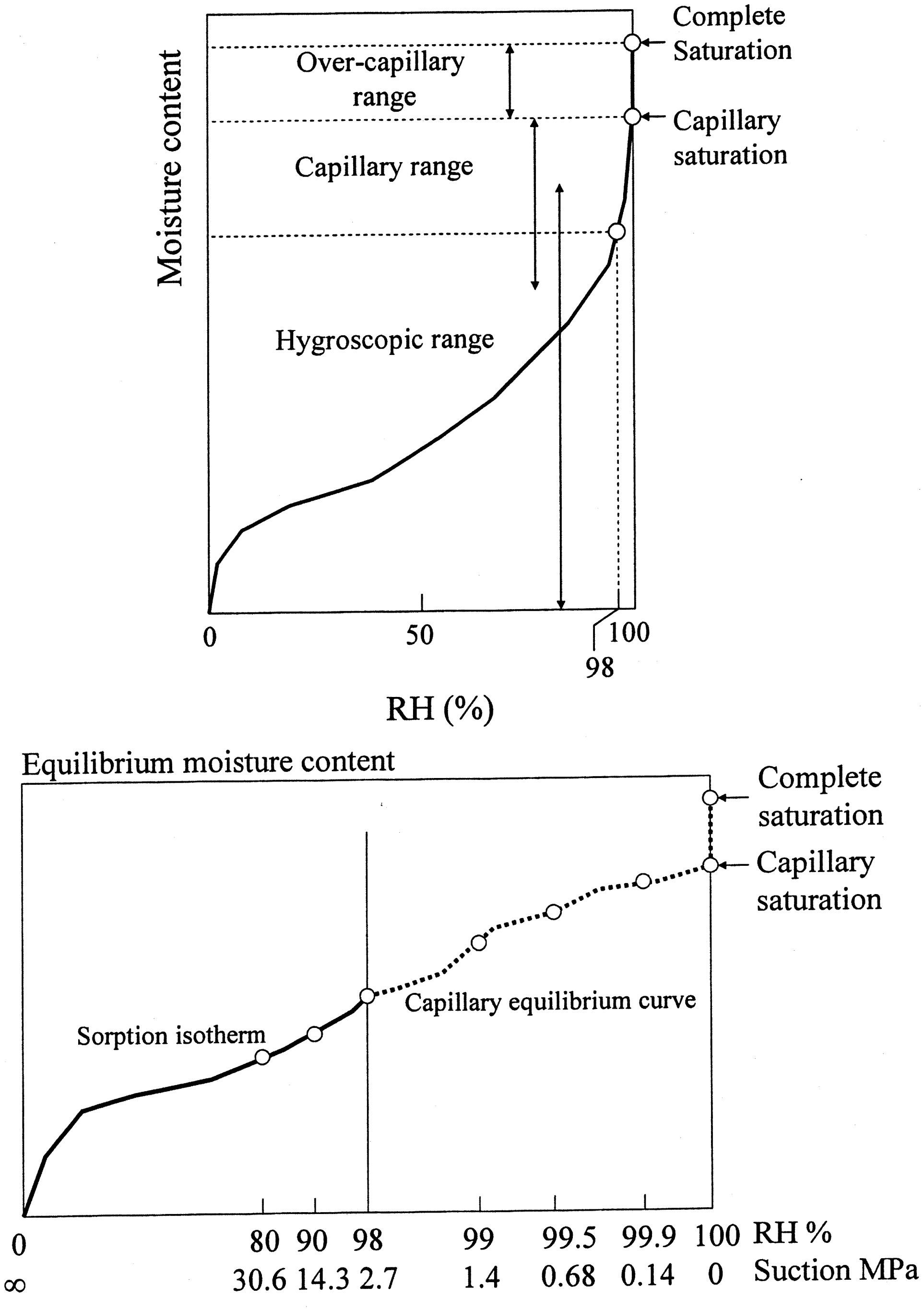

Figure 1.1: Different moisture ranges as regards the basic water absorption mechanism. Upper figure: The sorption isotherm. Lower figure: The capillary equilibrium curve.

There is a relation between the capillary pressure given by the Laplace law and RH given by the Kelvin law for capillary condensation:

$$\Delta p = -(R \cdot T/v_w) \cdot \ln(RH) \qquad (1.1)$$

Where, Δp is the capillary under-pressure (Pa) (the "suction"), R is the gas constant (8.314 mole/degree), T is the absolute temperature (degree), and v_w is the molar volume of water ($18 \cdot 10^{-6}$ m^3/mole).

Thus, each capillary pressure corresponds to a certain RH. In the upper moisture range (above about 98% RH) it is only possible to use the capillary equilibrium curve. In the lower moisture range it is most convenient to use the sorption isotherm, since RH is the only practical way to experimentally obtain the moisture state aimed at.

Moisture range 1: The "hygroscopic range" (0%RH to ≈98% RH)

Upper Figure 1.1.

Water within this range can be taken up by pure adsorption on the pore walls and by capillary condensation of water vapour. This process continues to 100% RH, but at high RH it is often overshadowed by capillary absorption.

Moisture range 2: The "capillary range" (up to 100% RH, capillary pressure 0 Pa)

Lower Figure 1.1.

Water uptake normally takes place by absorption of "free" water in contact with the surface of the material. *Capillary saturation* is reached when all through pores are water-filled. Capillary saturation is seen in a capillary absorption experiment as the "breaking-point" when absorption is plotted versus the square-root of absorption time; Figure 1.2. The capillary range is represented by the sloping line before capillary saturation is reached.

There is no distinct border between the hygroscopic and the capillary ranges, since capillary suction in a material with an initial RH<<100% will also fill such pores that are only filled by hygroscopic action when free water is not available.

Moisture range 3: The "over-capillary range" (RH=100% ,ΔP=0 Pa)

Water can continue to be absorbed in the material also after capillary saturation has been reached; see the slowly increasing water content in "Range 3" in Figure 1.2. This absorption is due to a gradual dissolution of air that has been entrapped in coarser "isolated" pores. The mechanism is described in (Fagerlund 2004).

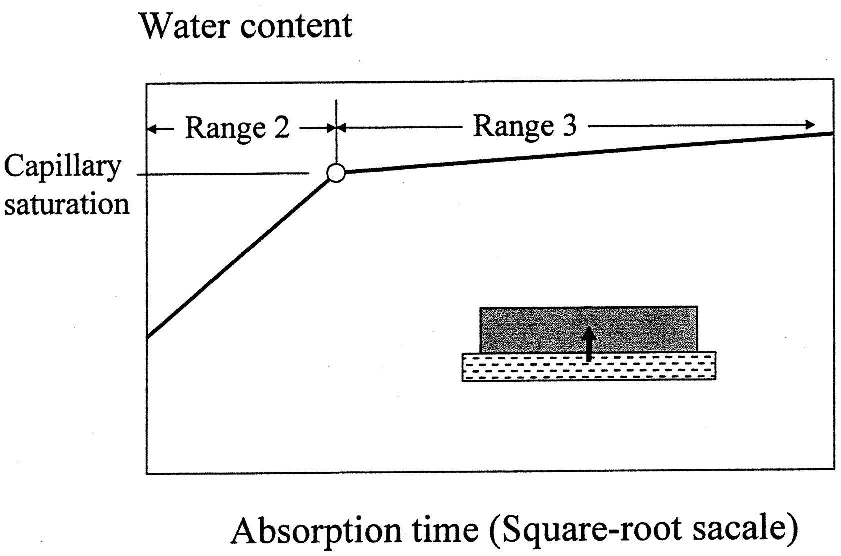

Figure 1.2: A capillary absorption experiment. Definition of capillary saturation. Illustration of moisture ranges 2 and 3.

2 THE ROLE OF WATER IN DESTRUCTION PROCESSES A SHORT OVERVIEW

2.1 Types of attack influenced by water

Many of the most frequent destructive processes in building materials and components are intimately coupled to moisture. Water takes part in the destruction processes in many ways, as exemplified below.

1. *Internal frost attack (Moisture range 3):*
   Water is the expanding medium at freezing causing internal destruction.

2. *External salt-frost attack (Moisture range 3)*
   Water is attracted to ice bodies in pores causing surface scaling when growing.

3. *Reinforcement corrosion in concrete and brick-work (Moisture range 1):*
   Water is the electrolyte needed for the corrosion process.
   Water is the transport medium for chloride transport into the material.
   Water is a blocking medium for gas transport influencing the corrosion process; like transport of carbon dioxide causing carbonation in concrete, and transport of oxygen needed for the corrosion process.

4. *Chemical attack on mineral-based materials (Moisture range 2):*
   Water is the solvent required for chemical reaction to take place between the aggressive agent and the mineral.
   Water is a solvent, dissolving the mineral.

5. *Chemical attack on polymers (Moisture range 2):*
   Water is causing hydrolysis of the polymer.

6. *Biological attack on wood-based materials (Moisture range 1):*
   Water is required for the metabolism of mould and fungi.

7. *Emission of volatile compounds from organic building materials (Moisture range 1):*
   Water (particularly at high pH) is a dissolving and/or catalytic agent for emission.
   Water is a transport medium for emitted substances.

8. *Emission of radon from materials (Moisture ranges 1 and 2):*
   Water is the transport medium for radon penetrating building materials.

9. *Loss of bond between a substrate (like concrete) and a surface material (like polymer-based flooring materials) (Moisture range 1):*
   Water is weakening the adhesive between the substrate and the surface material.
   Water is absorbed in the surface material causing expansion and bubbling of this.

10. *Destruction of concrete during fire (Moisture ranges 2 and 3):*
    Pore water vapour pressure caused by high temperature causes spalling of concrete surfaces.

As shown above, there are two principally different types of effect of water in destruction:

Type 1: Water is the direct aggressive agent
Type 2: Water makes destruction possible, but does not take active part in destruction

Examples of these two types of destructive action of water will be given in the next paragraphs.

An overview of effects of moisture on different material properties, including also other properties than those related to durability, is made in (Nilsson 2004).

2.2 Attack where water is the direct aggressive agent

2.2.1 Internal frost destruction

The clearest example of water being the direct aggressive agent is *internal frost destruction* in mineral-based materials like clay brick, natural stone or concrete. Water in pores freezes, and the 9% increase in volume, taking place at ice formation, causes internal stresses that are big enough to fracture the material, provided the water content is above a critical level. Only one single freezing is enough to severely harm the material. One example, showing the big effect of water, is given in Figure 2.1. The material is a clay brick that has been freeze-thaw tested in moisture insulated conditions. Before the test, a number of specimens were pre-conditioned to different degrees of saturation, S (S = total pore water volume/total pore volume). Below a critical degree of saturation of 0.755 the material is unharmed (defined by loss in the E-modulus smaller than 10%). Above this, it is normally completely destroyed. Similar results have been found for many types of mineral-based materials; see (Fagerlund 1972).

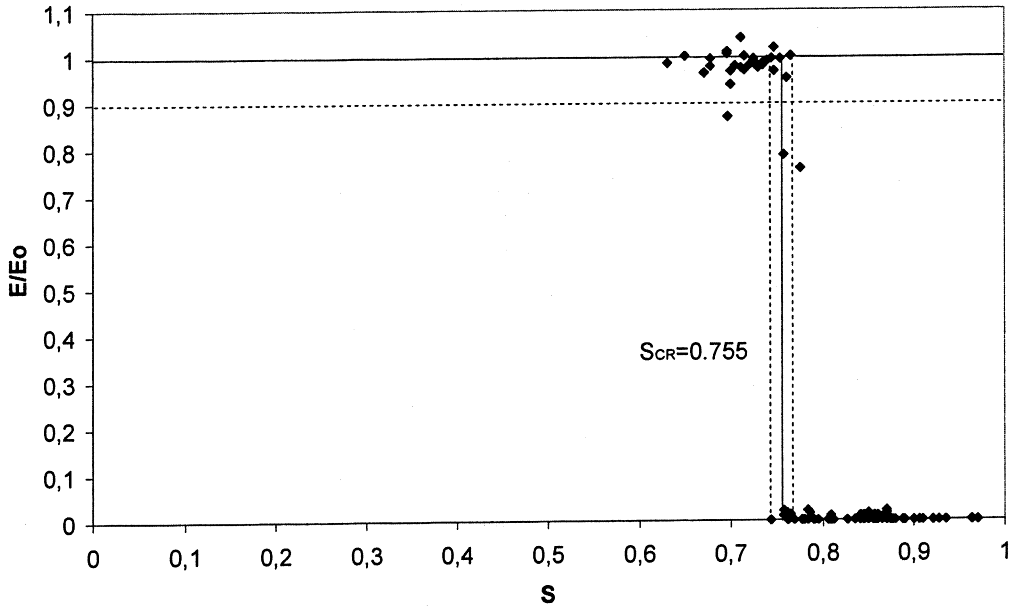

Figure 2.1: Example of a determination of the critical water content for a clay brick. E/E_o is the ratio of dynamic E-modulus before and after freeze/thaw. S is the degree of saturation.

The destruction mechanism is not altogether clear. Mechanisms have been described in a number of reports, e.g. (Powers 1945), (Powers 1949), (Powers & Helmuth 1953), Powers (1956), (Everett 1961), (Setzer 1998). A comprehensive experimental study of internal frost damage in concrete, and of the effect of different external factors on frost damage, has been presented in (Fridh 2005).

2.2.2 Salt-frost scaling

A second example of water being the primary destruction cause, is *salt-frost scaling* of surfaces that freeze in a saline environment, like sea water or de-icing salt. The destruction mechanism is not quite clear, but there are clear indications that ice-bodies formed in pores close to the surface attract unfrozen water from the moist surface. The ice-bodies thereby grow, and exert a pressure to the pore walls. The pressure is big enough to cause fracturing of the surface and scaling of this. The mechanism is experimentally examined and discussed in (Lindmark 1998). The mechanism has also been discussed in other reports like (Powers 1965), (Tange Jepsen 2002).

The mechanism is most important for concrete, but has also shown to be relevant to natural stone like sandstone and limestone, (Wessman 1997). An example of the salt scaling of a sandstone specimen is shown in Figure 2.2 (upper part). Already 2 weight-percent NaCl in the water surrounding the specimen was high enough to cause severe scaling. Pure water and very high salt concentrations gave low scaling. Another example valid for a dense high performance concrete is shown in Figure 2.2 (lower part), (Lindmark 1995). Pure water gave almost no scaling, why all other concentrations, both low and big gave high scaling that was almost independent of the salt concentration, which was varied from 1% to 5%.

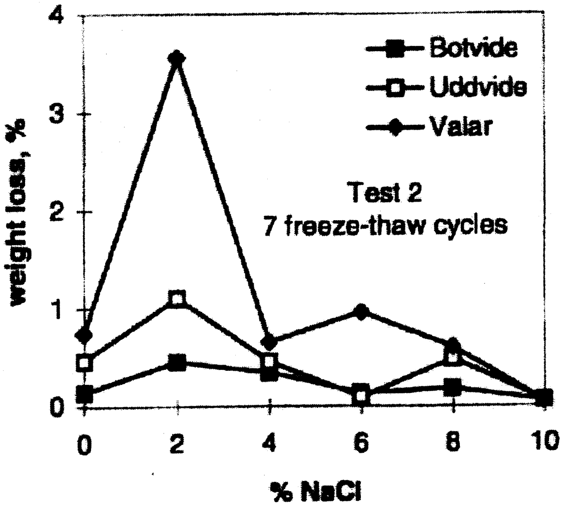

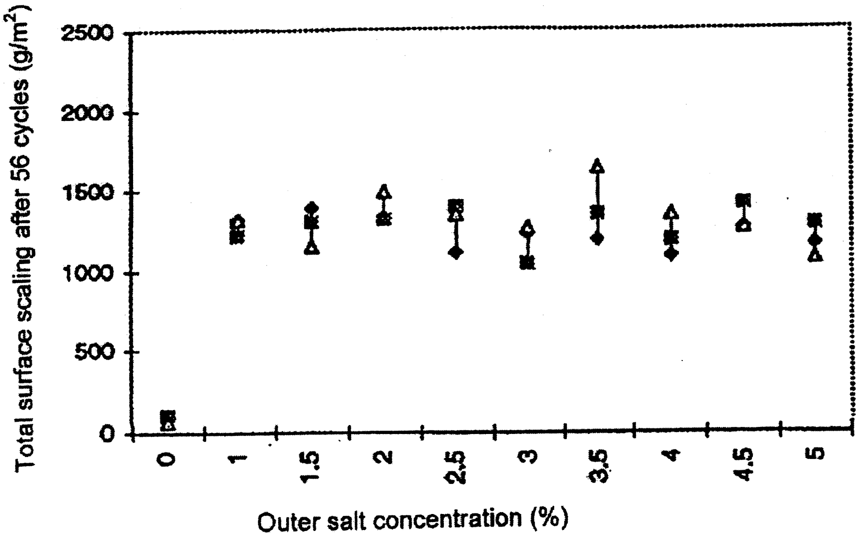

Figure 2.2: Examples of salt-frost scaling.
Upper figure: Sandstone. Lower figure: High performance concrete.

2.2.3 Leaching of concrete

A third example is *leaching of lime from concrete*. Water percolating the concrete structure dissolves lime-containing minerals in the concrete, mainly calcium hydroxide (portlandite). This results in a gradual reduction of strength and stability of the structure. The process and its effects are described in (Fagerlund 2000A). An example of surface leaching of concrete is shown in Figure 2.3a, (Locher&Sprung 1975). Examples of the effect of leaching on the residual strength are shown in Figure 2.3b presenting a compilation of different results in (Halvorsen 1966).

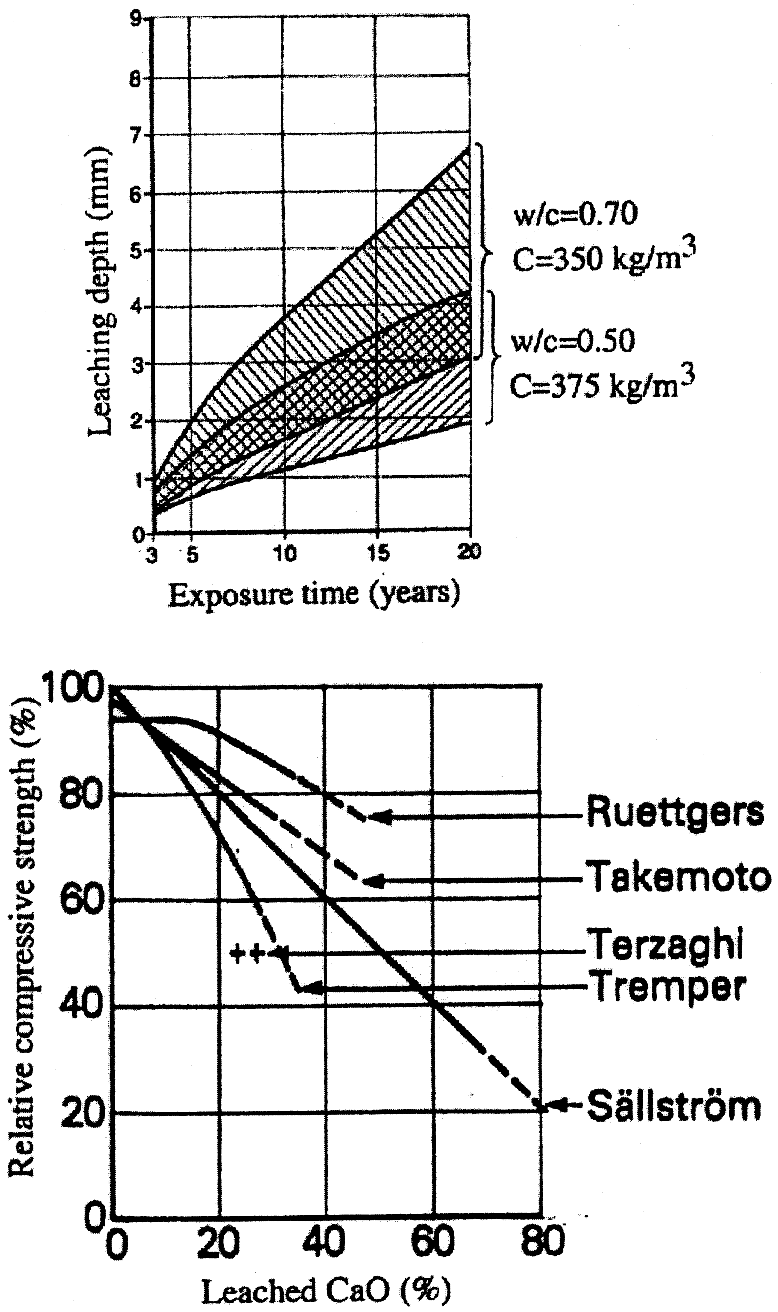

Figure 2.3: Effect of leaching of concrete.
Upper figure: Leaching of concrete surface in water with aggressive CO_2.
Lower figure: Strength loss as function of loss in CaO.

2.2.4 Spalling due to fire

A fourth example is *spalling of dense concrete during fire*. Water in surface pores will evaporate during fire. Very high vapour pressure could be built up in concrete that has low permeability, like concrete with low water-cement ratio also containing puzzolanic materials like silica fume. At 200°C the saturation vapour pressure is 1.6 MPa, and at 250°C it is 4 MPa. These values are of the same order as the tensile strength of concrete, or higher. Thus, explosive spalling could occur if the vapour is stopped from escaping inwards or outwards.

The risk increases with increasing mechanical stresses in the component. Examples of the measured pore pressure 25 mm from the fire exposed surface as function of temperature is shown in Figure 2.4, (Long Phan 1996). The maximum pressure occurs somewhat above 200°C. Spalling in one concrete occurs at a temperature of 225°C and at a pressure of 1.7 MPa. This pressure is 65% of the saturation vapour pressure at the actual temperature, indicating that some pressure relief occurs also in this dense concrete. However, it is not high enough to hinder spalling.

The risk of spalling increases with decreased water content, since empty channels through which vapour can escape is created at lower water contents.

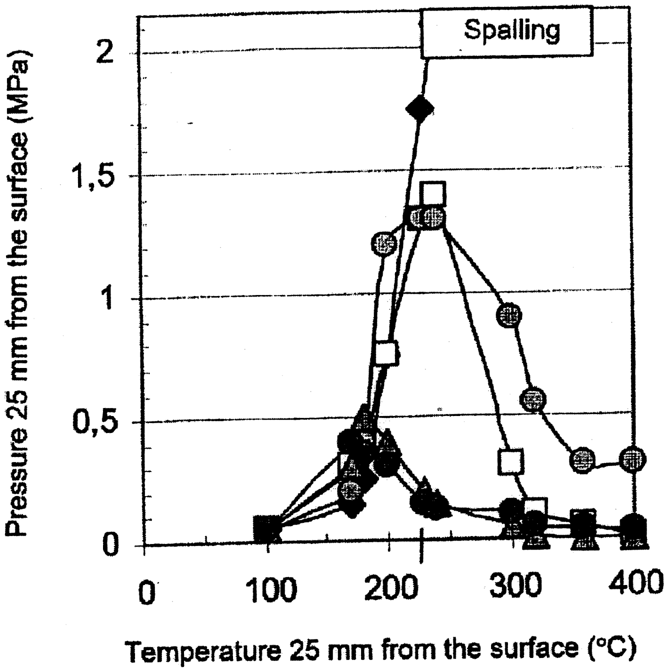

Figure 2.4: Internal vapour pressure versus temperature during fire test of 5 types of concrete with and without polypropylene fibres. Spalling only occurs in the high performance concrete without fibres.

2.2 5 Deterioration of bond

A fifth example is *deterioration of bond* between organic surface materials and mineral surfaces like concrete. Water taken up by the adhesive weakens this, which might cause total loss of bond, particularly when the surface material is also exposed to mechanical load. One example of the relation between the relative humidity in the concrete and the bond strength to a PVC-carpet is shown in Figure 2.5.

A secondary effect is that the surface material itself might take up moisture which makes it swell. Swelling of the order 10‰ has been measured for some PVC-carpets exposed to water. Then, if the bond is also lost, the swelling might cause considerable bubble formation of the carpet.

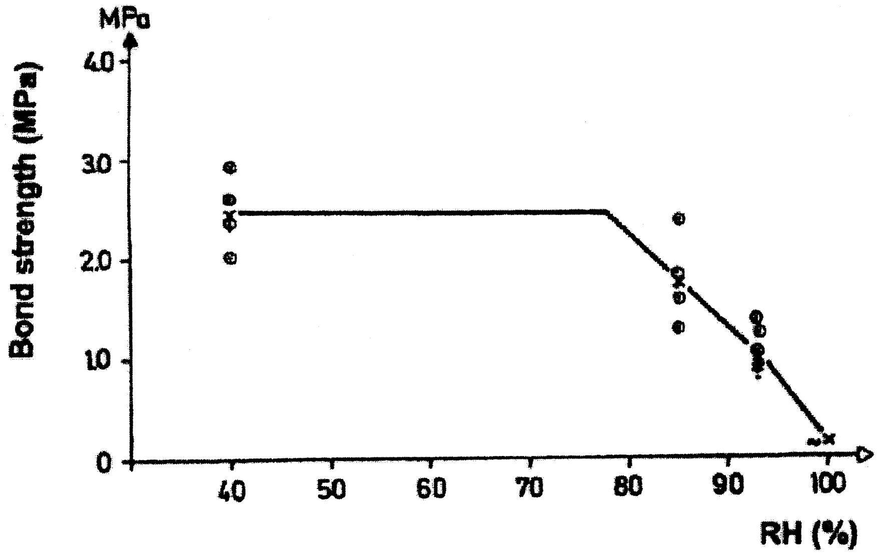

Figure 2.5: Example of the effect of RH at the interface on the bond between concrete and a PVC-based carpet (Hedenblad & Nilsson 1997).

2.2.6 Emission

A sixth example is *emission of volatile organic compounds* from organic surface materials bonded to moist concrete. Alkaline moisture in the interface between the concrete and the surface layers stimulates reactions in the adhesive and/or the surface material, that produces volatile compounds that penetrate the surface and enters the surrounding air. The process has been described in many reports. Two of the most comprehensive are (Gustafsson 1990), (Gustafsson 1992). An example of the effect of the relative humidity inside the concrete on the total amount of volatile organic compounds (TVOC) is shown in Figure 2.6, (Wengholt-Jonsson 1995).

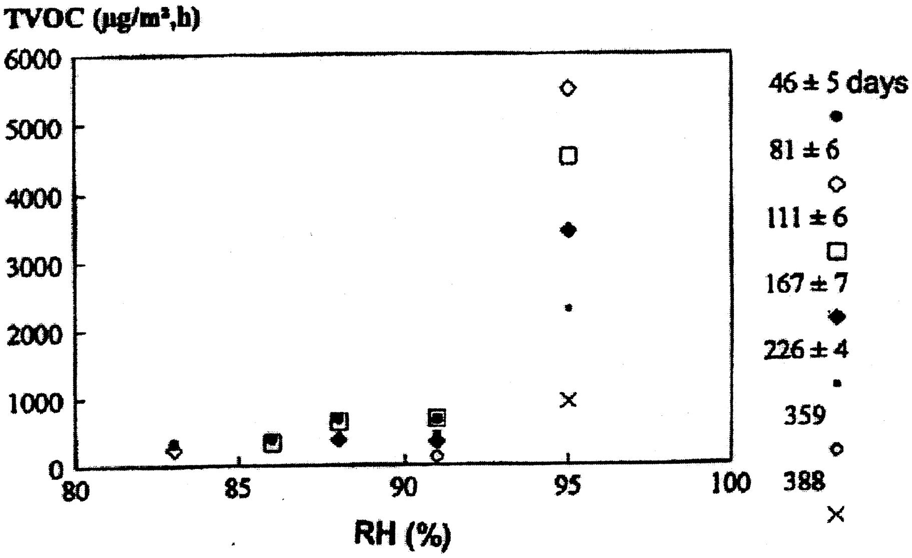

Figure 2.6: Total emission of volatile organic compounds (TVOC) from a PVC-carpet glued to concrete having different RH at gluing. The RH-measurement is made at different time after gluing.

2.3 Attack where water makes destruction possible, but where it does not take active part in destruction

Many destruction processes require the presence of water to occur, although water is not the main reason for destruction. In some cases water acts as the medium through which products from decay is transported. In other cases it is a sort of "catalyst" required for the destructive process to take place. Some examples will be given.

2.3.1 Reinforcement corrosion

Reinforcement corrosion in concrete is a destruction type in which water plays a very important role. Corrosion can only occur if the reinforcement steel has been de-passivated by ingress of carbon dioxide causing carbonation of the concrete, or ingress of chloride ions. These transport processes are highly determined by water in the pore system.

(i) Carbonation, which is the reaction between calcareous components in concrete and carbon dioxide from air, needs some pore water to occur. On the other hand, if the water content is too high, the influx of CO_2 into the concrete is obstructed. Therefore, the maximum carbonation rate occurs at about 50% to 60% relative humidity (RH) in the concrete. At lower RH the water content is so low that the carbonation rate is reduced. At higher RH the pores are so full with water that diffusion is very slow; the diffusivity of gas in water is only about 10^{-4} of that in air. Measurements of the oxygen diffusivity in cement paste as function of its relative humidity are shown in Figure 2.7, (Tuutti 1982).

Examples of the effect of RH in different types of concrete on carbonation is shown in Figure 2.8, (Houst 1993)).

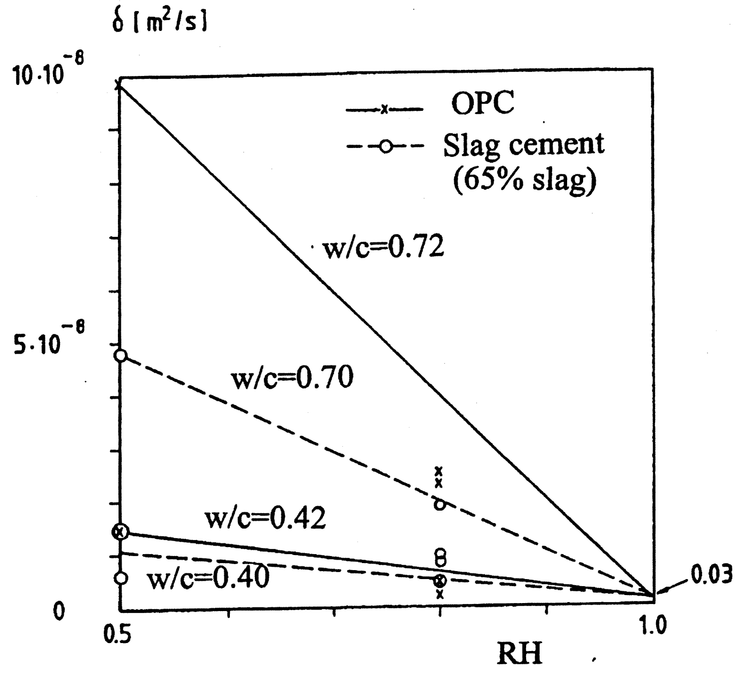

Figure 2.7: Effect of RH in concrete on the diffusivity of oxygen. Data from (Tuutti 1982).

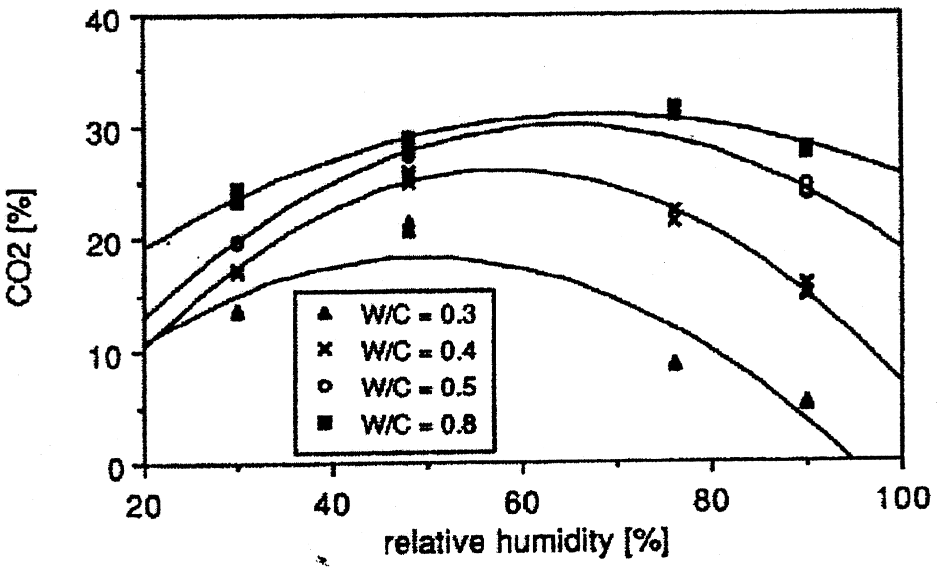

Figure 2.8: Effect of RH in concrete on the carbonation rate.

(ii) Transport of chloride ions only occurs in water phase. Therefore, it increases with increasing RH in concrete, and it reaches its maximum when the concrete is saturated. A calculated effect of RH on the transport coefficient of chloride ions in concrete with different RH is shown in Figure 2.9. It is based on the assumption that the diffusivity is directly proportional to the amount of capillary water (water in concrete at RH> 50%). It was calculated from desorption isotherms given in (Nilsson 1977).

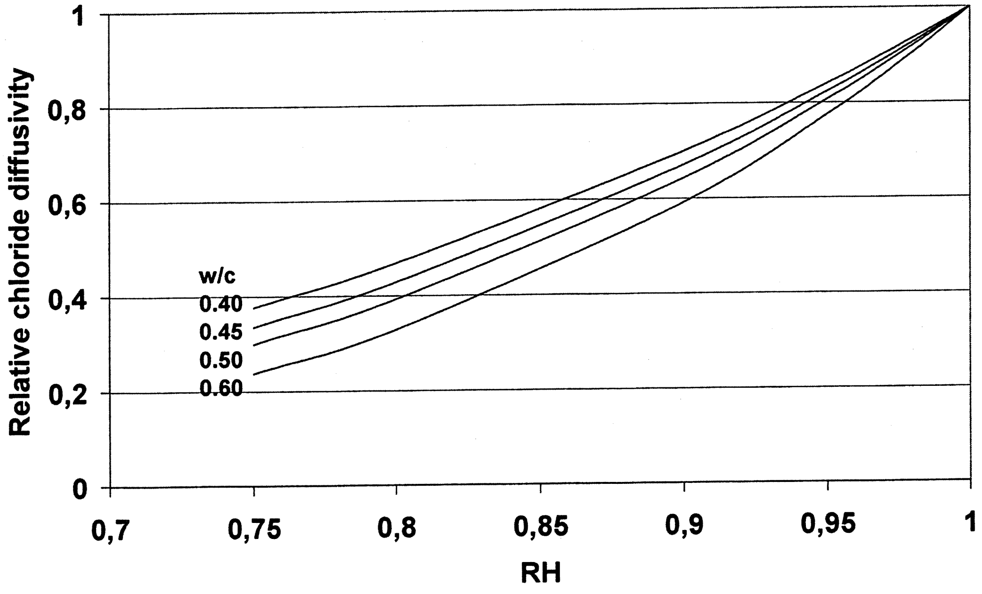

Figure 2.9:Calculated effect of RH in concrete on the diffusivity of chloride ions. w/c is the water-cement ratio.

Once corrosion has been initiated, its rate is a function of the inner relative humidity in the concrete. At low RH there is so small amount of electrolyte (pore solution) that corrosion is obstructed. At very high RH the transport of required oxygen to the cathode is obstructed by water in the pores. The consequence is that a maximum corrosion rate occurs at a certain RH-level, which is often of the order 90 to 95%. One example of the effect of RH in concrete on the corrosion current (the corrosion rate) is shown in Figure 2.10 (Tuutti 1982).

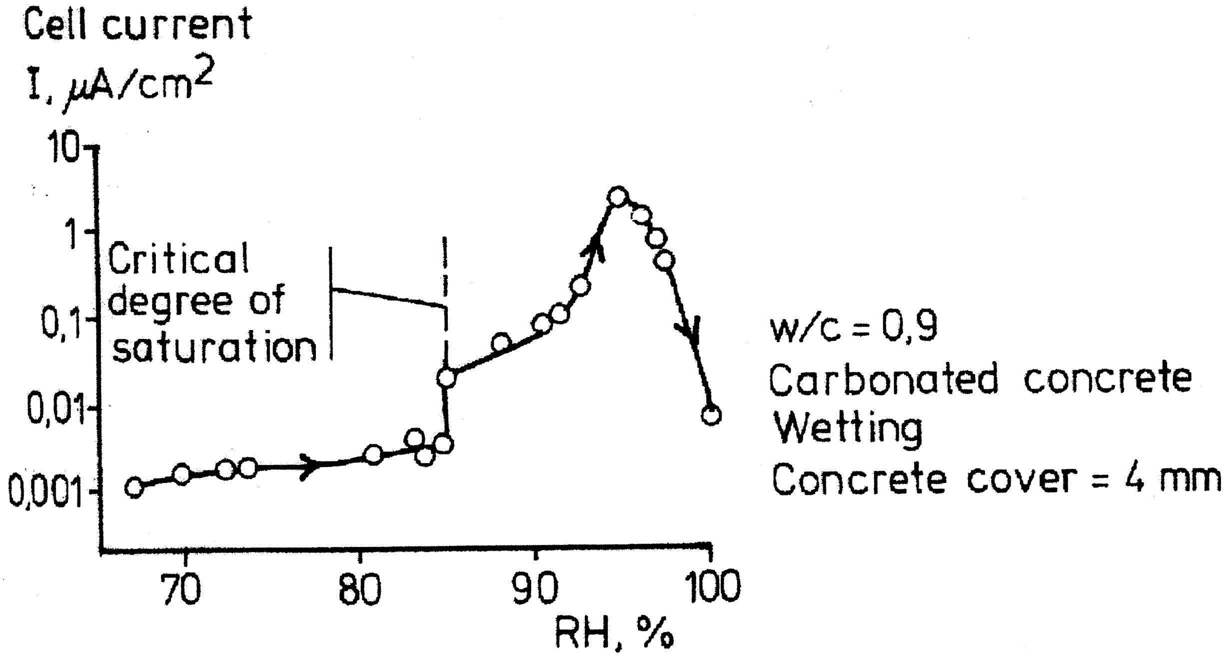

Figure 2.10: Example of the effect of RH in concrete on the corrosion rate (cell current) of cast-in steel.

The effect of moisture on corrosion can be summarised as follows, see also Figure 2.11:

- The time before onset of corrosion caused by *carbonation* is increased with increased moisture content, since the diffusivity of CO_2 is reduced with increased moisture content.
- The time before onset of corrosion caused by *chloride* ions is decreased with increased moisture content, since the diffusivity of chloride ions is increased with increased moisture content.
- The rate of corrosion has its maximum at a certain moisture level; both higher and lower moisture contents give lower corrosion rate, since oxygen diffusivity is decreased and electrical conductivity is increased with increased moisture content.

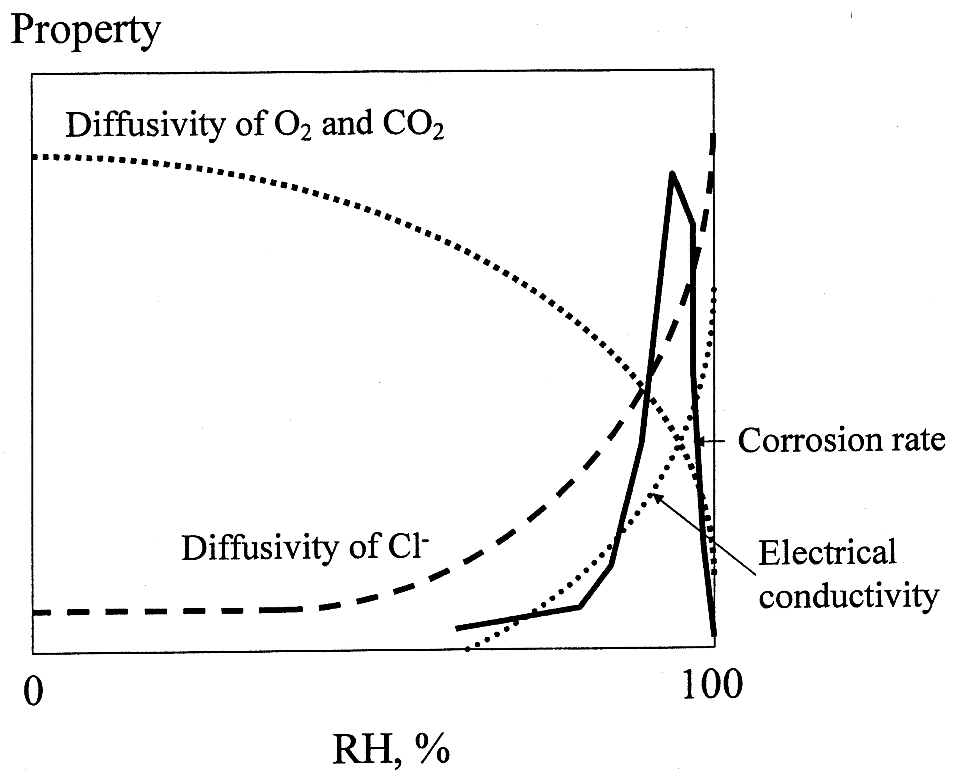

Figure 2.11: Principal effects of RH in concrete on different processes determining corrosion of reinforcement steel.

2.3.2 Decay of wood and other organic materials

Mould growth does only occur if the relative humidity in the organic substrate (e.g. wood) is above a certain level. The mould growth rate is also reduced if RH is too high. There is also an effect of temperature; high and low temperatures obstruct mould growth. The rate of mould growth has its maximum at a certain combination of RH and temperature. Examples of the effect of temperature and water activity (RH) on mould growth of two types of mould fungi are shown in Figure 2.12, (Adan 1994).

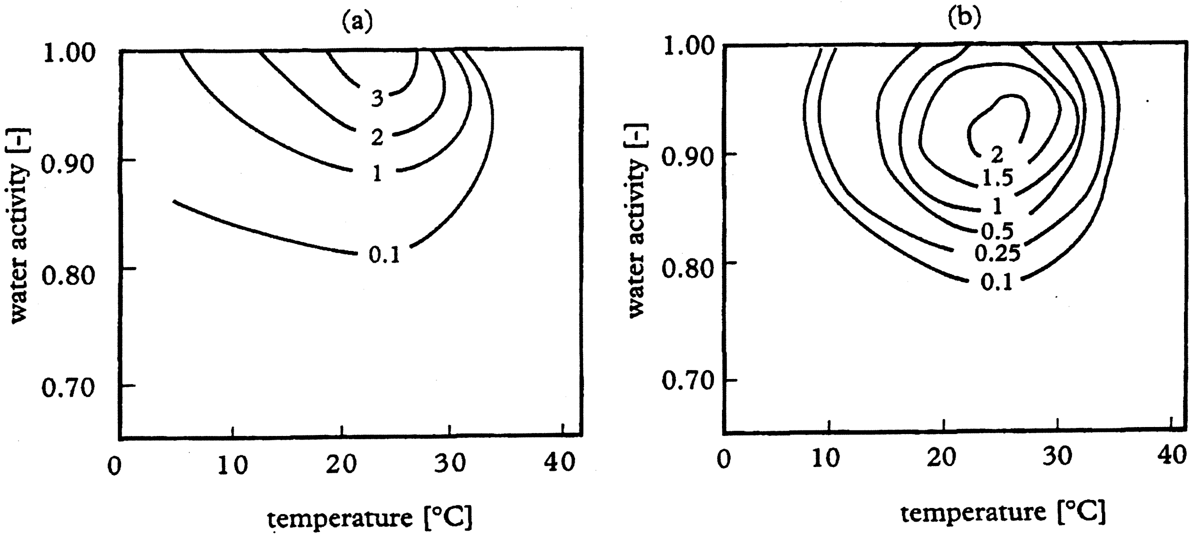

Figure 2.12: Examples of the effect of temperature and RH on the rate of mould growth. Each curve is valid for a constant growth rate (mm/day). (a) Penicillum Martensii growing on a type of agar. (b) Aspergillus versicolor growing on another type of agar.

The risk of unacceptable mould growth is also a function of the duration of the high RH. This is exemplified by Figure 2.13 showing the risk of initiated mould growth on wood at different values of temperatuere, RH and duration of RH; (Viitanen 1996). Examples from this diagram are:

+20C:
    75% RH: Mould growth probably impossible
    85% RH: Required duration 2.5 months
    95% RH: Required duration 0.5 month
+10C:
    75% RH: Mould growth probably impossible
    85% RH: Required duration 4 months
    95% RH: Required duration 1 month

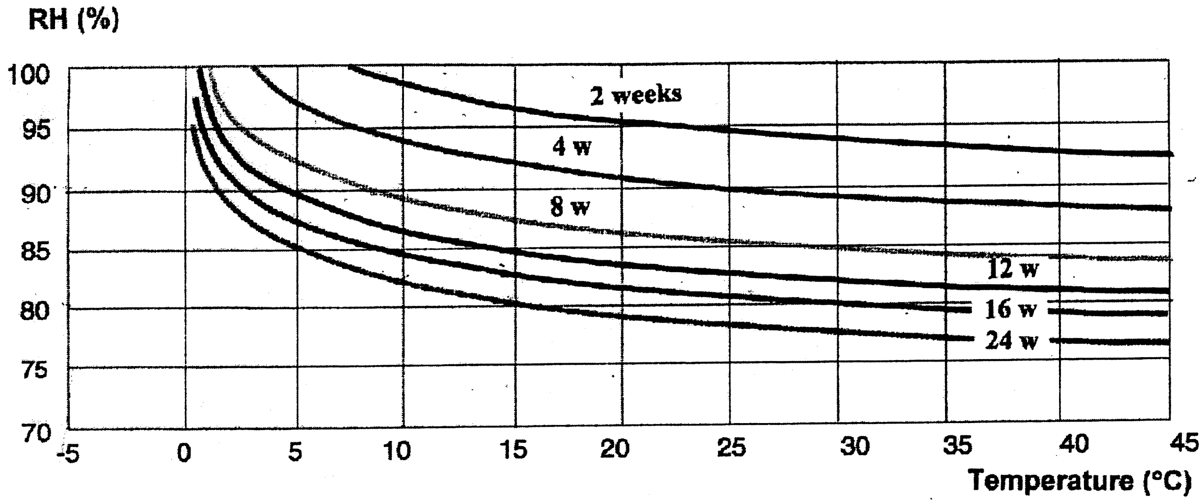

Figure 2.13: Effect of temperature and duration of moisture on the critical RH-level for onset of mould growth on wood.

In practice the moisture level varies; periods with low RH, giving slow rate of mould growth, alternates with periods with higher RH giving high mould growth rate. Mould growth that has been initiated at higher RH will almost completely stop when RH is lowered to 50% or lower. However it will start again when RH is once again raised, but the renewed growth might occur at a lower rate. Two examples are shown in Figure 2.14 (Adan 1994). The two gypsum boards, one (plain) without paper surfaces, and one (coated) with paper surfaces, was repeatedly exposed to 6 hours at 97% RH and 6 hours at a lower RH that was varied; 10%, 33%, 58% and 85%. There is a slowing down of mould growth when the board is dried occasionally. The lower the RH during the drying phase, the bigger the retardation of mould growth. However, mould growth did never stop entirely.

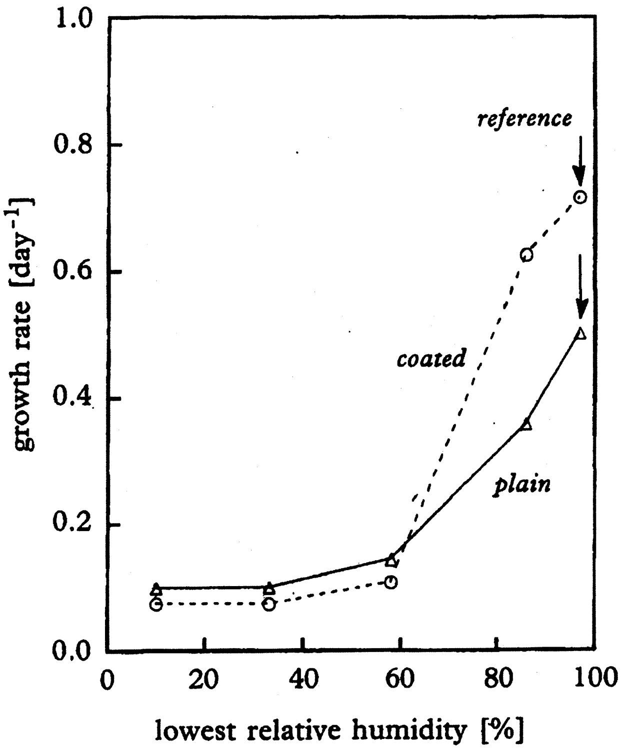

Figure 2.14:Effect on mould growth on gypsum board of drying from 97% RH to a lowest RH (10, 33, 58 and 85% RH), and moistening again to 97% RH. Repeated drying-wetting cycles, 6h drying+6h wetting, Mould type, Penicillum chrysogenum.

2.3.3 Atmospheric attack on stone

Natural calcareous stone, like limestone and marble, might be attacked by acid rain and other pollutants. Water is needed for the destructive process to take place. One example is shown in Figure 2.15, (Elfving 1994). The stone was exposed to SO_2 and NO in a reactor which was adjusted to different RH-levels.

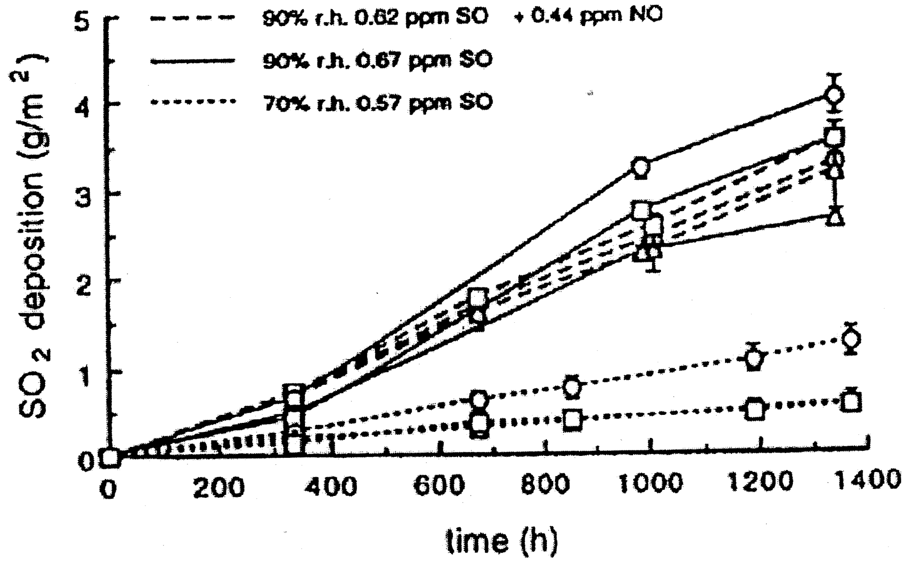

Figure 2.15: Effect of RH on the acid attack on limestone caused by SO (sulphuric acid) alone, or in combination with NO (nitric acid).

3 THE CRITICAL WATER CONTENT

3.1 The critical water content is well-defined and independent on duration of the moisture state

In some cases it is possible to identify a well-defined critical water content that marks a fairly distinct border between durability and non-durability. At moisture levels below the critical no damage occurs, at higher levels the material is completely destroyed. This type of behaviour is illustrated by Figure 3.1.

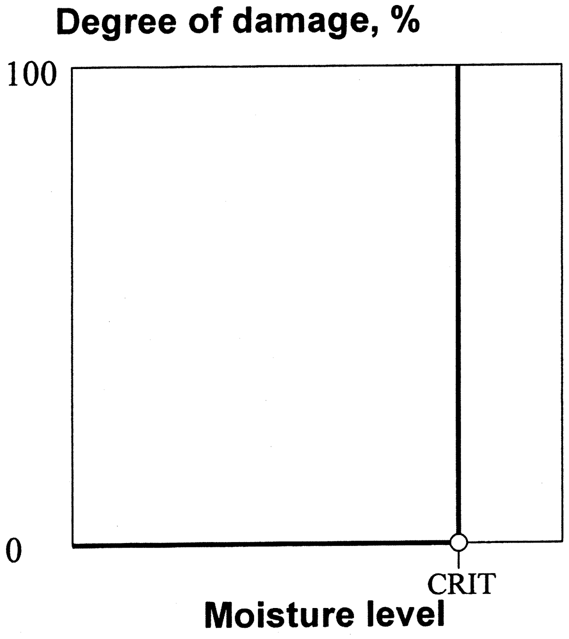

Figure 3.1: Distinct critical moisture level.

This behaviour is similar to mechanical fracture; the material is destroyed when a certain fracture load is transgressed. Below that level, the material is intact (provided fatigue of static or dynamic nature is neglected).

The relation between moisture content (W) and degree of damage (D) can be described in the following way:

$$\begin{array}{ll} W \leq W_{CR}: & D=0 \\ W>W_{CR}: & D=100\% \end{array} \tag{3.1}$$

Where D=0 means that the damage is zero or negligible. D=100% means that the material is so destroyed that it cannot fulfil its intended function.

In reality, the transition from durability to non-durability is often a bit less drastic than shown in Figure 3.1. In such cases there is a small moisture range within which damage is gradually increasing until the material is completely destroyed. This is illustrated by Figure 3.2.

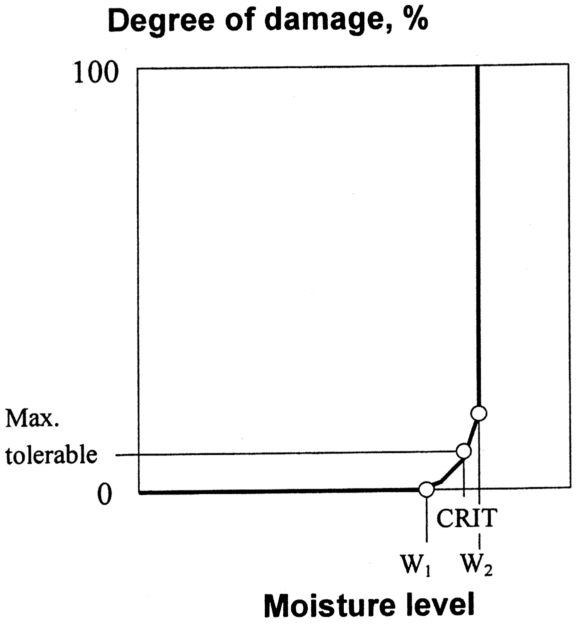

Figure 3.2: Transition moisture zone between no damage and complete destruction.

In this case a maximum tolerable damage level must be defined. The relation between moisture content and degree of damage is described by:

$$\begin{array}{ll} W \le W_1: & D=0 \\ W_1 < W \le W_2: & D=f(W) \\ W > W_2: & D=100\% \\ W = W_{CR}: & D=D_{\text{max. tolerable}} \end{array} \qquad (3.2)$$

The damage is gradually increased within the range between W_1 and W_2 at a certain moisture level W_{CR} the maximum tolerable damage is reached.

Damage of these well-defined types is internal frost destruction, salt-frost damage and surface spalling due to fire. The most studied case is internal frost damage, where numerous studies on many different types and compositions of mineral-based materials show that a critical water content shall not be transgressed during freeze/thaw if the material shall not be more or less completely destroyed by one single freeze-thaw. One example valid for a certain clay brick is shown in Figure 2.1 above. Another example valid for a certain concrete is shown in Figure 3.3. In both cases the maximum tolerable decrease in dynamic E-modulus is assumed to be 10% (i.e. $E/E_0=0.9$).

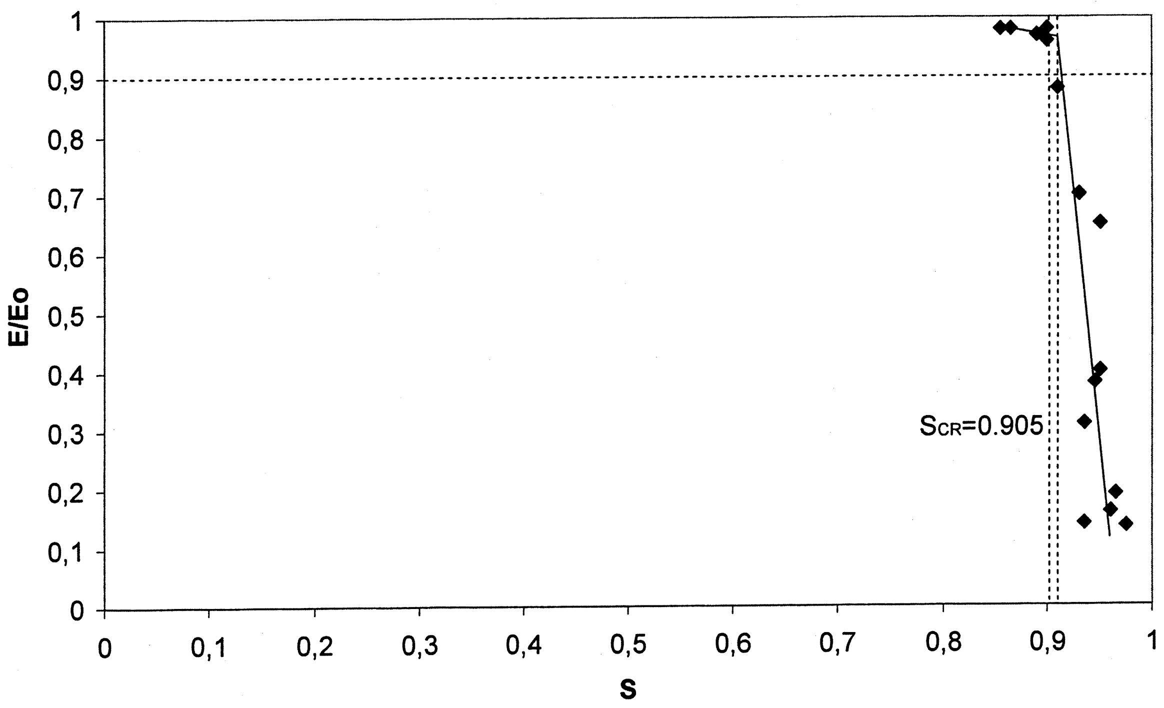

Figure 3.3: Example of the critical moisture content with regard to internal frost damage. Air-entrained concrete, water-cement ratio 0.46, air content 4.7% (S is the degree of saturation. E/E_0 is the ratio of E-modulus after and before freeze-thaw.)

Other examples are given in Chapter 6 below. These types of critical water content are *independent on the duration* of the water content. Thus, the critical water contents of the brick in Figure 2.1, and the concrete in Figure 3.4 are the same independently of how long time the actual water contents have existed in the material before freezing. They are also independent of the number of occasions at which the critical water content is transgressed. Thus they are not dependent on fatigue. The effect of fatigue in connection with frost attack is further discussed in (Fagerlund 2004).

3.2 The critical water content is less well-defined and dependent on the duration of the moisture state

In many cases the amount of damage depends on how long time the actual moisture conditions have been prevailing. One example valid for mould growth on wood is shown in Figure 2.13. In these cases the critical water content will partly be a function of the amount of damage that can be accepted, partly be a function of the duration of the moisture level. The behaviour and definition of critical moisture level is illustrated by Figure 3.4. The critical moisture level will land within a certain interval.

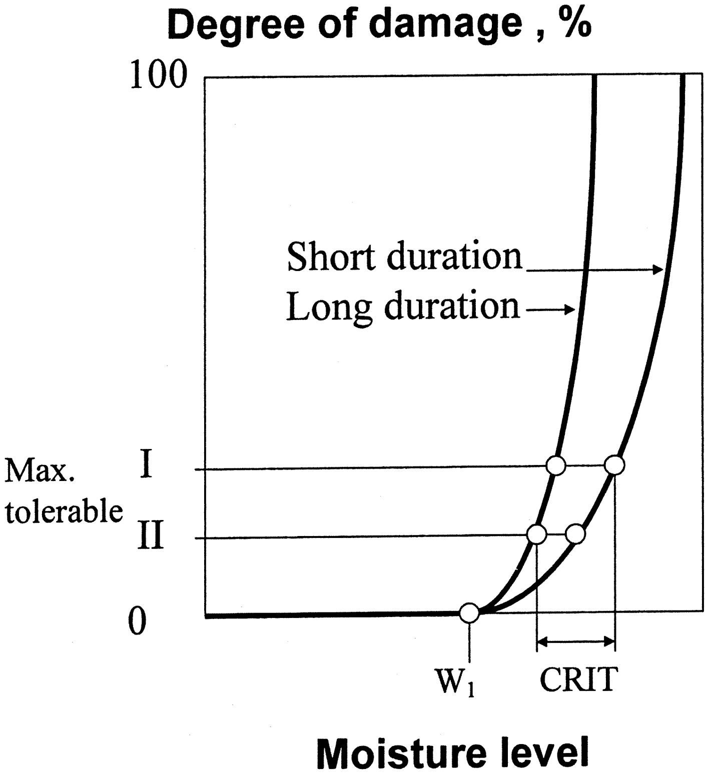

Figure 3.4: Damage is gradually increasing with increased moisture level and with increased duration of the high moisture condition.

The relation between moisture content (W) and degree of damage (D) can be described in the following way:

$$W \le W_1: \quad D=0 \qquad (3.3)$$
$$W > W_1: \quad D=f\{(W-W_1);t\} \quad 0 \le D \le 100$$

Where W_1 is the highest moisture content for which no damage can be observed. $f\{(W-W_1);t\}$ is a time dependent function describing the damage curve for $W>W_1$.

The damage function is different for different damage types. The simplest function imaginable is where damage is supposed to be directly proportional to the difference between W and W_l, and directly proportional to the exposure time:

$$D=C(W-W_l)\cdot t \tag{3.4}$$

Where C is a coefficient, which is different for different types of destruction.

The equation is illustrated by Figure 3.5. It predicts complete destruction also for small transgression of the moisture content W_l provided the exposure time is long enough.

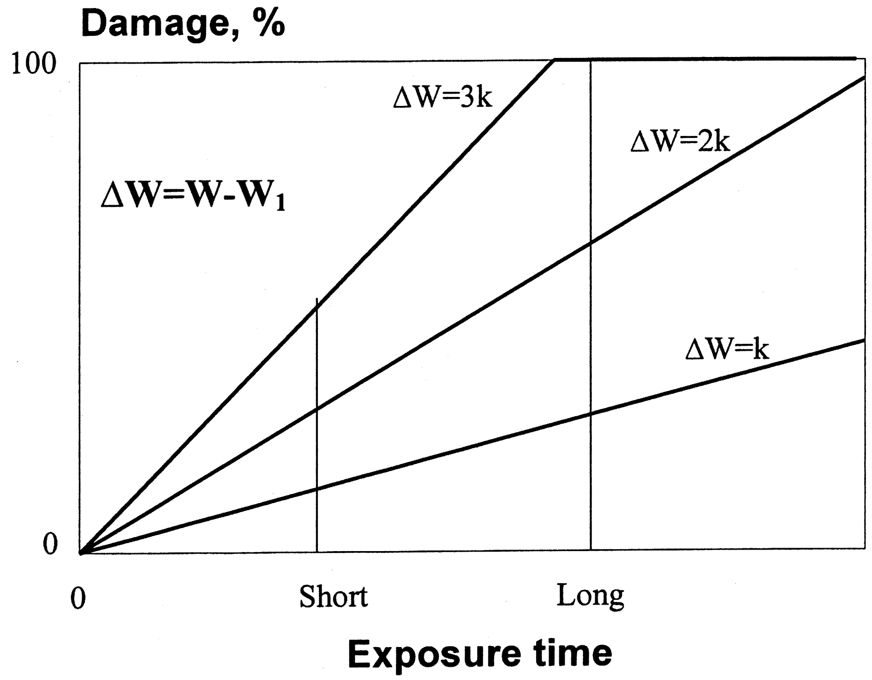

Figure 3.5: Damage function of type (3.4). Direct proportionality between damage, exposure time, and moisture level.

For most destruction types it is more likely that damage approaches an asymptote, which is a function of the amount by which W_l is transgressed. Furthermore, it is likely that damage is more rapidly increasing with increased transgression of the level W_l. An expression that considers these requirements is:

$$D=C\cdot(W-W_l)^a\cdot[A\cdot t/(B+t)] = C\cdot\Delta W^a\cdot[A\cdot t/(B+t)] \tag{3.5}$$

Where a>1. The coefficients A and B depend on the type of destruction. This equation leads to a maximum destruction at long exposure times. This asymptote is given by:

$$D_{t=\infty} = C\cdot(W-W_l)^a\cdot A = C\cdot\Delta W^a\cdot A \tag{3.6}$$

An example of application of this expression is given below.

Example

The following coefficients are used in the example:

C=1; W is expressed in terms of relative humidity, RH; thus, $\Delta W=\Delta RH$; a=3, B=5; A is determined by the condition that the asymptote is defined by $80\cdot\Delta RH^2$, thus, according to equation (3.6) $A= 80/\Delta RH$.

The damage function becomes:

$D=\Delta RH^3\cdot(80/\Delta RH)\cdot[t/(5+t)]=80\cdot\Delta RH^2\cdot t/(5+t)$ where D=1 means total destruction (3.7)

The relative humidity below which no damage occurs is assumed to be $RH_l=0.70$.

The result is shown in Figure 3.6.

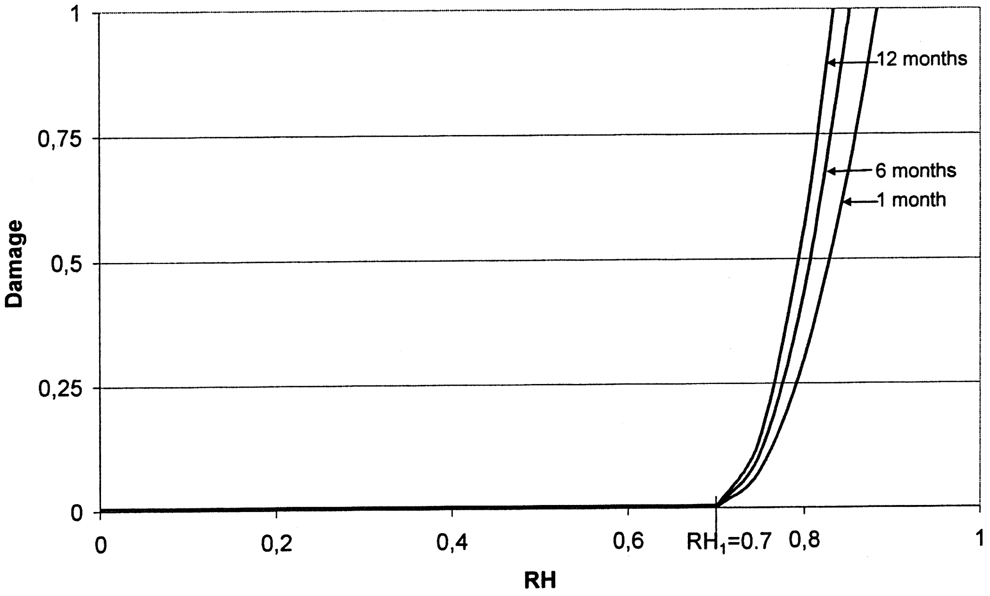

Figure 3.6: The example. Evolution of damage as function of the exposure time.

3.3 Critical water contents causing environmental problems

In some cases moisture does not harm the material itself but it stimulates emissions from the material that might cause environmental problems to the interior of the building. Examples are emission of volatile organic compounds, or emission of radon. For these types of moisture damage it is often difficult to find well-defined critical moisture conditions for at least four reasons:

(i) The relation between moisture level and rate of emission is often obscure and depends not only on the moisture content but also on the pH of the moisture and its contents of ions. It also depends on interaction between different materials in contact with each other.

(ii) The emission is often very complex and contains numerous components, only few of which are really harmful.

(iii) The concentration of emitted substance in air surrounding the emitting material is not only depending on the rate of emission from the material, but also on the rate of removal by ventilation.

(iv) The maximum acceptable concentration of the hazardous substances emitted, i.e. the effect on man, is often not known. In many cases there are no official limits for the maximum tolerable concentration. Probably, the acceptance level is highly different for different individuals; some persons can accept a high concentration, while others are annoyed also at very low concentrations. In many cases it is not only one of the emitted compounds that is hazardous, but the synergetic effect of a combination of two or more substances.

This complex problem is illustrated by Figure 3.7.

These difficulties mean that the relation between the moisture level in the material (or construction element) and the maximum tolerable negative environmental effect is often very unclear. One possibility is to use the “principles of caution” and define the critical moisture condition as the value below which practically no emission can be detected. This might, however, lead to a situation where some materials and materials combinations cannot be used, since emission, which are not caused by moisture, can occur. In such cases emissions will occur also at very low moisture conditions. The concept “critical moisture” therefore looses its meaning.

Since emission often increases progressively with increased moisture level one might define the critical moisture level as the intersection between two tangents to the emission-W-curve; see Figure 3.8.

The best solution is to base the criterion on maximum tolerable values in indoor air stipulated by the authorities.

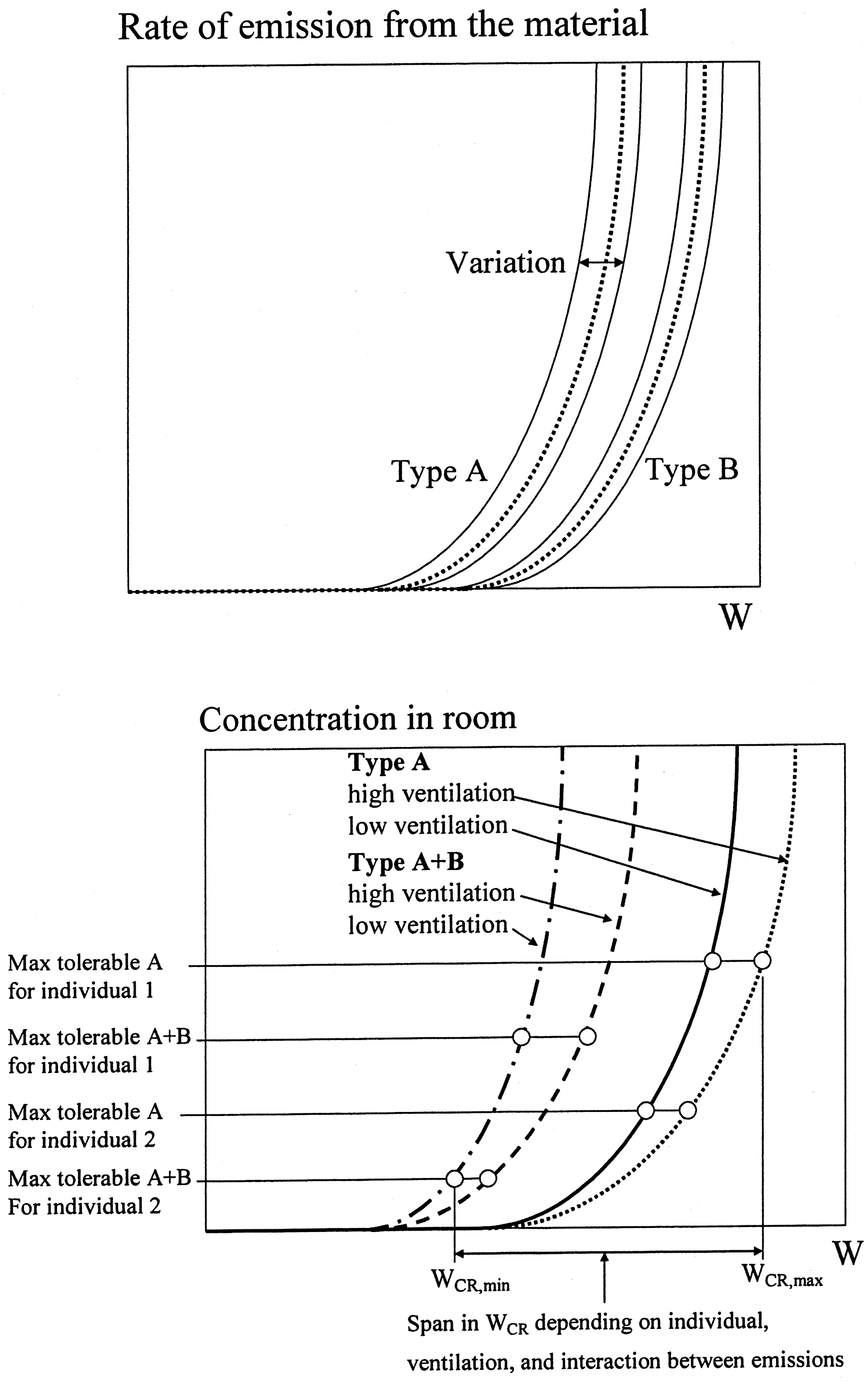

Figure 3.7: Upper: Rate of emission of compounds A and B as function of the moisture content.
Lower: Concentration of compound A and of the combined compounds A and B in air around the emitting material (or structure). Definition of the critical moisture condition depends also on the sensitivity of individuals, and on the amount of ventilation.

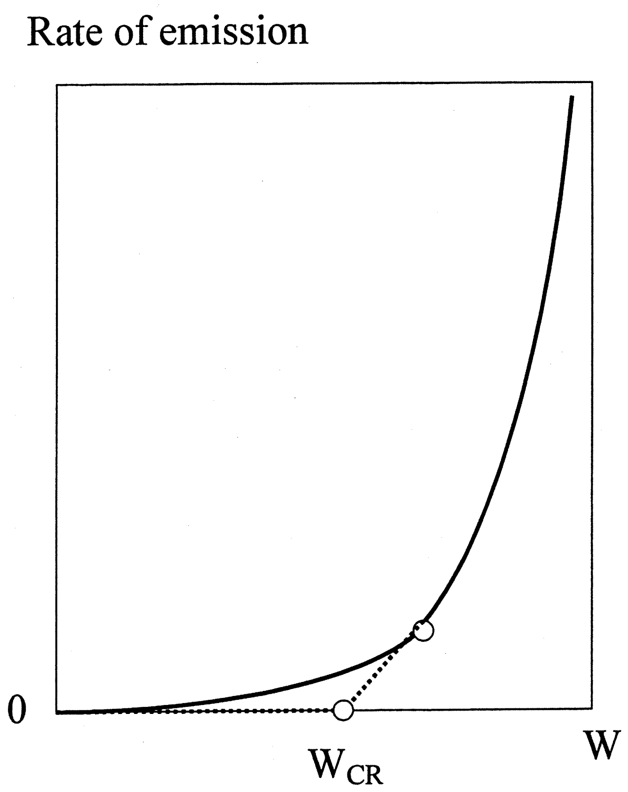

Figure 3.8: The critical moisture content defined as the intersection between two tangents to the emission-W-curve.

3.4 Critical water content of combined materials

A material, which in itself is rather insensitive to moisture, or that can stand very high moisture conditions, might be harmed by moisture if it is used in combination with other materials. Typical examples are polymer-based flooring materials on concrete slabs. Often the flooring systems consist of 4 different materials, (i) a concrete slab, (ii) a self-levelling cement-bound screed, (iii) a glue, (iv) a polymer-based flooring material. See Figure 3.9.

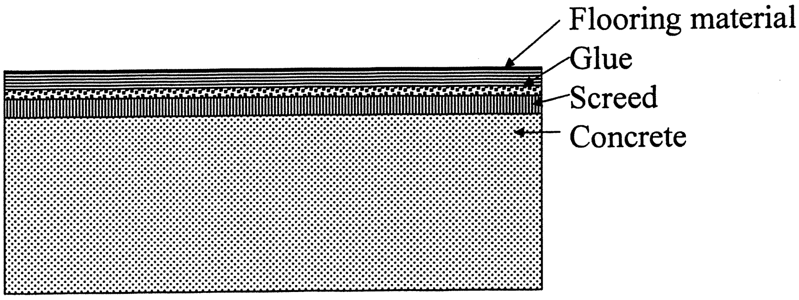

Figure 3.9: Example of a materials combination. Covered concrete floor.

The concrete and the screed are insensitive to moisture, their RH_{CR} is 100%. Also the glue and the flooring materials themselves are often durable at very high moisture conditions. The function of the combined four materials, however, might be severely impaired at moisture levels far below 100% RH. The reason is that one of the four materials might negatively affect the behaviour of one of the other materials. Examples of this are: (i) screeds containing casein have been found to emit ammonia in alkaline environment, which causes discolouring of cork-plates and oak parquet, (ii) alkaline moisture from concrete and/or screed might cause decomposition of phthalate plasticizer in PVC-carpets with evil-smelling emission as consequence, (iii) alkaline moisture from concrete and/or screed might negatively affect the strength of the glue and thereby impair the bond to the flooring material, one example is shown in Figure 2.5.

In these cases it is not meaningful to test the individual materials for their critical moisture levels. Instead, the whole "package" of materials should tested, and the critical moisture level of the package be found.

Another case is *frost attack* on combined porous materials like external rendering on brick, or exterior porous surface layers on concrete. Each material has its own critical moisture level, which can be expressed in terms of a critical degree of saturation, see Figure 2.1. If there is no interaction between the two materials during freeze/thaw, these critical values will be unchanged. The critical moisture level of the combination is therefore determined by the two individual critical moisture levels. This case is illustrated by Figure 3.10 (a).

When a combination of the two materials are frozen there is a possibility that surplus water caused by the 9% increase in volume when water freezes is transferred from one material to the other. This will increase the moisture level close to the interface. Possibly, for some combinations the water content is so much increased that the assembly is destroyed, despite the fact that the individual moisture contents in the two materials before freezing was below their critical values. The case is illustrated by Figure 3.10(b). This risk has never been investigated theoretically or experimentally. The risk can be investigated by frost testing both the combination and the individual materials with regard to their critical moisture levels.

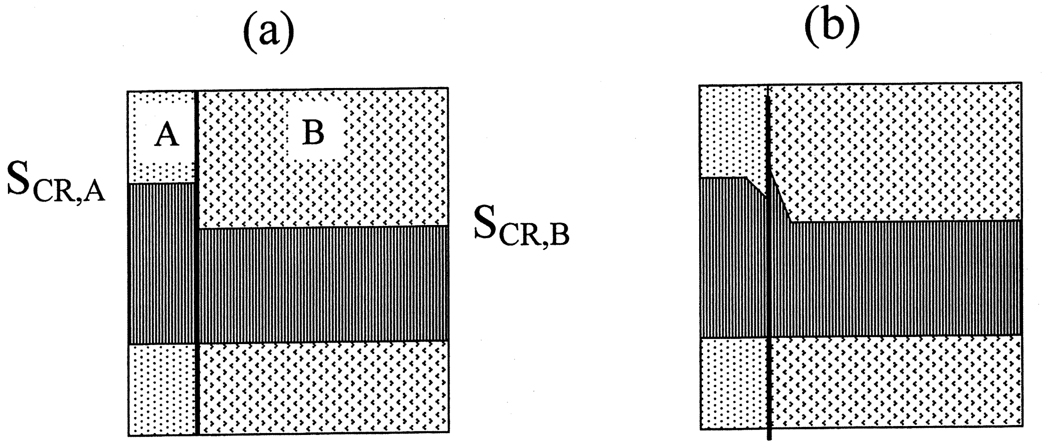

Frost resistance determined by $S_{CR,A}$ and $S_{CR,B}$

Frost resistance independent of $S_{CR,A}$ and $S_{CR,B}$

Figure 3.10: Critical moisture conditions in combined materials without, (a), and with, (b), redistribution of water at the interface during freezing.

In combined materials there is an interface zone with properties that is normally different from properties of the two adjacent materials. This is an additional cause that makes the composite differ from the materials used isolated.

4 THE RISK OF MOISTURE INDUCED DAMAGE

4.1 Well-defined critical moisture level independent of the duration of moisture load

4.1.1 Principles

At critical moisture contents of the type shown in Figure 3.1 and 3.2 the damage risk can be calculated according to the same principles as the risk of failure is calculated in structural design. The following analogy with structural design can be used:

Type of design	Actual stress	Fracture stress	Required safety level
Structural	σ	f	$P\{f>\sigma\} > p_1$
Durability	W_{ACT}	W_{CR}	$P\{W_{CR}>W_{ACT}\} > p_2$

$P\{x>y\}$ is the probability that the "fracture load" transgresses the "actual load".

The required probabilities p_1 and p_2 could of course be quite different for the two types of design. Traditionally p_1 is very high since the consequences of structural collapse are normally very big. p_2 can be considerably lower, since damage caused by lacking durability will often give small risk of immediate collapse.

In a most simple case both the W_{CR}-value and the W_{ACT}-value have fixed values, which will however normally be a function of time. This case is illustrated by Figure 4.1.

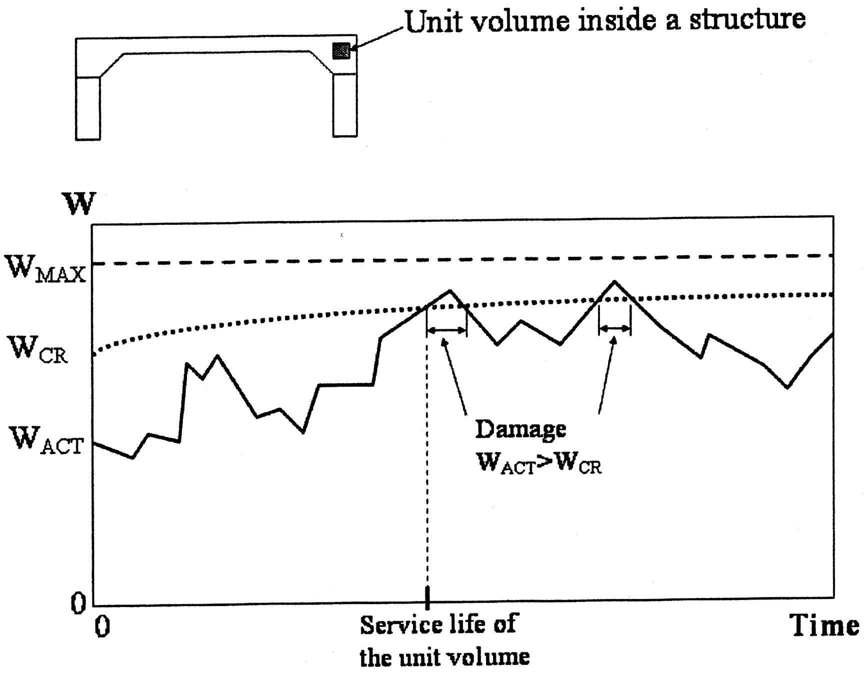

Figure 4.1: Example of time-dependent variations of the critical and actual moisture condition inside a unit volume in a structure. Damage in the unit volume occurs when $W_{ACT}> W_{CR}$. W_{MAX} *is the moisture content at full saturation.*

In reality, W_{CR} and W_{ACT} are stochastic variables which depend on variations in material properties and in climatic conditions. This is illustrated by Figure 4.2 in which mean values and "variation ranges" are shown. Normally, the variation in S_{ACT} is much bigger than in S_{CR} since it is entirely determined by climate variations, which are normally very big and uncertain. There is risk of damage when the value of W_{ACT} transgresses the value of W_{CR}; the bigger the transgression, the bigger the risk.

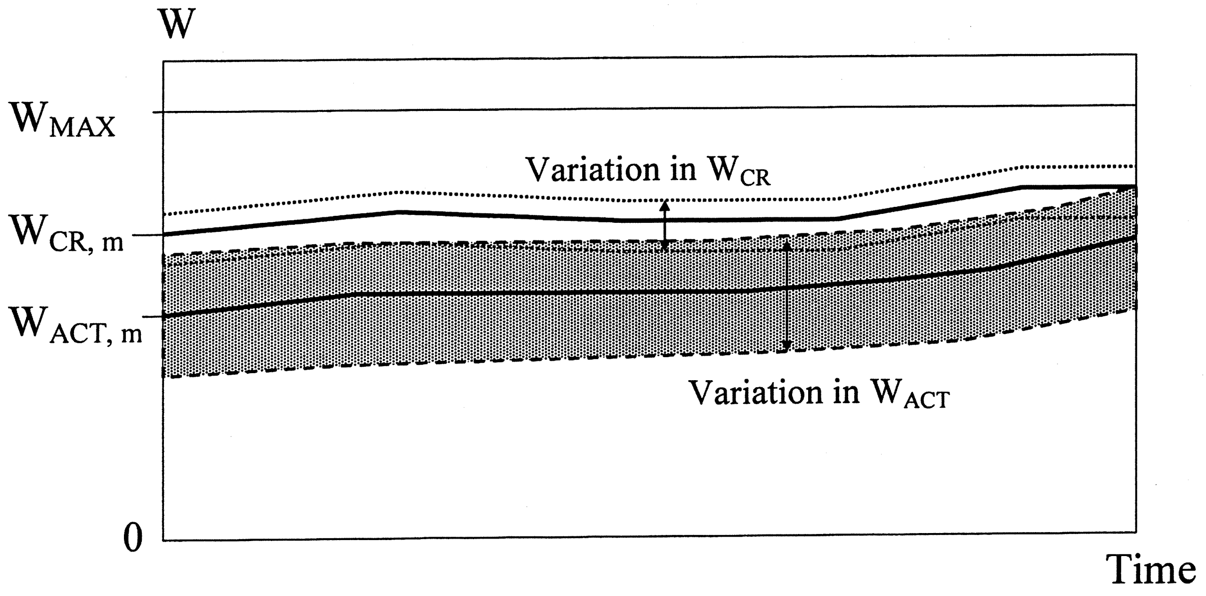

Figure 4.2: Mean values and ranges of variation of W_{ACT} and W_{CR}.

The risk of failure can be calculated by the following equation:

$$P\{W_{ACT}>W_{CR}\} = \int_{0}^{W_{max}} F(W_{CR})\cdot f(W_{ACT})\cdot dW \tag{4.1}$$

Where $F(W_{CR})$ is the distribution function of the critical moisture condition. $f(W_{ACT})$ is the (normalized) frequency function of the actually occurring moisture condition. W_{max} is the maximum possible moisture condition (at full saturation). These functions are illustrated by Figure 4.3.

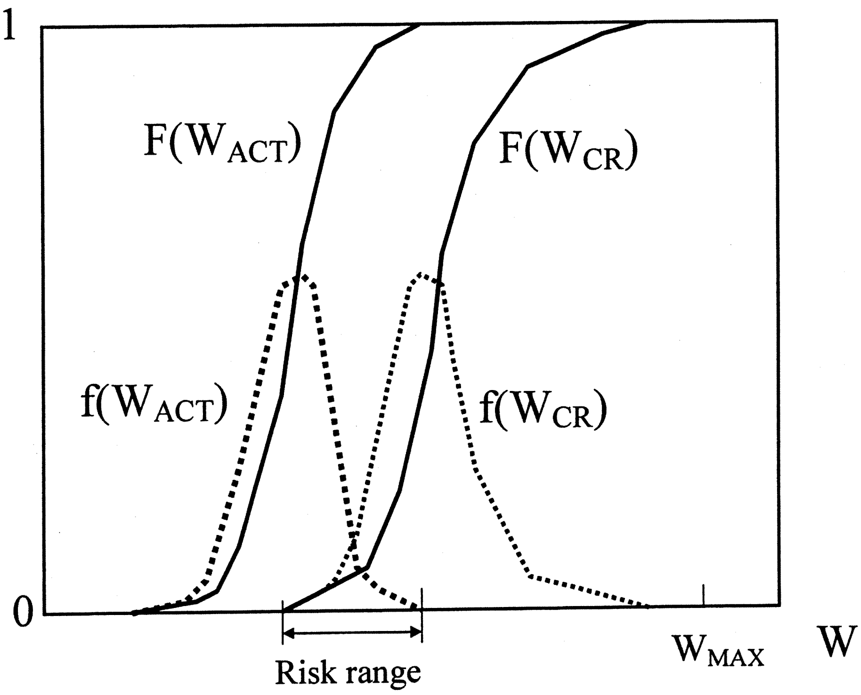

Figure 4.3: Frequency functions (f) and distributions (F) of critical and actual moisture conditions (W). Areas under the frequency curves are 1.

Example

Moisture content is expressed in terms of relative humidity RH ($0 \leq RH \leq 1$). Both RH_{CR} and RH_{ACT} are supposed to be normal distributed. The mean value and the standard deviation are:

RH_{CR}:	Mean value: 0.62	Std. dev.: 0.03
RH_{ACT}:	Mean value: 0.76	Std. dev.: 0.08

The risk of moisture is calculated by equation (4.1) with the general moisture content W exchanged for RH:

$$P\{RH_{ACT}>RH_{CR}\} = \int_0^1 F(RH_{CR})\cdot f(RH_{ACT})\cdot dRH \qquad (4.2)$$

The probability of damage becomes **0.23 (23%)**

Example

The standard deviation in RH is supposed to be higher, 0.15 instead of 0.08. The other values are unchanged:

RH_{CR}:	Mean value: 0.62	Std. dev.: 0.03
RH_{ACT}:	Mean value: 0.76	Std. dev.: 0.15

Then, the probability of damage is increased to **0.33 (33%)**

4.1.2 Effect of the exposure time

For some exposure types, and some types of materials, the risk of moisture damage will change with exposure time. This will be the case when:

1. The actual moisture level (W_{ACT}) gradually increases with time. A typical case is a concrete column founded in water. During the whole exposure time, water will be sucked into the concrete, causing steadily increased moisture content.
2. The critical moisture level (W_{CR}) changes with time due to ageing of the material. One example is concrete where the gradual hydration might cause such changes.

The principles are illustrated by Figure 4.4; the frequency function of W_{ACT} is supposed to move towards higher values of W with time, while the frequency function for W_{CR} is supposed to move towards lower values. The net effect is that the damage risk increases with increased exposure time, which is illustrated by Figure 4.5. Numerical examples are given in paragraph 5.4.3.

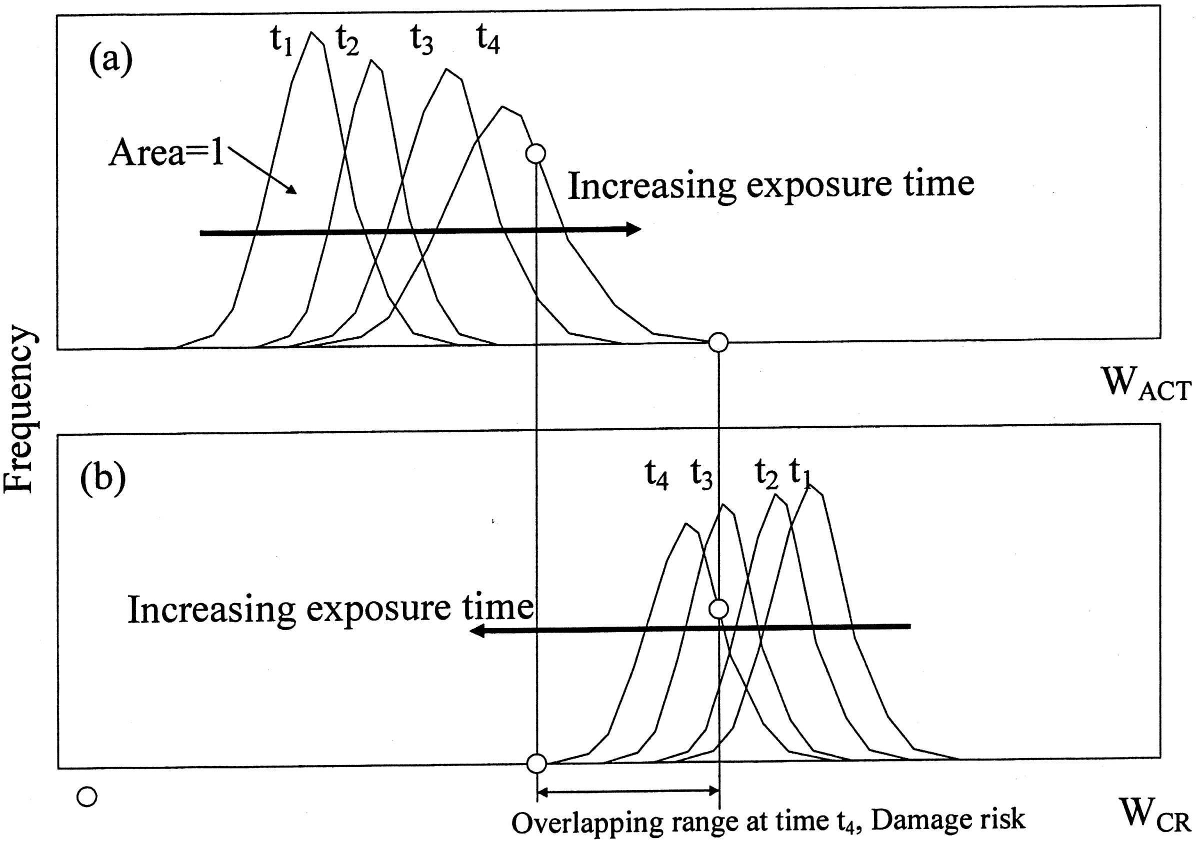

Figure 4.4: Time variations of the frequency functions of W_{ACT} *and* W_{CR}*; principles.*

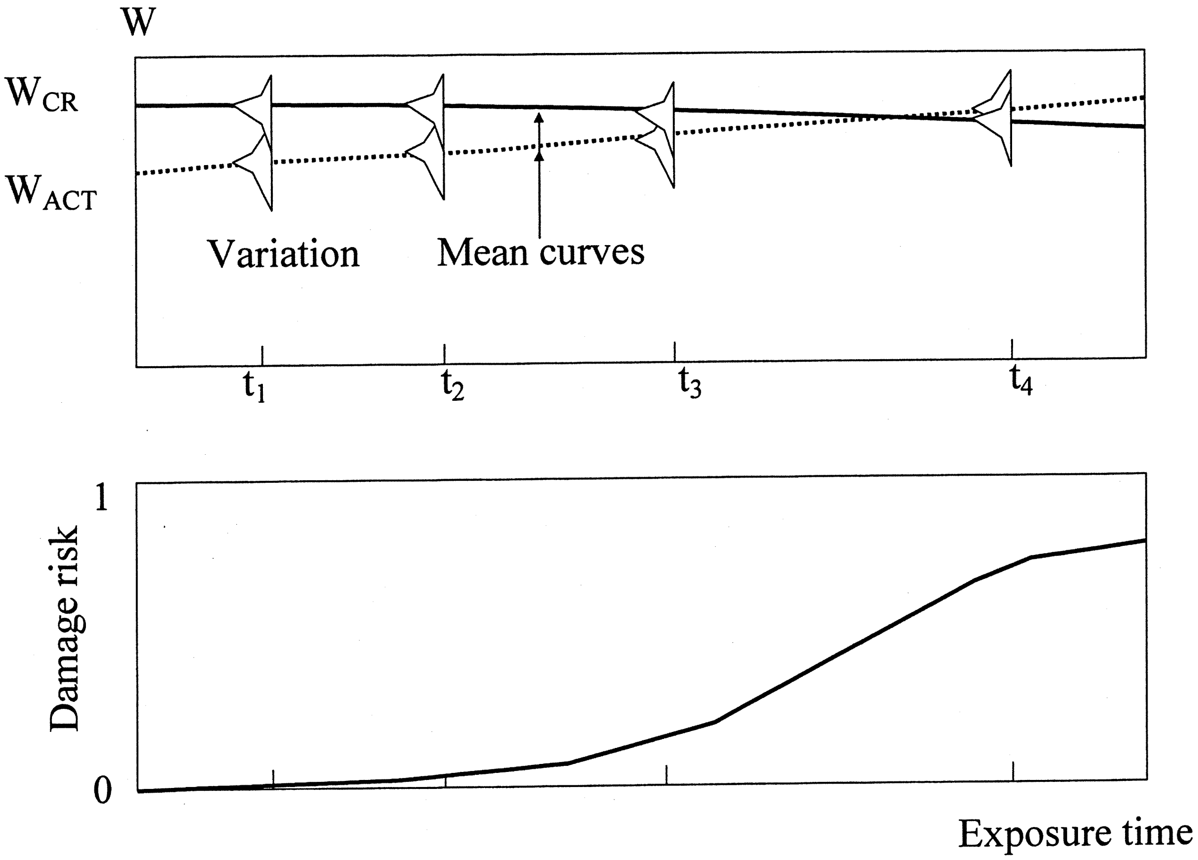

Figure 4.5: Increase in the damage risk with time when the W_{CR} and/or W_{ACT} are time dependent according to the principles in Figure 4.4.

4.2 The critical moisture level is influenced by the duration of the moisture state

Often the critical moisture condition is not very well defined, and it might also be influenced by the duration of the moisture state; see Figure 3.4 above. In such cases the risk of moisture damage will depend on both the moisture state and the duration of this.

Total damage (D) can be calculated as the sum of partial damages occurring at many occasions.

$$\Delta D = f(\Delta W_{ACT};\Delta t) \qquad (4.3)$$

$$D=\Sigma\Delta D_i=\sum_{1}^{i} f(\Delta W_{ACT,i};\Delta t_i) \qquad (4.4)$$

$$\Delta W_{ACT,i}=W_{ACT,i}-W_1 \quad \text{and} \quad \Delta t_i=t_i-t_0 \qquad (4.5)$$

Where ΔW_{ACT} is the moisture content transgressing a limiting value W_1 below which no damage occurs; Figure 4.6. t_0 is the time when the moisture content $W_{ACT,i}$ is first reached and t_i is the time when this moisture level disappears. Thus moisture damage is supposed to be accumulated *in similar manner as damage in dynamic fatigue.*
The principles are illustrated by Figure 4.6.

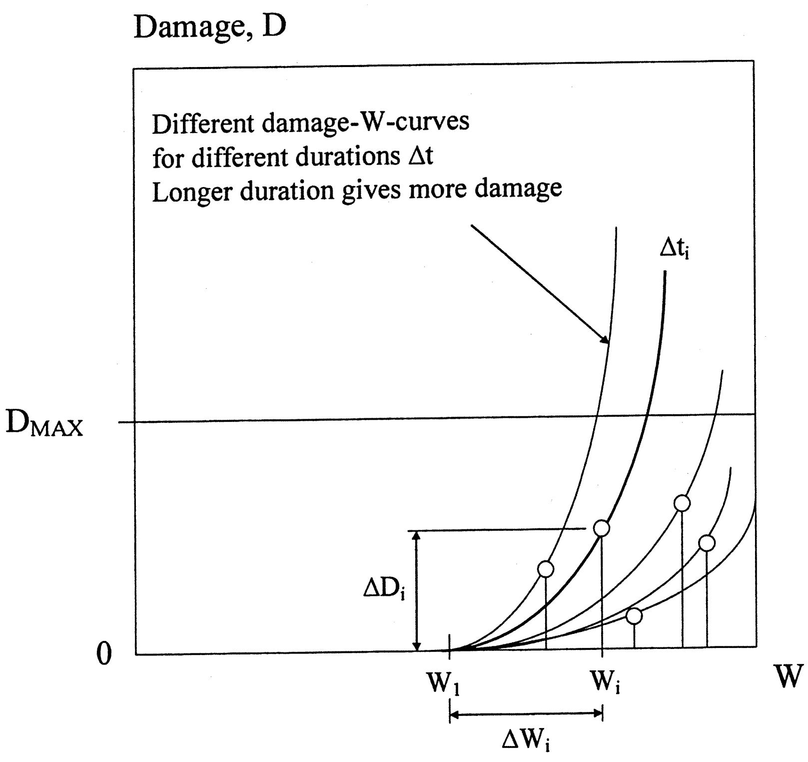

Figure 4.6: Damage caused by a transgression with duration Δt of the limiting value W_1. Each curve in the diagram is valid for one constant duration; the longer the duration, the higher the curve.

In order to calculate the risk that a certain damage level shall be reached, the variation of the D-W curve for different constant duration of the moisture load must be know; see Figure 4.7.

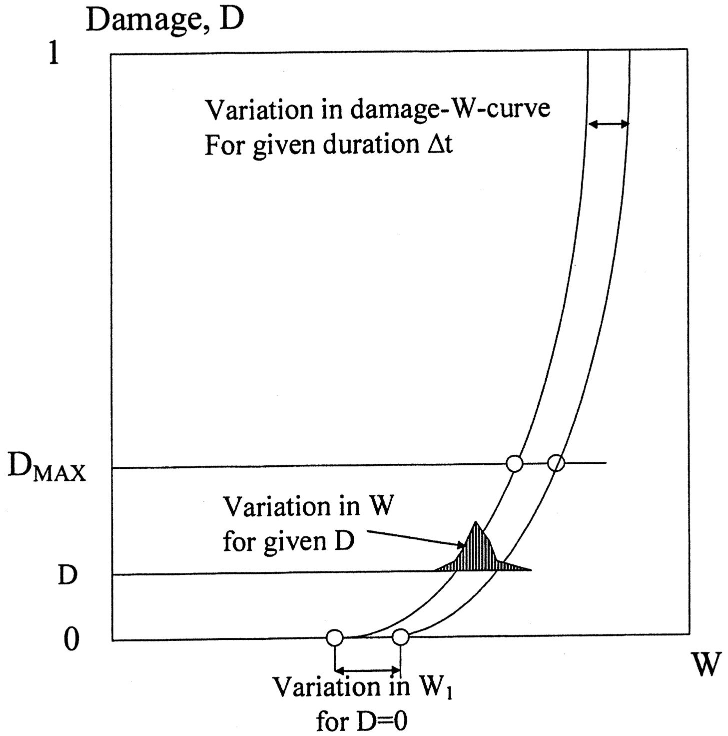

Figure 4.7: Variation in the D-W-curve valid for a constant duration of the actual moisture load.

The damage curve can be described by an equation. Therefore, the variation in the damage curve can be described by variations in the parameters included in that equation. An imaginable expression for the damage curve is given by equation (3.5). It contains four parameters (A, B, C, a). The variations in these give the variation in expected damage for different transgressions of the limiting value W_l. This is illustrated by Figure 4.8.

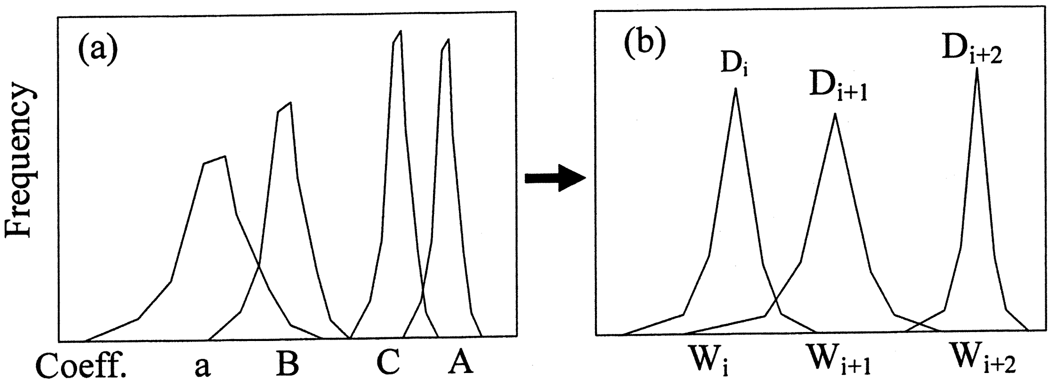

Figure 4.8: Damage equation (3.5) for a certain ***constant duration*** *of the moisture load. (a) Variation in the coefficients a, A, B and C. (b) The resulting variation in moisture level W_i for different damage levels D_i.*

The "D-W-field" according to Figure 4.8 corresponds to W_{CR} in the risk analysis and is valid for a constant duration Δt_i of the moisture load. Each point within the field corresponds to a moisture content $W_{CR,i}$ which will with a certain probability give a certain damage, D_i.

In order to calculate the risk that a certain damage D_i shall also occur it is necessary to find the frequency function of the moisture level $W_{ACT,i}$ with the given duration Δt_i. Such functions are illustrated by Figure 4.9.

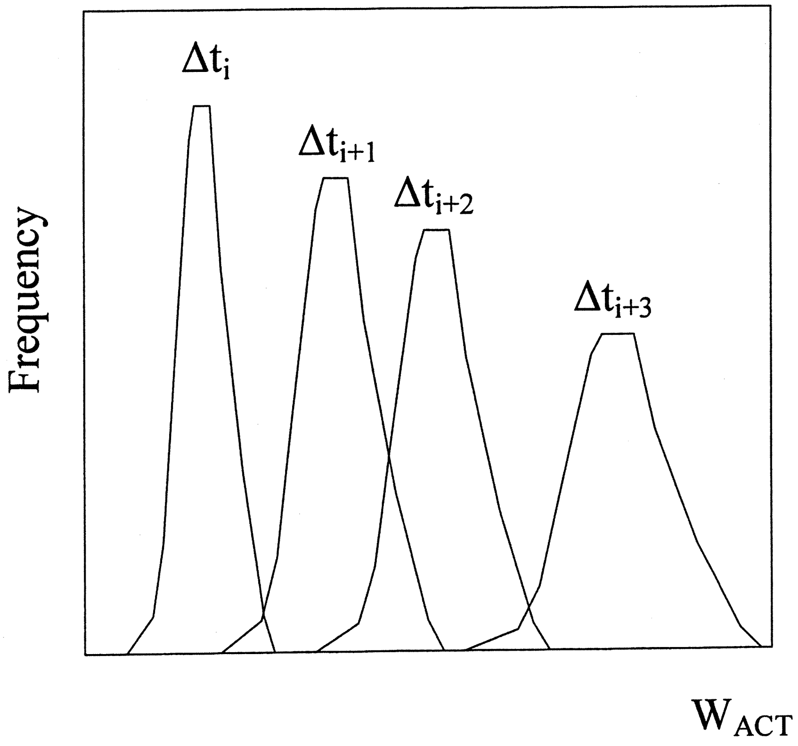

Figure 4.9: Frequency functions of W_{ACT} for different constant duration of the moisture load.

The risk for occurrence of damage D_i for duration Δt_i is then calculated by:

$$P\{D_i\} = \int_0^{W_{max}} F(W_{CR,i}) \cdot f(W_{ACT,i}) \cdot dW \qquad (4.6)$$

This calculation can be made for different damage levels D_i and for different durations Δt_i. This gives an indication of the total risk of moisture induced damage.

5 SERVICE LIFE

5.1 Different types of attack

Some types of moisture induced attack are *destructive*, i.e. the attack is such that the basic function of the structure can no longer be fulfilled. Such destruction types are different types of frost attack, reinforcement corrosion, different types of chemical attack on structural materials, rot on wood. All these attacks will cause so big destruction, that the safety of the structure becomes too low. In these cases one can talk about the *service life of the structure* since the destruction will normally increase with increased exposure time.

Other types of moisture induced attack will not harm the structure itself but cause *unacceptable annoyance* to the inhabitants of the building, or to the environment. Such types of attack are emission of hazardous compounds, mould on organic materials, aesthetic decay of surfaces, etc. In these cases it is less meaningful to talk about service life of the structure or building. Instead one shall design the building in a way that such damage does not occur at any time.

5.2 Service life with regard to structural safety - principles

Service life is ended when damage has become so big that the intended function of the material, or structure, in question is no longer fulfilled. For the well-defined critical moisture condition W_{CR} of the type shown in Figure 3.1 or 3.2, service life is ended the first time W_{CR} is transgressed. The principles are illustrated by Figure 4.1. This figure shows the moisture conditions for *one single unit volume* (or *unit cell*) inside a structure, and its service life.

The service life of the *entire structure* is not ended until a larger number of unit volumes (unit cells) have become damaged. Thus, there is a difference between the "local" service life of a piece of the material, and the "global" service life of a whole structure. This is also illustrated by Figure 5.1 showing the destruction of a concrete beam.

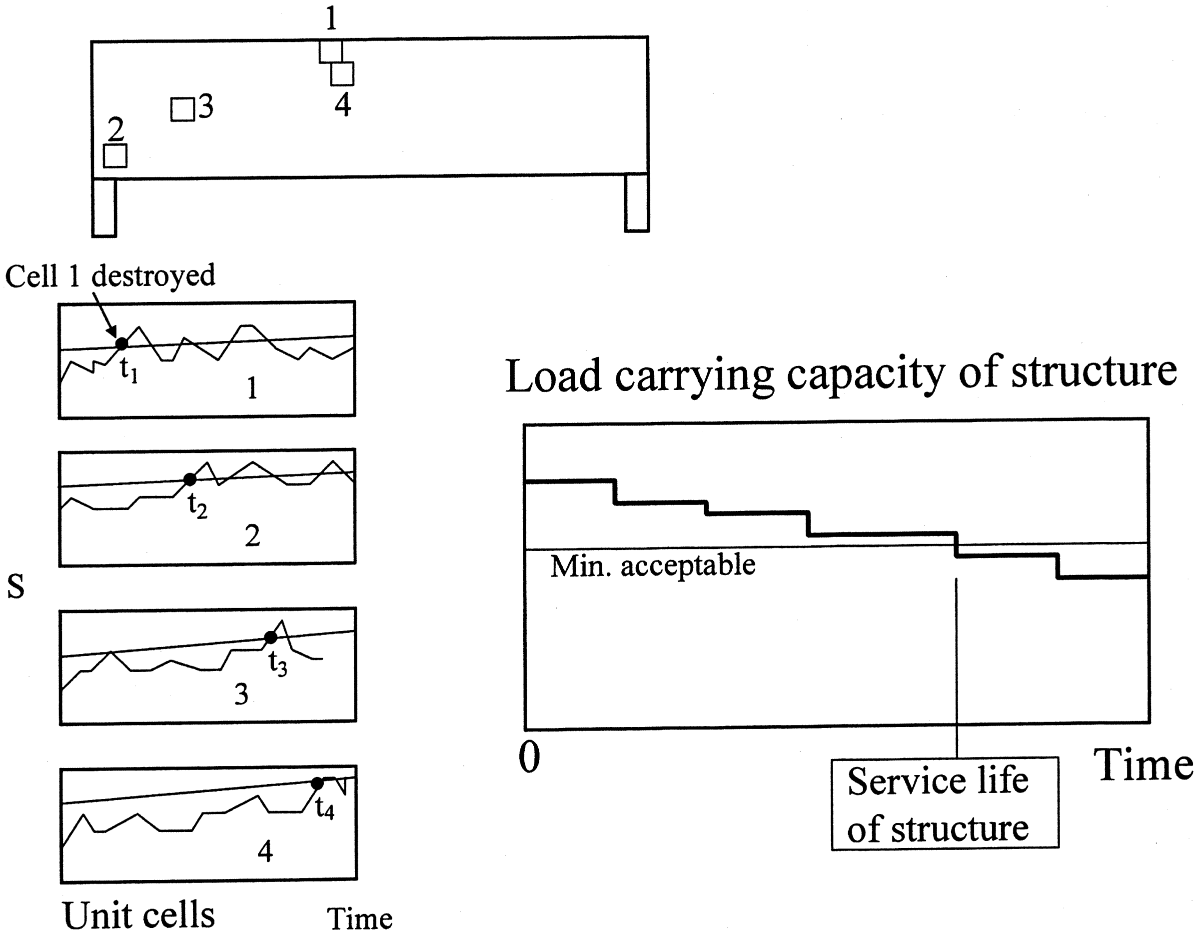

Figure 5.1: The service life of the entire structure is determined by the service life of individual unit cells inside the structure.

Each unit cell has its own service life determined by its own value of the critical moisture content W_{CR} and its own time evolution of the actual moisture content, W_{ACT}. Service life of cell 1 is ended at time t_1, which causes a certain reduction of the function (in this case load carrying capacity) of the beam. Thereafter, more and more cells are "lost", and after a certain exposure time the service life of the entire structure is ended.

The *risk* that a certain unit cell is damaged is calculated according to the principles described in paragraph 4.1 (equation (4.1)). By combining the risk for different cells, the risk of failure of the entire structure as function of exposure time can be calculated.

5.3 Representative environment - the "representative service life"

5.3.1 Principles

A precise calculation of service life requires that the moisture-time field inside the structure can be calculated (estimated) by high precision; see Figure 5.1. This also means that the future outer moisture conditions in macro- and micro-scale around the structure can be estimated by high precision, and that it is possible to translate the outer moisture-time conditions to an inner moisture-time field. This is of course not possible. Therefore, even if the critical moisture level in different parts of the structure is known, it will not be possible to calculate the true service life.

Instead of calculating the *true* service life one can calculate a sort of *representative* service life by exchanging the real complex environment by a representative environment that gives similar moisture levels in the structure as the real environment. In the following, principles and methods for calculation of the inner moisture field are presented in brief.

5.3.2 Structures only exposed to variations in RH

Some structures are only exposed to *air of varying relative humidity,* but are not exposed to free water; i.e. the moisture variations are located to the *hygroscopic range 1* defined by Figure 1.1. The relative humidity has an annual variation that can be estimated from climate statistics, combined with information on other moisture sources, like moisture emanating from indoor activities. In such cases the real complex environment might be exchanged for a representative environment that is supposed to give about the same internal moisture field (RH-field) as the real environment. The principles are illustrated in Figure 5.2.

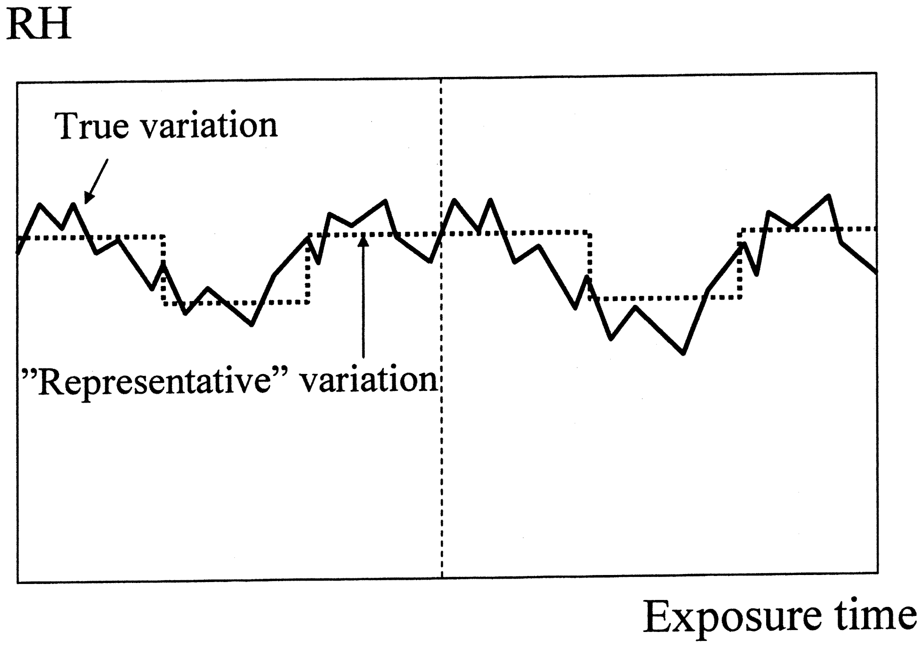

Figure 5.2: Structures only exposed to variations in outer RH. Real RH-variation and representative RH-variation.

The translation of the external representative environment to the internal environment can be made by means of traditional moisture mechanics, provided the sorption isotherm and the moisture transport coefficient of the material are known. For Portland cement concrete, sorption isotherms are given in (Nilsson 1997) and transport coefficients as function of RH given in (Hedenblad 1993). Transport data for other materials are given in (Hedenblad XXX). Sorption isotherms for other materials are given in (Ahlgren 1972).

Moisture transport is calculated by:

$$q = -\delta_c \cdot dc/dx \qquad (5.1)$$

Where q is the moisture flux ($kg \cdot m^{-2} \cdot s^{-1}$), dc/dx is the water vapour gradient ($kg \cdot m^{-3} \cdot m^{-1}$). δ_c is the water transport coefficient ($m^2 \cdot s^{-1}$). The vapour concentration c ($kg \cdot m^{-3}$) is proportional to the relative humidity; $c = c_0 \cdot RH$ where c_0 is the concentration of saturated vapour.

Figure 5.3 shows examples of calculated moisture-time fields for a concrete exposed to a certain step-wise variation of the outer RH between 60% and 95% (Fagerlund & Hedenblad 1993) The effect of other types variations can be calculated in the same manner, using the same material data. In order to find the representative environment, comparisons can be made between really measured RH in some structures and calculated RH for different simulated outer RH-variations.

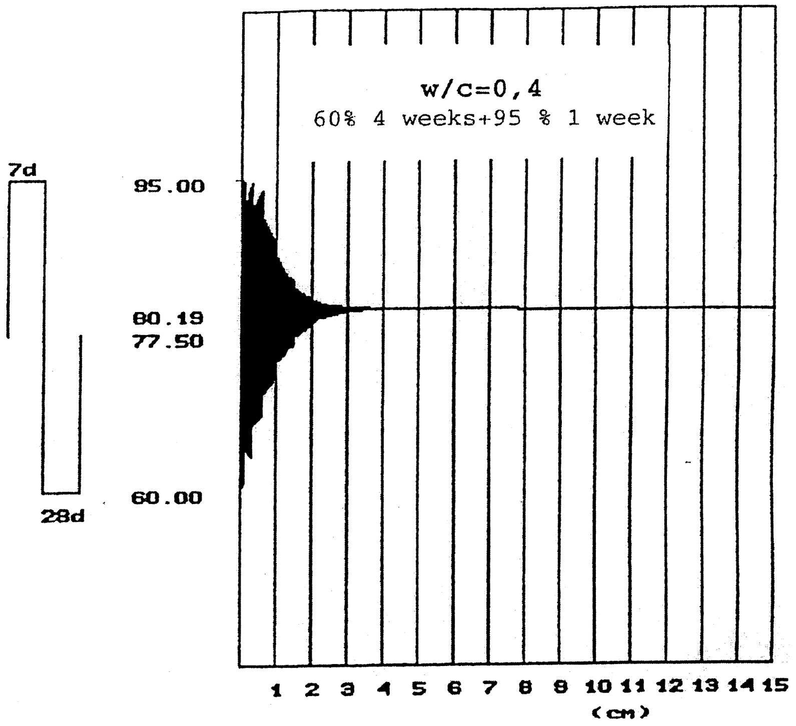

Figure 5.3: Concrete with w/c-ratio 0.40 exposed to a cyclic variation in outer RH between 60% and 95%.

5.3.3 Structures sometimes exposed to liquid water

When the structure is *intermittently exposed to free water,* like rain, melting snow, sea water splash etc., a representative environment involving both the *hygroscopic range 1* and the *capillary range 2* defined by Figure 1.1 can be used. Cyclic variations in RH below 100% are interrupted by periods of water suction. See Figure 5.4.

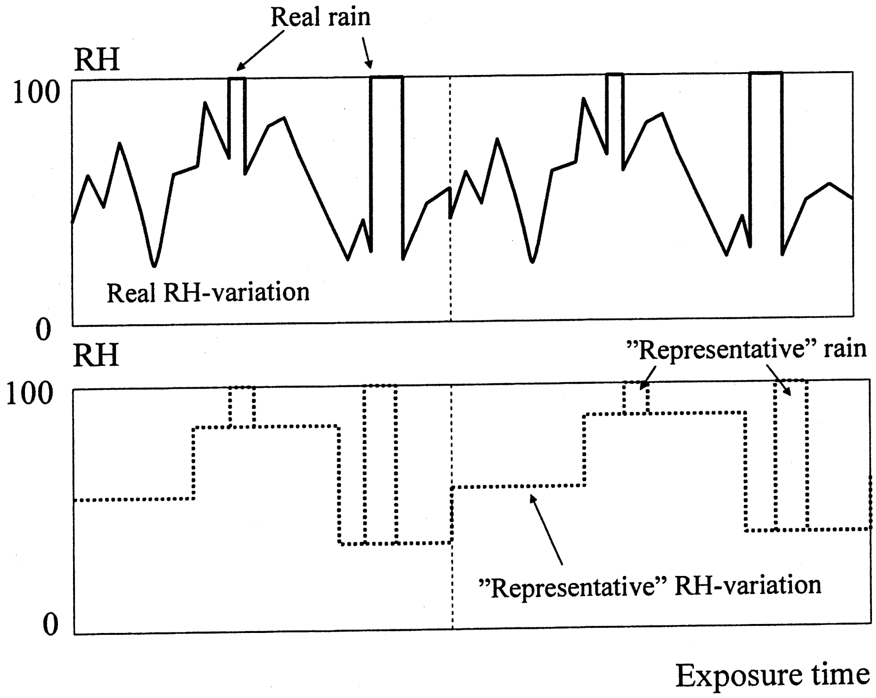

Figure 5.4: Structures exposed to variations in outer RH with intermittent rain. Real RH-variation and representative RH-variation.

It is considerably more complex to translate this type of moisture variation to an internal moisture-time field in the structure, since the material data at the very high moisture levels reached at exposure to free water are unknown for most materials. Both the capillary equilibrium curve (see Figure 1.1) and the moisture diffusivity in the capillary range must be known. Experimental methods that can be used are described and used in (Janz 2000) and (Johansson 2005).

Calculation of moisture transport within the capillary range can be made in the same manner as for the hygroscopic range; equation (5.1). As driving potential it is however more convenient to use the *capillary under-pressure* ("suction") Δp instead of the vapour concentration c.

$$q = \delta_{\Delta p} \cdot d(\Delta p)/dx \qquad (5.2)$$

Where $\delta_{\Delta p}$ is the transport coefficient (s), and $d(\Delta p)/dx$ is the capillary pressure gradient ($Pa \cdot m^{-1}$).

Equation (5.2) is equivalent to equation (5.1). The relation between Δp and c is, see equation (1.1):

$$\Delta p = -K \cdot \ln(c/c_0) = -K \cdot (\ln c - \ln c_0) \tag{5.3}$$

Where the constant $K = R \cdot T/v_w$ (Pa), where R is the gas constant (8.314 $J \cdot mole^{-1} \cdot degree^{-1}$), T the absolute temperature, and v_w the molar volume of water ($18 \cdot 10^{-6} m^3 \cdot mole^{-1}$). At +20C $K = 1.35 \cdot 10^8$ Pa.

The relation between the transport coefficients $\delta_{\Delta p}$ and δ_c is:

$$\delta_{\Delta p} = (c/K) \cdot \delta_c \tag{5.4}$$

Thus, moisture transport coefficients δ_c determined within the hygroscopic range (RH<98%) can be transformed to transport coefficients to be used in equation (5.2). This can therefore be used over the entire moisture range. The sorption isotherm has to be transformed to a capillary absorption curve. This is made by the Kelvin equation (1.1).

A calculated moisture field in the same concrete as in Figure 5.3, but this time exposed to 7 days rain alternating with 7 days drying periods at 60% RH, is shown in Figure 5.5 (Fagerlund & Hedenblad 1993).

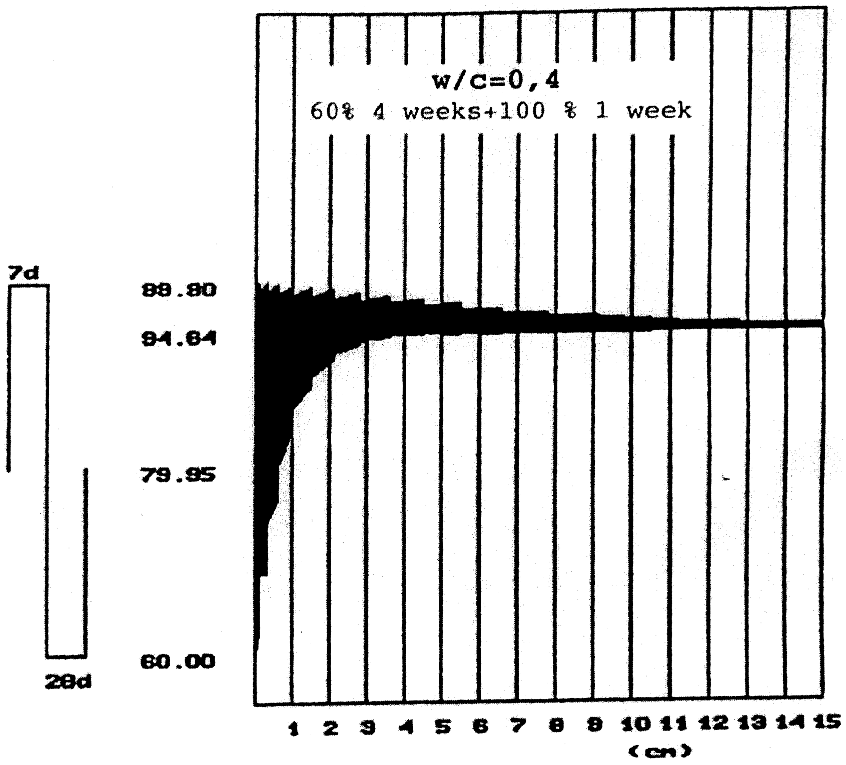

Figure 5.5: Concrete with w/c-ratio 0.40 (same as in Figure 4.3) exposed to cyclic variation of 7 days rain and 7 days at 60% RH.

After calculation, the moisture-time field can be compared with the critical moisture level in order to find the risk of damage after different exposure times.

The concept "representative environment" has been used for carbonation of steel in concrete. The carbonation rate depends on the moisture level in the concrete cover. Carbonation is reduced with increased moisture level, since water blocks the inflow of carbon dioxide. Thus, concrete *exposed to rain* is likely to have a lower carbonation rate than concrete *protected from rain*. Figure 5.6 shows a *service life diagram* based on this idea (Tuutti 1982). Structures are divided in these two moisture groups. The lines (depth versus square-root of time in log-log scale) describe the expected carbonation depth as function of time. The lines for the group "protected from rain" give the shortest service life.

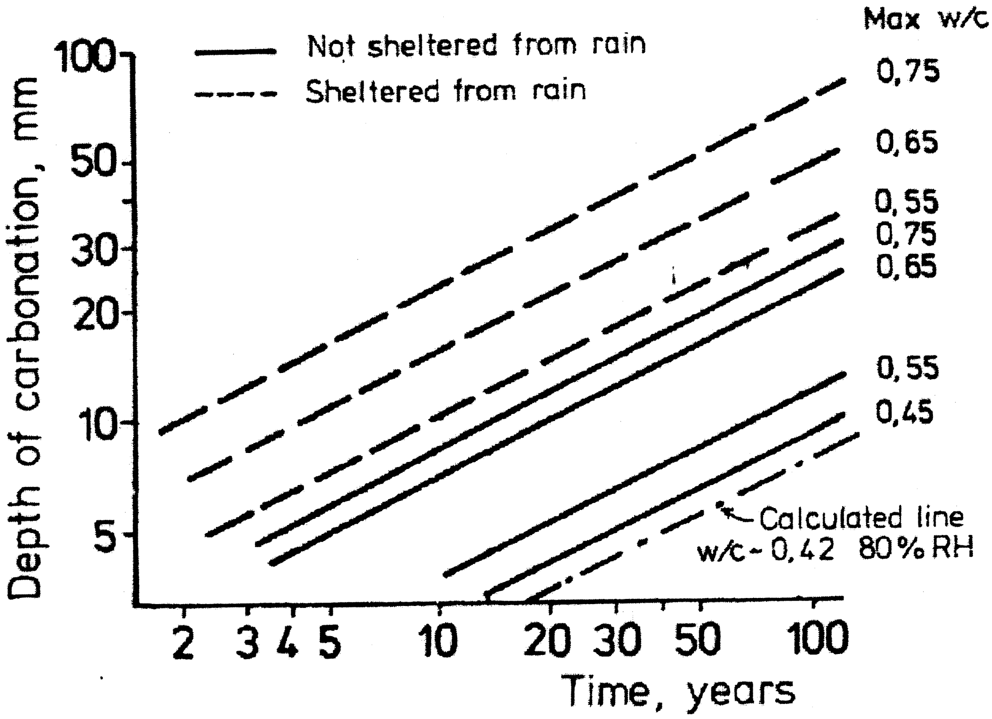

Figure 5.6: Carbonation of concrete with different quality and in different environment.

5.3.4 Structures permanently, or for long periods, exposed to liquid water

Structures permanently sucking water, like structures founded below the ground water level, or in sea water, or certain hydraulic structures, will slowly take up water in the *over-capillary range 3* as illustrated by Figure 1.2. The rate of water absorption is determined by the rate of dissolution of air in coarse pores like air-pores in concrete or air-pockets ("non-permeable open pores") in ceramic materials. Examples of such pores are given in Figure 5.7.

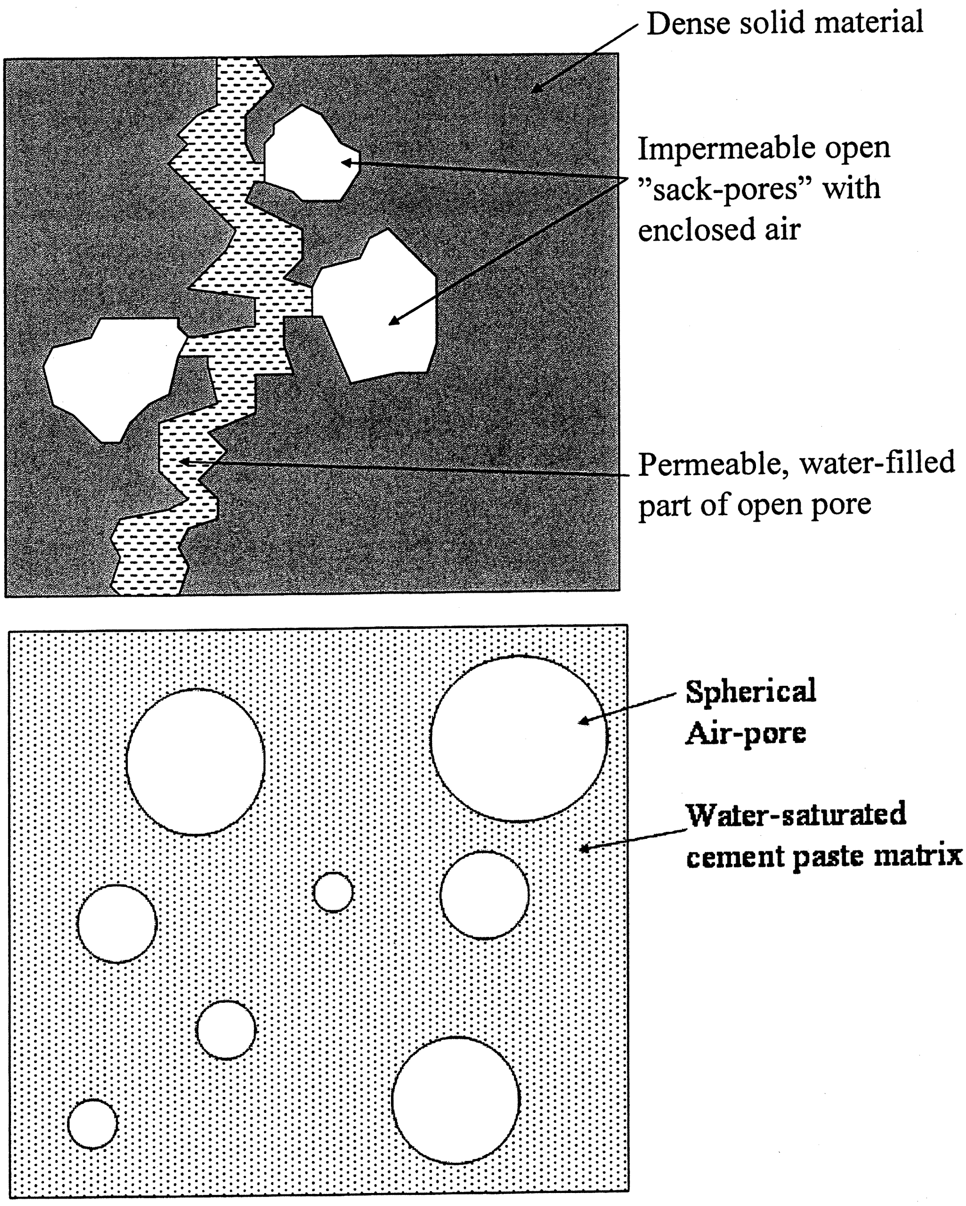

Figure 5.7: Examples of non-permeable open pores

Air can also be enclosed by the mechanism illustrated by Figure 5.8. In a straight pore with varying pore diameter, sucking water from one end, the entire pore will become easily water-filled. In a real material, coarse parts of the pore is surrounded by numerous bifurcation pores. If the coarse part of the main pore has a diameter above about 1 μm and the bifurcation pore is much smaller (<0.1 μm), an air-bubble will be enclosed in the coarse part during the initial absorption process. The mechanism is described in (Fagerlund, 2004). This is the reason why air-pores in concrete are not water-filled during a capillary absorption test. The capillary pores surrounding the air pores are much smaller than 0.1 μm, while the air pores are bigger than about 10 μm.

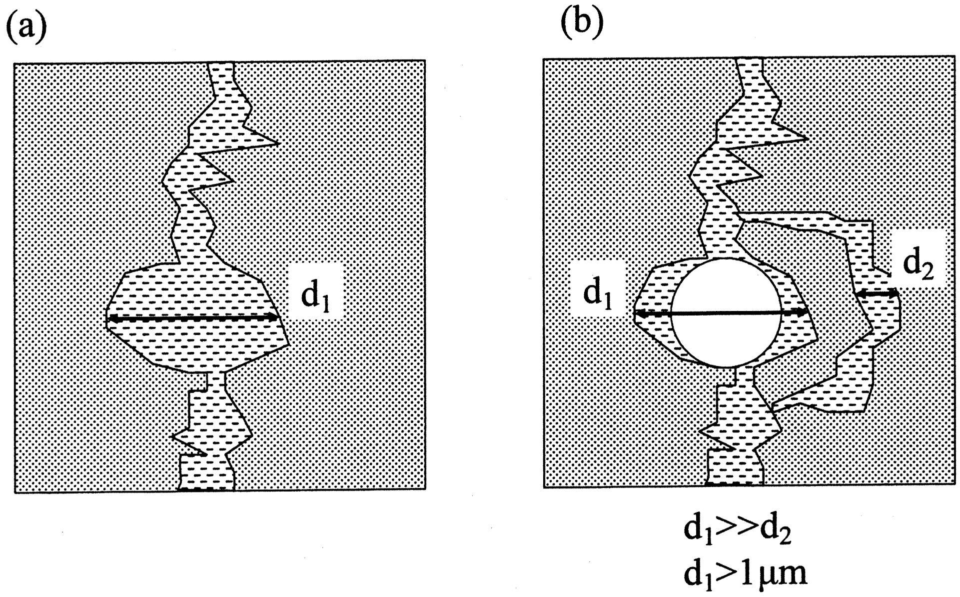

Figure 5.8: Enclosure of air-bubbles in pores with varying diameter. (a) Straight pore without bifurcation. (b) The same pore with a narrow bifurcation pore.

The primary rate-determining parameters for water absorption are; (i) the diffusivity of dissolved air within the water-filled part of the pore system, (ii) the fineness of the initially air-filled pore system. Theoretically, also the location of the unit cell inside the structure is of importance, the closer to the surface, the more rapid the absorption.

Based on a simple geometrical model for pores that are still air-filled at the breaking-point in the capillary water absorption curve (see Figure 1.2), the following expression for the time needed to completely dissolve all air in a pore with radius r and thereby fill it with water is derived in (Fagerlund 2004):

$$t \approx 9.0 \cdot 10^6 \cdot r^3 / \delta \qquad (5.5)$$

Where t is time (s), r is the pore radius (m), and δ is the diffusivity of dissolved air in the pore water ($m^2 \cdot s^{-1}$). This equation shows that the long-term absorption is quite slow. In Table 5.1 examples are given on the time needed to fill air-pores of different size.

Table 5.1: Required time to water-fill pores of different size, equation (5.5).

Pore radius (μm)	Required time	
	Diffusivity of dissolved air, δ (m^2/s)	
	10^{-11}	10^{-12}
10	15 minutes	2.5 hours
20	2 hours	20 hours
50	31 h	129 days
200	83 days	2.3 years
500	3.5 years	35 years

Thus, the absorption time needed to fill a pore is very long for coarse pores and for materials with low permeability.

The water uptake mechanism, and examples of calculated water absorption curves are described in (Fagerlund 2004).

The long-term absorption in Range 3 at un-interrupted water storage can be described by an empirical equation of the following type:

$$W=a + b(t-t_b)^c \tag{5.6}$$

Where W is the water content (kg/m^3). a, b and c are coefficients, which are different for different materials. $c<1$, which means that the water absorption in Range 3 is always retarded. t is the total absorption time, while t_b is the absorption time when capillary saturation is reached (the "breaking-point" in an absorption curve; see Figure 5.10.) Thus, the coefficient a is the absorption at the breaking-point ($t=t_b$).

An example of an experimental determination of the long-term water absorption in the same concrete as in Figure 3.3 is shown in Figure 5.9. The water content is expressed in terms of degree of saturation, S which is defined:

$$S=V_W/P \qquad 0 \leq S \leq 1 \tag{5.7}$$

Where V_W is the volume of water in the material (m^3/m^3), and P is the total open porosity of the concrete, obtained by water absorption after vacuum-treatment (m^3/m^3).

In Figure 5.9 (upper part) the initial short-term absorption is shown with time in square-root scale. In Figure 5.9 (lower part) the long term absorption from 1 day to 15 days is shown in linear scale.

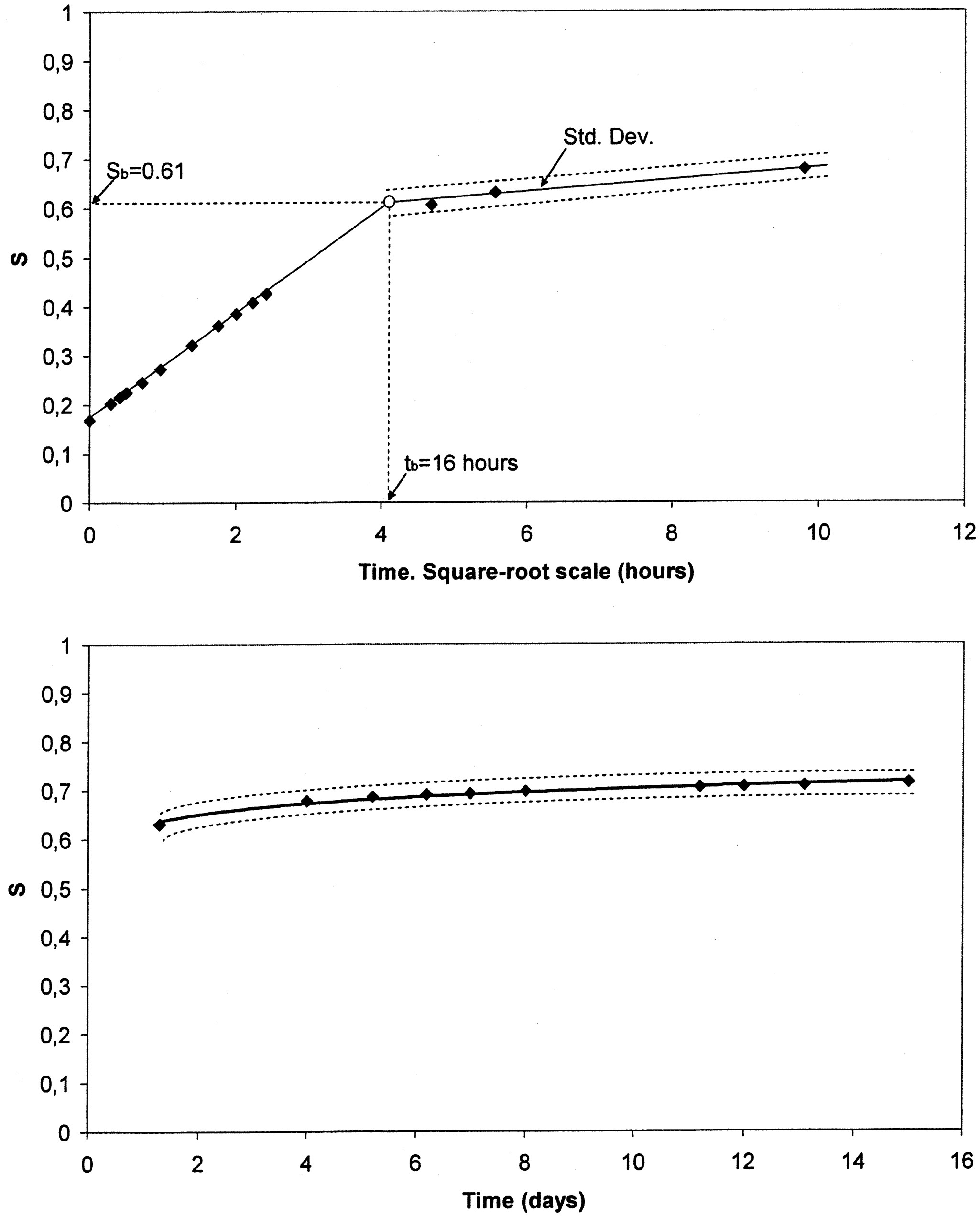

Figure 5.9: The capillary water absorption for the same concrete as in Figure 3.3.
Upper: The short-term absorption (Range 2) from 0 to 96 hours.
Lower: The long-term absorption (Range 3) from 1.3 to 15 days

The breaking-point time t_b is reached after fairly short time of absorption, compared with the total absorption time; 16 hours versus 15 days. For the long-term absorption $t-t_b$ is therefore replaced by t, which is the total absorption time from the start of absorption. Inserting $t_b=0$ and $t=0$ in equation (5.6) gives the intercept of the extrapolated long-term absorption curve on the S-axis.

The following equation describes the long-term water absorption within Range 3 with high precision:

$$S_{ACT} = 0.549 + 0.104 \cdot t^{0.17} \tag{5.6'}$$

Where the absorption time t is expressed in days. 0.549 is the extrapolated intercept of the absorption curve on the S-axis. This is not exactly the same as the absorption at the breaking-point, which is S_b=0.61. Inserting the breaking-point time 16 hours (0.67 days) in equation (5.6′) gives S_{ACT}=0.646.

5.4 Frost attack: The equivalent capillary water absorption time the "potential service life"

5.4.1 Principles

For frost exposed structures permanently or intermittently exposed to suction of water the concept *"equivalent capillary water absorption time, t_{eqiv}."* in a capillary absorption experiment can be used as a substitute to the more complex absorption in practice. This is illustrated by Figure 5.10.

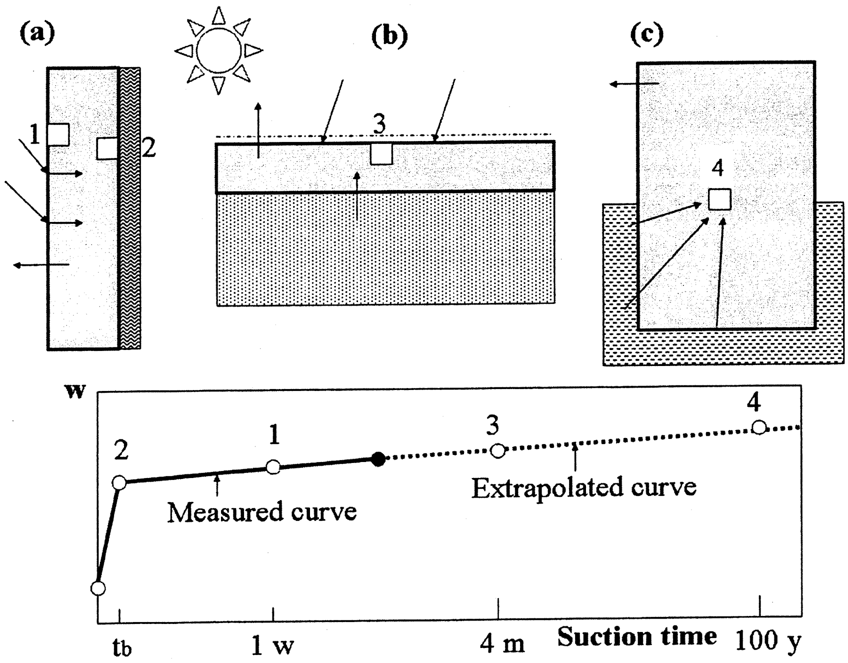

Figure 5.10: The equivalent capillary water absorption time, examples. 1-4 are different unit cells inside the structures.

The *façade element (a)* intermittently exposed to driving rain obtains a moisture level that depends on the location within the element. A unit cell at the surface (cell 1) corresponds to the breaking-point (t_b) in a capillary absorption experiment. A unit cell in the interior of the element (cell 2) might obtain somewhat higher moisture content because the drying between new rains is more restricted than at the surface. The moisture level is supposed to correspond to 1 week absorption in the experiment.

The *road surface (b)* is periodically exposed to rain, and for longer periods to melting snow. Water can be sucked up from the ground. The moisture level reached in a unit cell at the surface (cell 3) is supposed to correspond to 4 months in the absorption experiment. If this is shorter than 4 months the absorption curve has to be extrapolated according to principles described below.

The *foundation in ground water or sea water (c)* is permanently sucking water from casting until the end of its service life. Therefore, the equivalent capillary water absorption time of a unit cell in the interior of the structure (cell 4) corresponds to the required service life. The expected water content has to be found by extrapolation.

Cell 1: $t_{equiv.} = t_b$
Cell 2: $t_{equiv.} =$ 1 week
Cell 3: $t_{equiv.} =$ 4 months
Cell 4: $t_{equiv.} =$ required service life (sometimes as long as 100 years)

A capillary absorption experiment must be one-dimensional, and be performed in such a way that evaporation from the specimen is avoided; Figure 5.11. The specimen shall be as thin as practically possible in order that a well-defined breaking-point shall be obtained. It shall not be that thin, however, that it is no longer representative for the material.

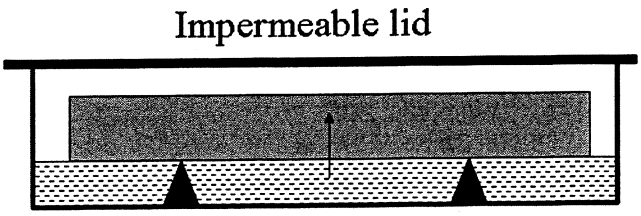

Figure 5.11: A capillary absorption experiment.

The long-term water absorption curve (after the breaking-point t_b) can normally be described by the following equation; same as equation (5.6):

$$W_{CAP}=W_b + b\cdot(t-t_b)^c \qquad (5.8)$$

Where W_b is water absorption at the breaking-point, t is the total absorption time, t_b is the absorption time at the breaking point. b and c are experimentally determined coefficients, which are different for different materials. Normally, $t \gg t_b$, therefore $t-t_b$ can be replaced by the total absorption time t.

$$W_{CAP}=A+B\cdot t^C \qquad (5.8')$$

Comparison of the absorption curve with the critical water content gives a quantitative measure of the potential service life. The calculation can be *deterministic* giving one single value of the mean service life, or it can be *stochastic* giving also the spread in service life.

5.4.2 Deterministic potential service life

Equation (5.8′) is used for extrapolation in order to find a potential mean service life, $t_{life,pot}$. This is reached when the capillary water absorption W_{CAP} reaches the critical value W_{CR}:

$$W_{CAP}(t_{life\ pot}) = W_{CR} \tag{5.9}$$

Using equation (5.8′) gives:

$$t_{life,pot} = [(W_{CR}-A)/B]^{1/C} \tag{5.10}$$

Example

The *mean* potential service life is calculated for the concrete in Figure 3.3 and 5.9. The following data are valid:

Figure 3.3: $S_{CR,\ mean}=0.905$

Figure 5.8: $S_{ACT,mean}=0.549+0.104\cdot t^{0.17}$ with t in days

The mean potential service life is:

$$t_{life,pot}=[(0.905-0.549)/0.104]^{1/0.17} = 1390 \text{ days } (3.81 \text{ years})$$

Thus, it is 50% chance that the concrete can stand almost 4 years of continuous water absorption before it is hurt by frost.

The 4 years in the example above is the *mean* service life. In reality, both S_{CR} and S_{ACT} are afflicted with uncertainties causing a certain spread in the calculated service life. Thus, it is a risk that the concrete can be damaged also after shorter absorption time than 4 years. This is treated in the next paragraph.

5.4.3 Stochastic potential service life

In reality, both the critical moisture content and the capillary absorption are subject to certain variations. Therefore, the potential service life will depend on the acceptable risk of damage. The principles are shown in Figure 4.5. Two examples are given below

Example 1

The splash zone of a concrete foundation in sea water and exposed to freezing and thawing. The moisture content is expressed in degree of saturation S ($0 \leq S \leq 1$). The hypothetical time variations of S_{CR} and S_{CAP} are shown in Figure 5.12.

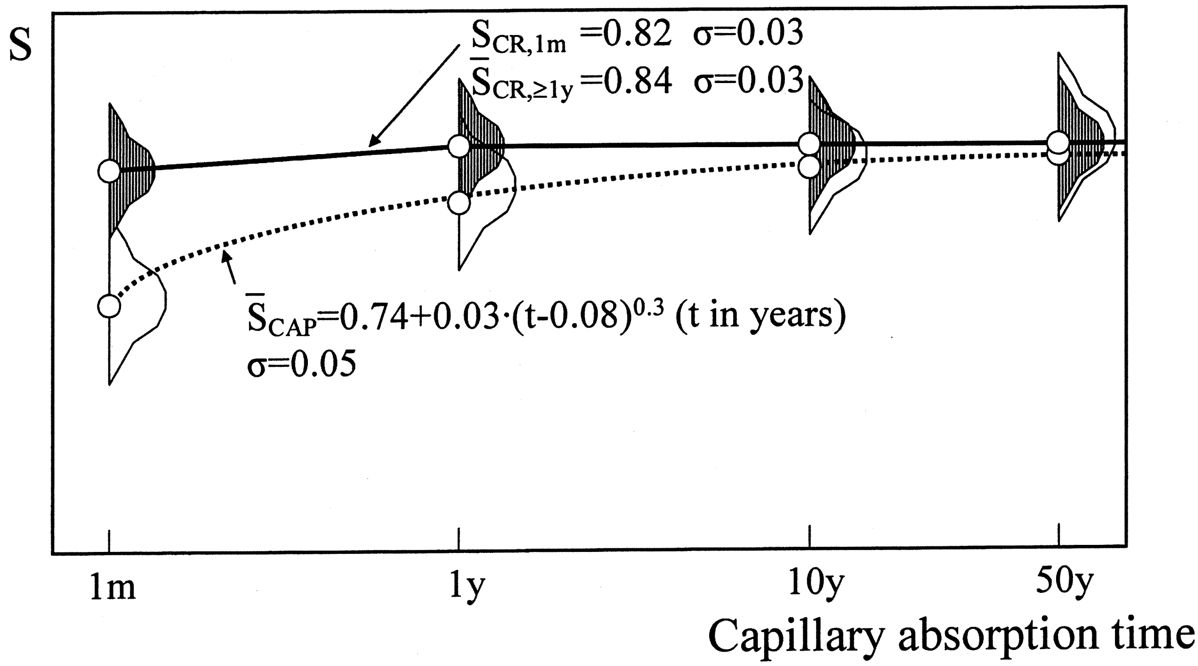

Figure 5.12: Time variations of S_{CR} and S_{CAP}.

The *critical degree of saturation* is supposed to increase with time.

Time 1 month:	$S_{CR,mean}$: 0.82	Std. dev.: 0.03
Time ≥1 year:	$S_{CR,mean}$: 0.84	Std. dev.: 0.03

The *actual degree of saturation* is described by the following equation

$S_{ACT,mean}= 0.74+0.03(t-0.08)^{0.3}$ (t in years)

Std. dev.: 0.05 (independent of exposure time)

Inserting these data in equation (4.1) gives the following damage risk at different exposure times:

1 month:	8%
1 year:	11%
10 years:	23%
50 years:	46%

These data are plotted in Figure 5.13. The service life will be about 5 years if only 20% damage risk is accepted.

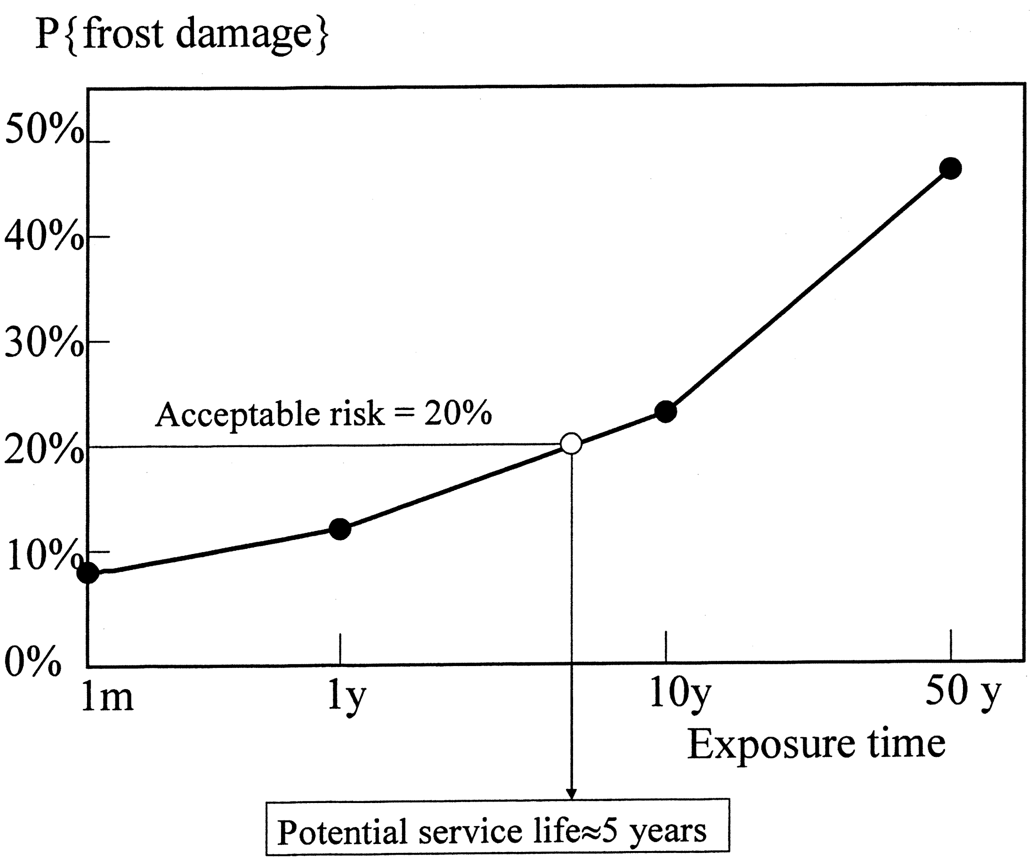

Figure 5.13: The example: Frost damage risk as function of exposure time.

Example 2

The previous example was based on hypothetical data. In the present example, really observed data will be used.

Data for the concrete in Figures 3.3 and 5.9 are used. The following mean values and spread were observed experimentally:

S_{CR}:

Mean value: 0.905

Standard deviation: 0.005

S_{ACT}:

Mean value: $0.549+0.104\cdot t^{0.17}$ (t in years)

Standard deviation: 0.040

Insertion of these data in equation (4.1) assuming S_{CR} and S_{ACT} being normal distributed gives the following damage risks for different absorption times:

1 year: 4 %
2.5 years: 30%
3 years: 38%
3.8 years: 50%
5 years: 66%
6 years: 77%

The result is also plotted in Figure 5.14. The spread in potential service life is quite high, which depends on the fairly big variation in the absorption curve. The variation in S_{CR} is very low.

The potential service life will be about 2 years if only 20% damage risk is accepted. This means that a structure built with the actual concrete will have 80% chance of survival in all situations where the un-interrupted exposure to water does not exceed 2 years. This condition is valid for all types of structures, except hydraulic structures permanently stored in water with no possibility to dry, but with possibility to freeze.

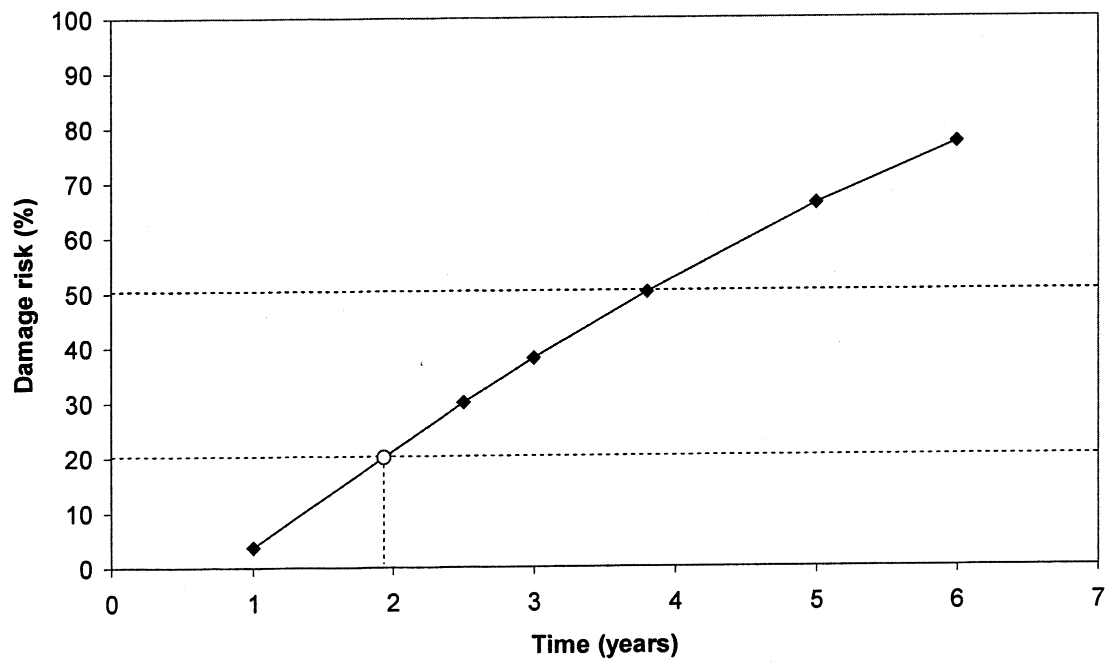

Figure 5.14: The concrete in Figures 3.3 and 5.9.
Damage risk versus water absorption time.

5.4.4 Effect of spread in S_{CR} and S_{CAP}

The spread in the values of S_{CR} and S_{CAP} will affect the frost damage risk for a given exposure time; the bigger the spread, the bigger the uncertainty in damage risk. An example is given below.

Example

$S_{CR}=0.800$

$S_{CAP}=0.730+0.007 \cdot t^{0.5}$ where t is in days

The standard variations in S_{CR} and S_{CAP} are either 0.01 or 0.03 for all exposure times.

The mean service life (50% damage risk) is calculated by equation (5.10).

$t_{life,pot}=[(0.800-0.730)/0.007]^{1/0.5}=100$ days.

The damage risk as function of exposure time is calculated by equation (4.1).The result for different combinations of standard deviations is shown in Figure 5.15.

The variation in potential service life varies between about 20 days and 65 days if only 20% risk is accepted. The effect of variation in S_{CR} is about the same as for the variation in spread in S_{CAP}.

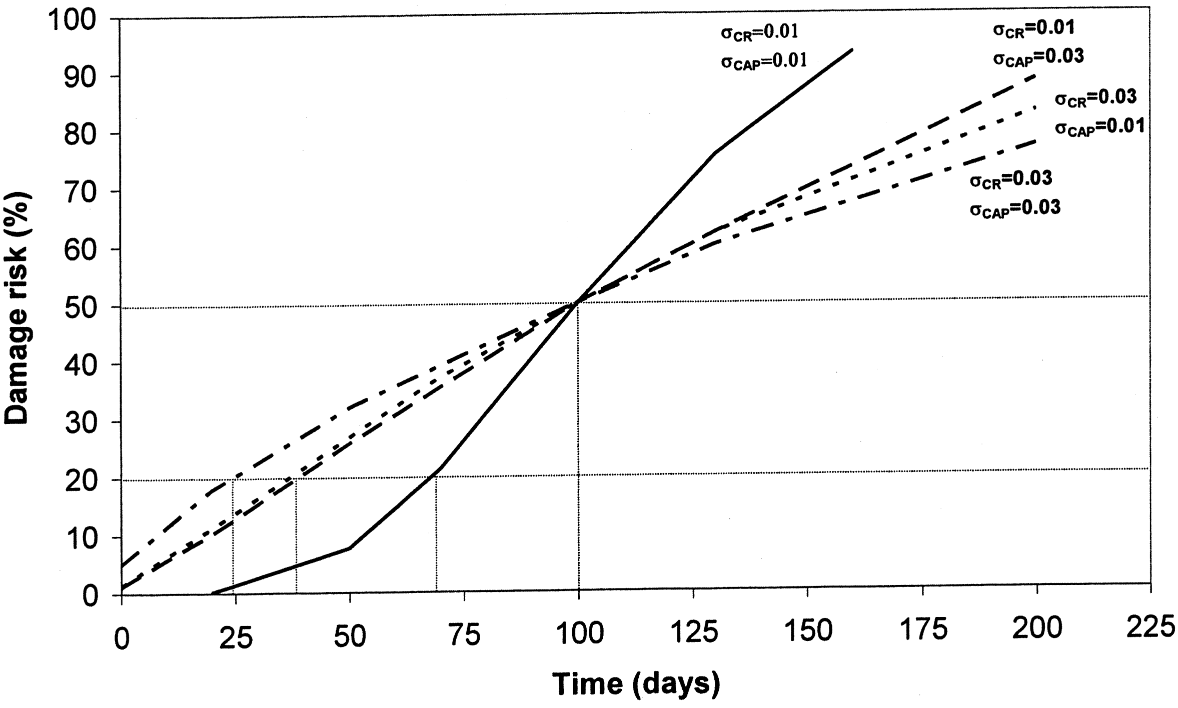

Figure 5.15: Effect of variations in S_{CR} and S_{CAP} on the frost damage risk

5.5 Moisture design with regard to service life

In order to design a structure for a desired service life, in cases where moisture is decisive for service life, the following information is required:

1. Information on the *critical moisture level* in crucial parts of the structure. Information is obtained by experiments. In rare cases the critical moisture level can also be found by theoretical calculation.

2. Information of the *future moisture-time field* in these crucial parts. Theoretical calculation, using moisture mechanics, can be used in certain cases, primarily when the critical moisture level is located to moisture range 1, i.e. the hygroscopic range. Material data for moisture fixation and moisture transport must be determined experimentally, however. Normally the concepts representative service life using representative environments, and potential service life using long-term water absorption must be used

The critical moisture level *at the desired service life* is compared with the estimated real moisture level in the selected parts of the structure. The effect of transgressions of the critical moisture level is estimated. If the moisture effect is un-acceptable other materials or material qualities must be selected until the service life is assumed to be acceptable.

The principles are shown in Figure 5.16.

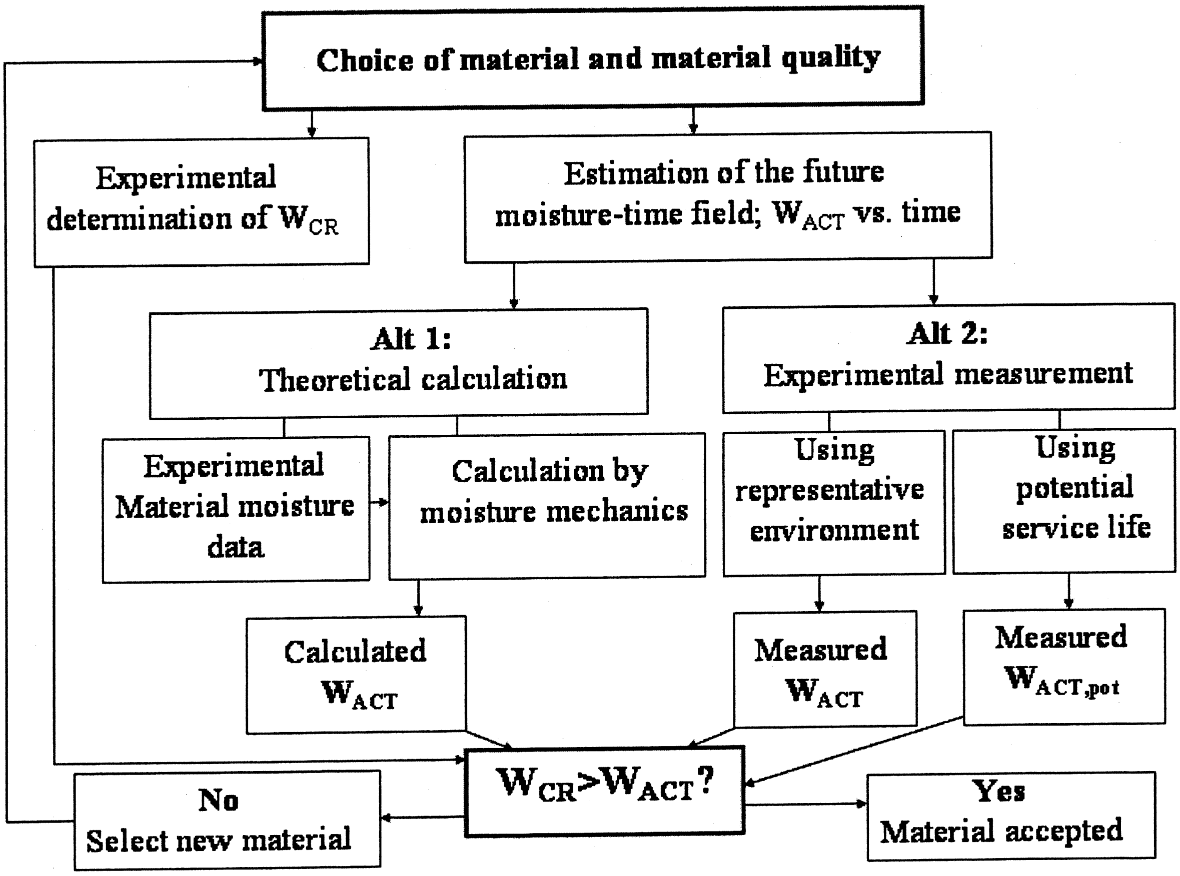

Figure 5.16: Service life design with regard to moisture induced damage - principles.

6 SERVICE LIFE WITH REGARD TO FROST DAMAGE. EXAMPLES

6.1 Principles

6.1.1 The critical water content

Frost damage is linked to well-defined critical water contents of the type illustrated by Figures 3.1 and 3.2. Examples are given above in Figures 2.1 and 3.3. Other examples for other materials will be given in this chapter.

The critical water content is determined by a few freezing and thawing cycles of a number of moisture isolated specimens that have been pre-conditioned to different moisture levels. Damage is detected as loss in E-modulus, loss in strength, permanent volume expansion, or change in any other property that is sensitive to loss in cohesion of the material. For the material in Figure 2.1, and 3.3, and for most other materials treated in this chapter, loss in dynamic E-modulus was used. Normally, the water content is expressed in terms of degree of saturation defined by equation (5.7), although any other definition can be used. The technique for determination of the critical moisture content is described in (Fagerlund 1977).

The critical water content (critical degree of saturation) is either defined as the intercept between the damage curve for water contents above the critical, and the zero-damage axis, or as the intercept between the damage curve, and the line for maximum acceptable damage (like maximum 10% loss in E-modulus). The difference between these two definitions is normally small, since the damage curve often is very "steep" for moisture levels above the critical. The two different principles of defining the critical degree of saturation are illustrated by Figure 6.1. Both the mean value and the standard deviation are determined experimentally.

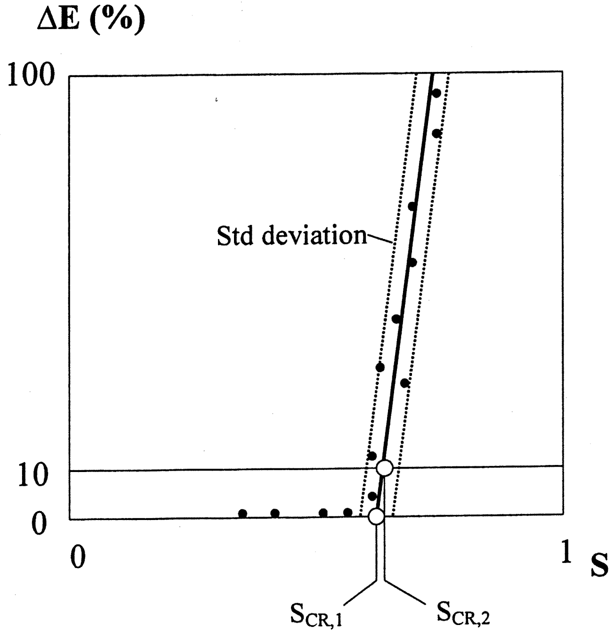

Figure 6.1: Alternative definitions of critical degree of saturation when E is used as damage criterion.

6.1.2 The actual water content

The critical water content for frost damage is almost always located to the over-capillary range defined in Figure 1.1. Since there are no reliable methods to calculate moisture transport in this area, it is not possible to theoretically calculate the water content likely to appear in the real structure. Instead, as a substitute, the long-term capillary water uptake experiment described in paragraphs 5.3.4 and 5.4 is used. Both the mean absorption curve and the standard deviation are determined.

The experimental technique is described in (Fagerlund 1977). The long-term absorption is calculated as the mean value for the whole specimen. If this is thick, the calculated water content might be underestimated for parts of the specimen close to the water surface and over-estimated for the more distant part. In (Fagerlund 2004) it is theoretically shown, however, that the long-term absorption will occur fairly homogeneously over the entire specimen thickness as long as this is not more than a few centimetres thick. This has also been confirmed experimentally (Fagerlund 1972).

The measured water absorption curve in Range 3 is extrapolated to longer times by equation (5.8) or (5.8′).

6.1.3 The frost damage risk. The potential service life

For each measured, or extrapolated, absorption time the frost damage risk is calculated by equation (4.1). In this way, the increase in the frost damage risk with increasing absorption time can be calculated according to the principles illustrated by Figure 4.5 and shown by the Examples in paragraph 5.4.3, Figures 5.13 and 5.14.

Each structure, and each part of the structure, corresponds to a certain equivalent capillary water absorption time; see Figure 5.10. Therefore, the real frost damage risk of a real structure can be assessed from the absorption results.

Also the potential service life at un-interrupted water absorption, and the spread in this, can be calculated by using the extrapolated absorption curve; see Figure 6.2.

In all calculations of the damage risk made below it is assumed that both the critical and actual moisture conditions are normal distributed.

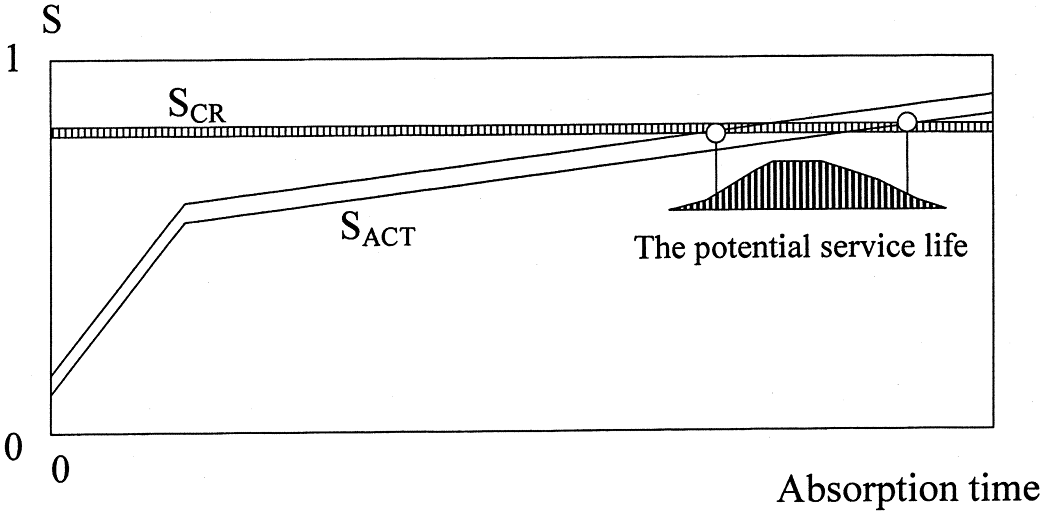

Figure 6.2: The potential service life.

6.2 Example 1; under-burnt clay brick

6.2.1 The material

Specimens, 30·30·120 mm, were produced from ordinary clay bricks that had been burnt at a lower temperature than the normal. Therefore, these bricks obtained higher porosity and higher permeability than the ordinary bricks burnt at the correct temperature (result for that material is discussed in paragraph 6.3).

The following material data are valid:

Bulk density: 1690 kg/m^3 (σ=11 kg/m^3) (σ is the standard deviation)
Total porosity: 39.5 % (σ=0.2%)

6.2.2 The critical water content

The determination of the critical degree of saturation is shown in Figure 6.3. Damage is defined by change in the dynamic E-modulus determined from the fundamental frequency of transverse vibration. If a loss in E of 10% is used as criterion the following mean value and standard deviation for the critical degree of saturation are valid:

$S_{CR,mean}$=0.850
$\sigma\approx$0.015

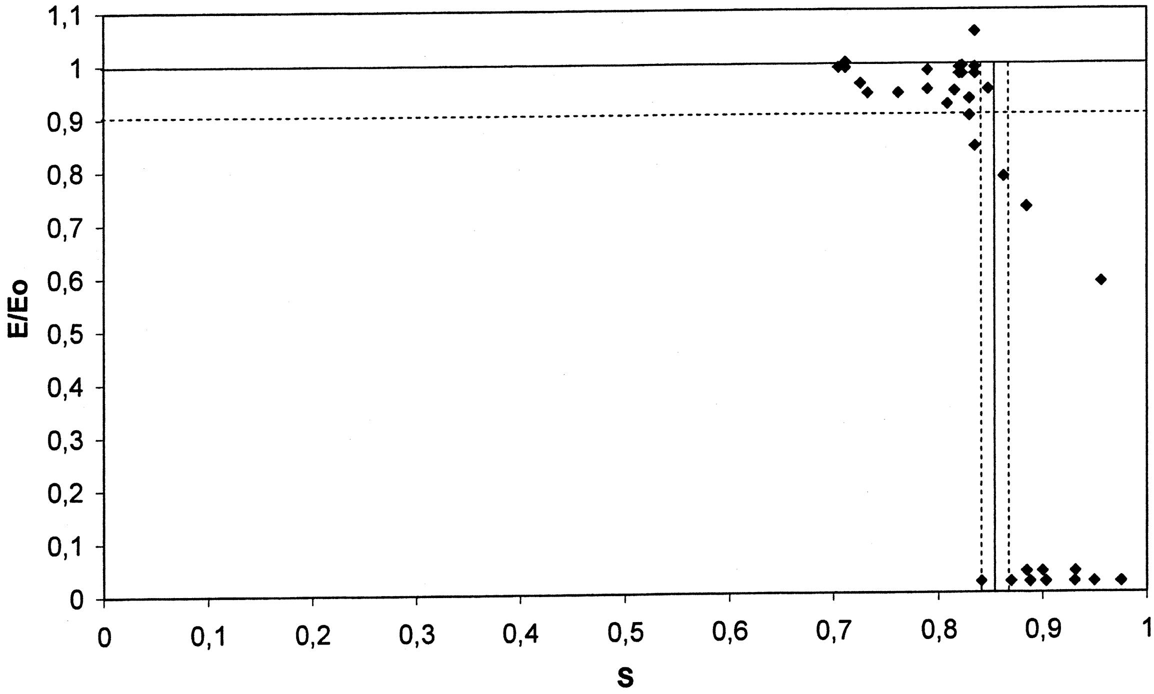

Figure 6.3: Under-burnt clay brick: Results of a determination of the critical degree of saturation.

6.2.3 The actual water content

The actual water content was determined by a 2-week capillary water uptake using the method shown in Figure 5.11. The specimen thickness was 30 mm.

The initial absorption, with a rising water front, is shown in Figure 6.4. Capillary saturation (the "breaking point" S_b) corresponds to S=0.70 ($\sigma \approx 0.007$). It occurs after an absorption time of only 13 minutes. Thus, the capillarity is very high. If the brick is used in a façade, also a very short period of rain would cause capillary saturation on a considerable depth from the surface.

$S_b=0.70$ ($\sigma \approx 0.007$)
$t_b=13$ minutes

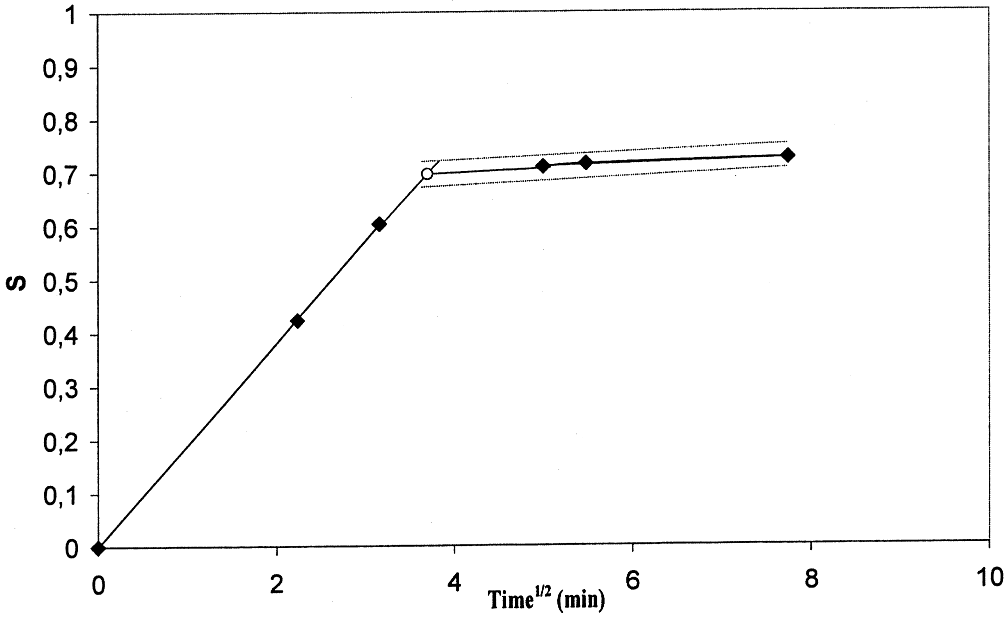

Figure 6.4: Under-burnt clay brick: Result of the determination of capillary absorption. The initial absorption with a rising water front.

The long-term absorption for t>1 day is shown in Figure 6.5. For t>1 day the degree of saturation can be described by equation (5.8′). Inserting actual data in this gives:

$$S_{ACT} = 0.747+0.0289 \cdot t^{0.55} \quad \text{t in days} \qquad (6.1)$$

$\sigma \approx 0.01$ for all t.

Inserting t_b=13 min (0.009 days) in equation (6.1) gives S_b=0.75, which is higher than the observed value, 0.70. This shows that equation (6.1) can only be used for absorption times bigger than about 1 day.

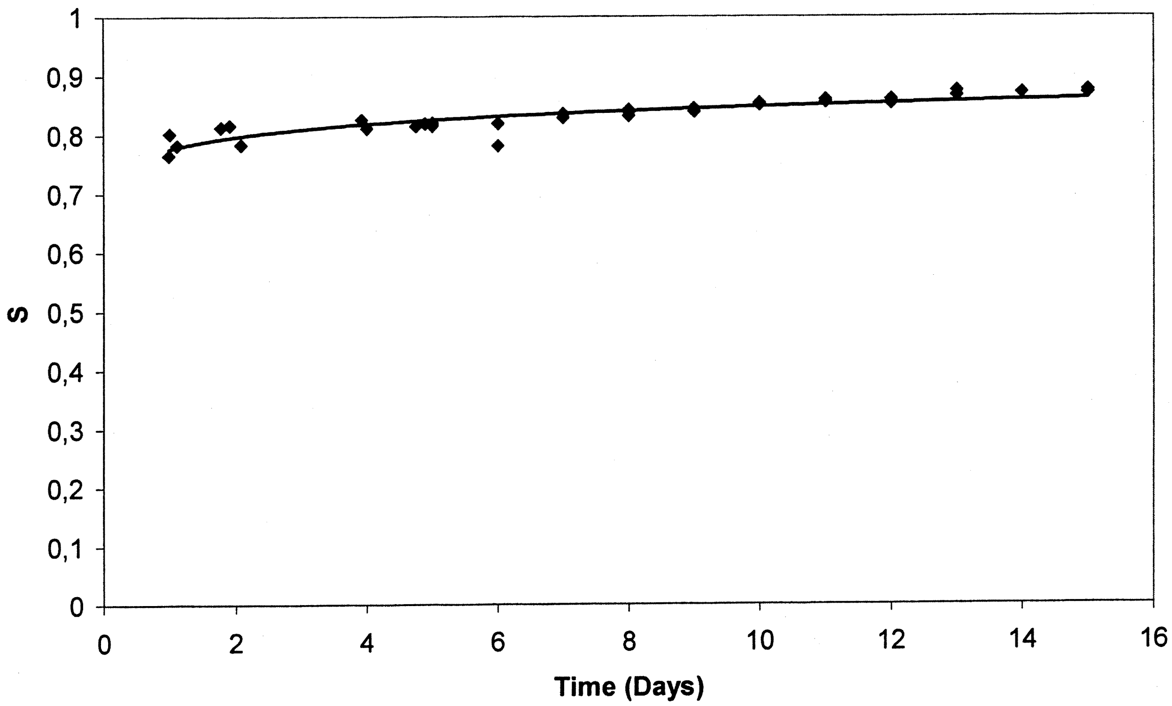

Figure 6.5: Under-burnt clay brick: Result of the determination of capillary absorption. The long-term absorption.

6.2.4 The frost damage risk and the potential service life

Deterministic calculation

The *mean* potential service life is obtained by using the mean values of the critical and actual degrees of saturation in equation (5.10).

$$t_{life,pot} = [(0.850-0.747)/0.0289]^{1/0.55} = 10.0 \text{ days} \qquad (6.2)$$

Thus, there is 50% risk that the brick cannot stand more than 10 days of continuous water absorption before it can become hurt by frost.

Stochastic calculation

A stochastic calculation of the damage risk as function of the capillary water absorption time is made by means of Equation (4.1) expressed in the following manner:

$$P\{\text{frost damage}\} = \Sigma\, F(S_{CR})\cdot f(S_{ACT}(t))\cdot \Delta S \qquad (6.3)$$

Where the functions F and f are divided in intervals of S. $F(S_{CR})$ is supposed to be independent of time. The same is also valid for all examples below.

The result of the calculation is shown in Figure 6.6. The "potential service life" is about 7 days if only 20% damage risk is accepted.

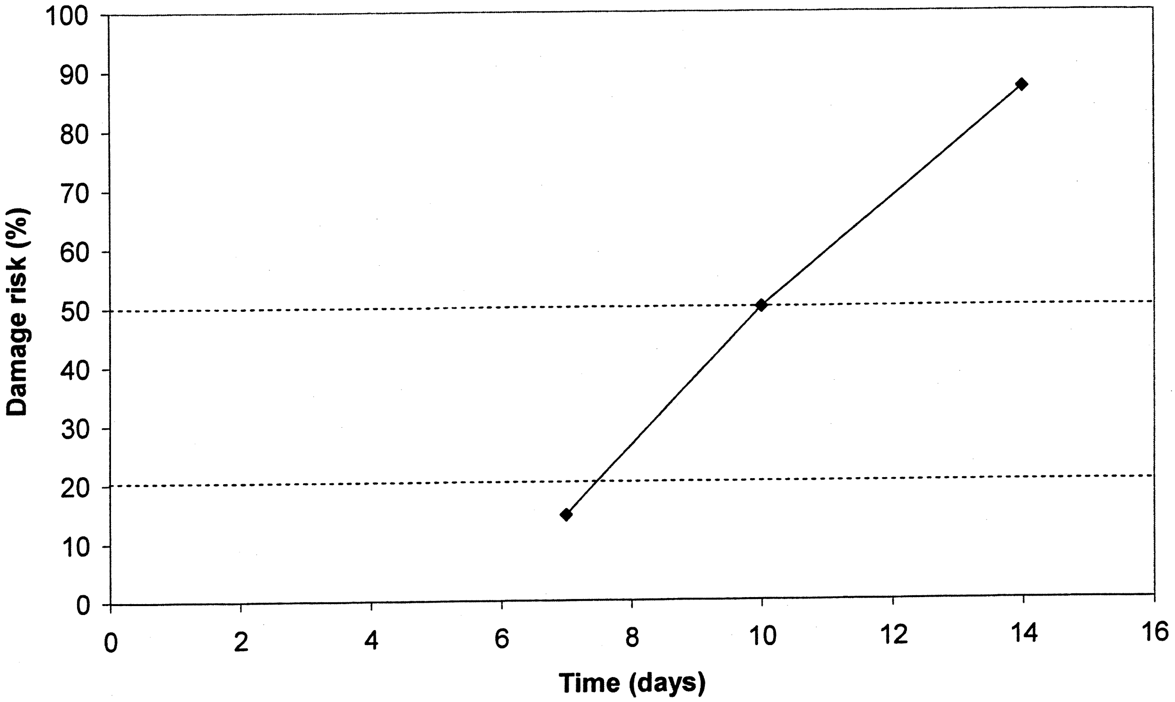

Figure 6.6: Under-burnt brick. Damage risk as function of the water absorption time.

6.3 Example 2; hard-burnt clay brick

6.3.1 The material

Hard-burnt clay bricks were produced from the same burning as was used for the under-burnt brick in paragraph 6.2. The bricks had been burnt at a heater part of the oven, which had the intended temperature. They were therefore considerably denser, and had lower porosity.

The following material data are valid:

Bulk density:	1860 kg/m^3 (σ=6 kg/m^3)
Total porosity:	31.1 % (σ=0.1%)

6.3.2 The critical water content

The results of the determination of the critical degree of saturation on specimens with size 30·30·120 mm are shown in Figure 6.7. Damage is defined by change in the dynamic E-modulus. If a maximum loss in E of 10% is used as criterion, the following mean value and standard deviation for the critical degree of saturation are valid:

$S_{CR,mean}$=0.755
$\sigma\approx$0.01

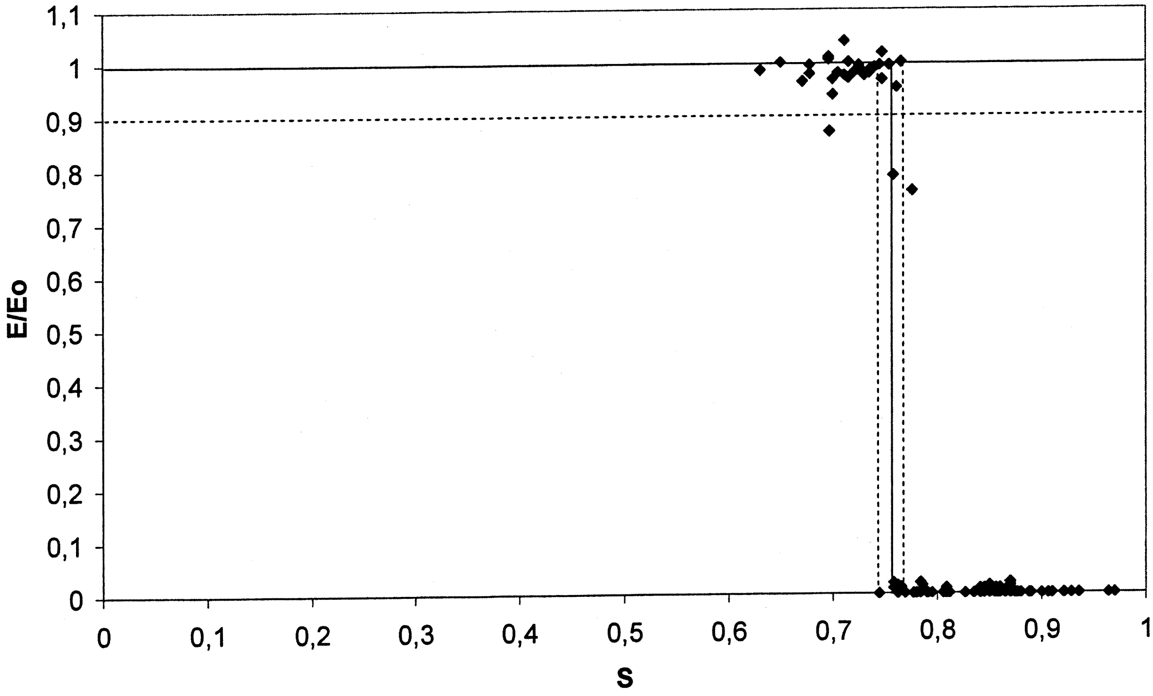

Figure 6.7: Hard-burnt clay brick: Results of a determination of the critical degree of saturation.

6.3.3 The actual water content

The actual water content is determined by a 2-week capillary water uptake by the method shown in Figure 5.11. The specimen thickness was 30 mm.

The short time absorption curve is shown in Figure 6.8. Capillary saturation is reached after 260 minutes (4.3 hours):

$S_b=0.51$ ($\sigma \approx 0.007$)
$t_b=260$ minutes

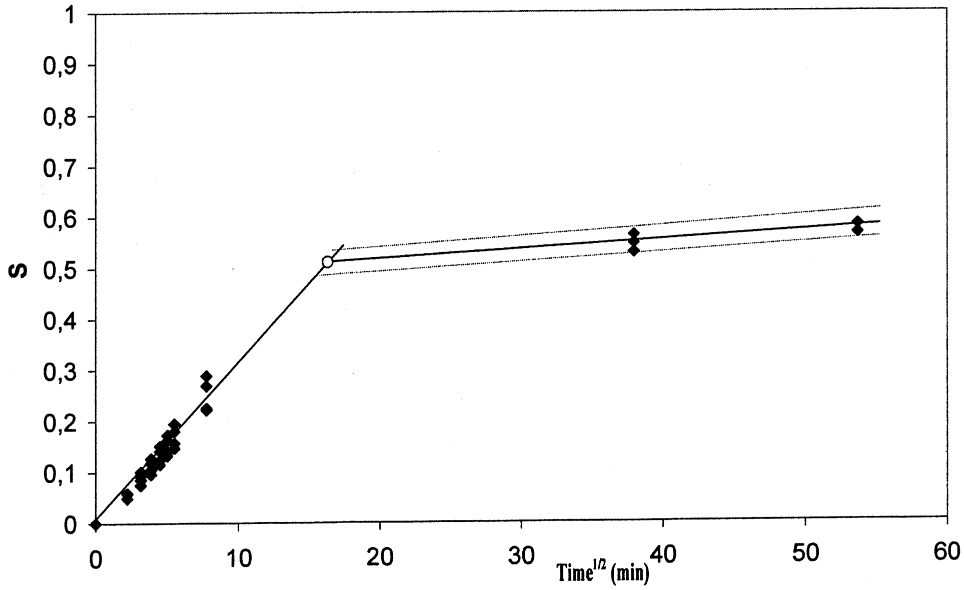

Figure 6.8: Hard-burnt clay brick: Result of the determination of capillary absorption. The initial absorption with a rising water front.

The long-term absorption is shown in Figure 6.9. For t>1 day the degree of saturation is described by:

$$S_{ACT} = 0.366+0.199 \cdot t^{0.172} \quad \text{t in days} \qquad (6.4)$$

$\sigma \approx 0.03$ for all t.

Inserting $t_b=260$ min (0.18 days) in equation (6.4) gives $S_b=0.51$, i.e. the same as the observed value. This shows that equation (6.4) can be used also for absorption times down to the breaking point in the absorption curve.

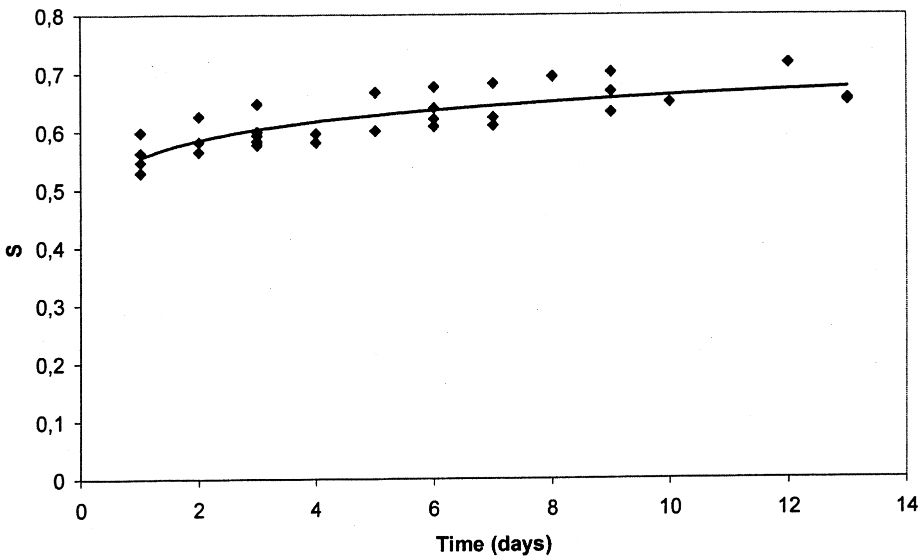

Figure 6.9: Hard-burnt clay brick: Result of the determination of capillary absorption. The long-term absorption.

6.3.4 The frost damage risk and the potential service life

Deterministic calculation

The mean potential service life is obtained by using the mean values of the critical and actual degrees of saturation in equation (5.10).

$$t_{life,pot} = [(0.755\text{-}0.366)/0.199]^{1/0,172} = 49.2 \text{ days} \qquad (6.5)$$

Thus, it is 50% chance that the hard-burnt brick can stand up to 1.5 months of continuous water absorption before it is hurt by frost.

Stochastic calculation

A stochastic calculation of the damage risk as function of the capillary water absorption time is made by means of equation (6.3). The result of the calculation is shown in Figure 6.10. The "potential service life" is 31 days if only 20% damage risk is accepted. Thus, the hard-burnt brick is considerably more frost resistant than the under-burnt brick produced from the same raw material.

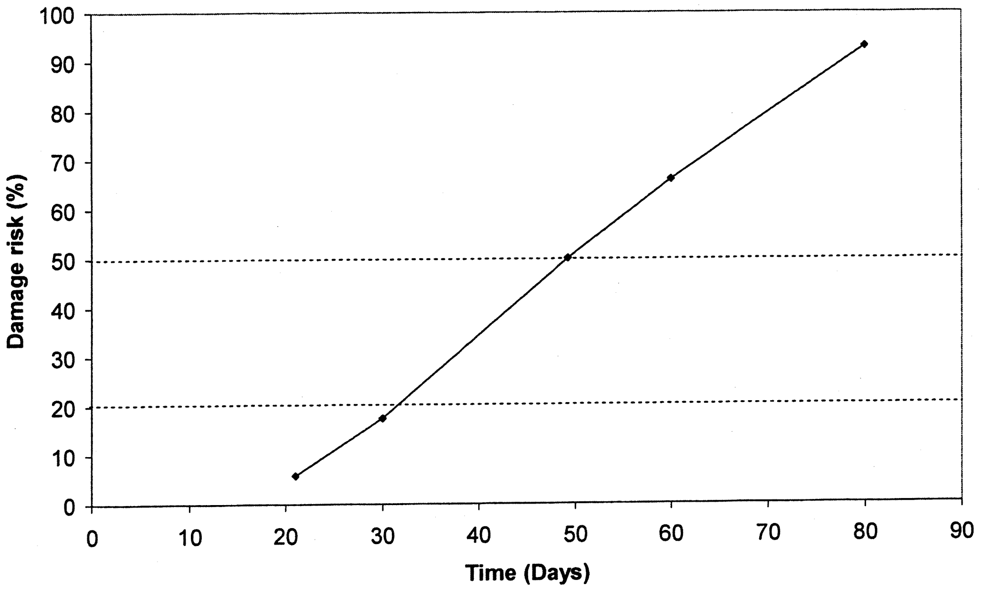

Figure 6.10: Hard-burnt brick. Damage risk as function of the water absorption time.

6.4 Example 3; autoclaved sand-lime brick

6.4.1 The material

The specimens 30·30·120 mm were prepared from factory-produced sand-lime bricks.

The following material data are valid:

Bulk density: 1840 kg/m^3 (σ=23 kg/m^3)
Total porosity: 30.9 % (σ=1.1%)

6.4.2 The critical water content

The determination of the critical degree of saturation is shown in Figure 6.11. Damage is defined by change in the dynamic E-modulus. If a loss in E of 12% is used as criterion the following mean value and standard deviation for the critical degree of saturation are valid:

$S_{CR,mean}$=0.805
$\sigma \approx 0.02$

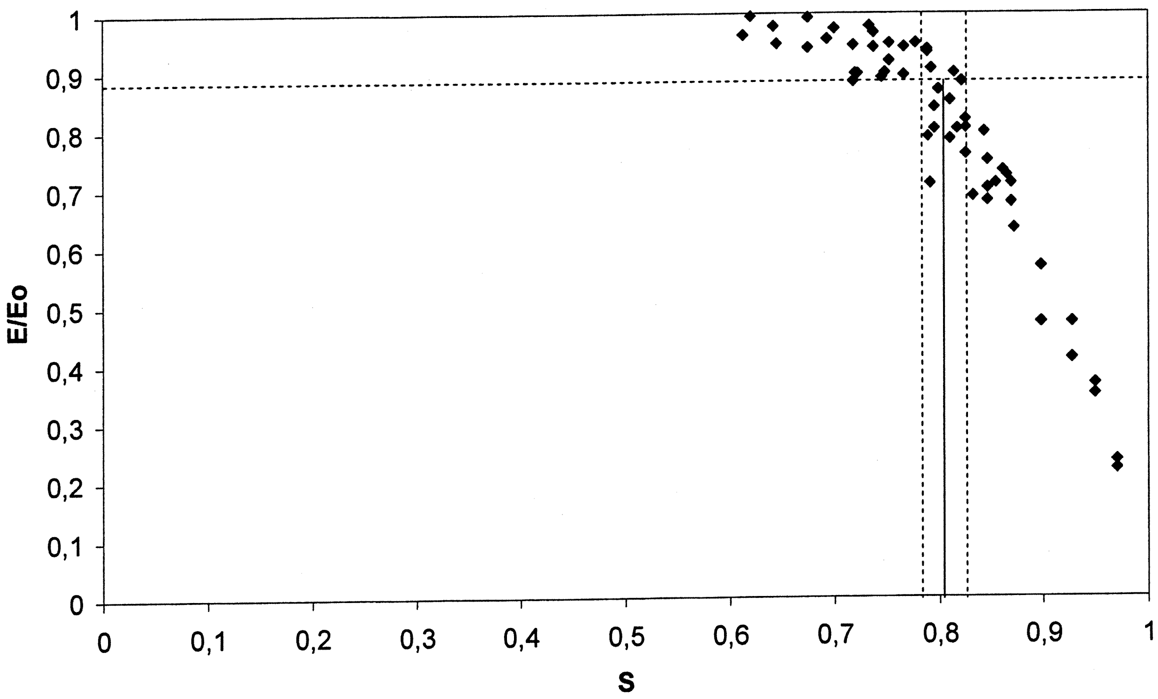

Figure 6.11: Sand-lime brick: Results of a determination of the critical degree of saturation.

6.4.3 The actual water content

The actual water content is determined by a 2-week capillary water uptake by the method shown in Figure 5.11. The specimen thickness was 30 mm.

The initial absorption curve is shown in Figure 6.12. Capillary saturation is reached after 110 minutes (1.8 hours):

$S_b=0.77$ ($\sigma \approx 0.01$)
$t_b=110$ minutes

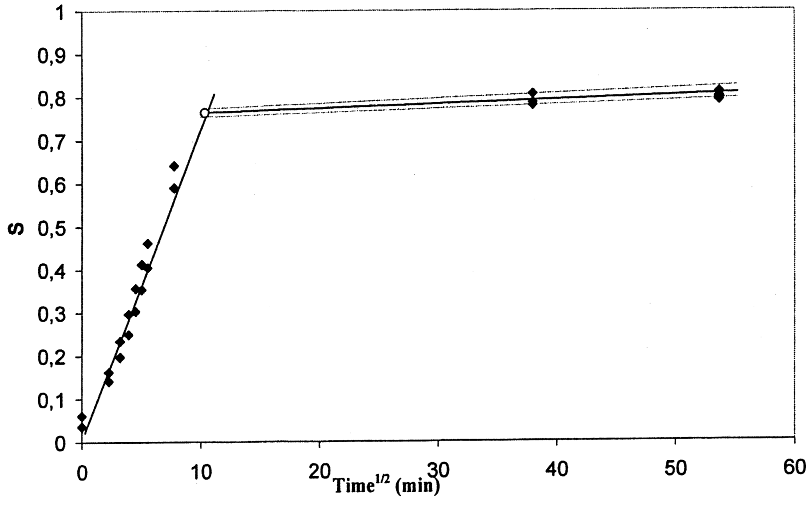

Figure 6.12: Sand-lime brick: Result of the determination of capillary absorption. The initial absorption with a rising water front.

The long-term absorption is shown in Figure 6.13. For t>1 day the degree of saturation is described by:

$S_{ACT} = 0.781+0.017 \cdot t^{0.63}$ t in days (6.6)

$\sigma \approx 0.03$ for all t

Inserting $t_b=110$ min (0.076 days) in equation (6.6) gives $S_b=0.78$, i.e. almost the same as the observed value 0.77. This shows that equation (6.6) can be approximately used for absorption times down to the breaking point in the absorption curve.

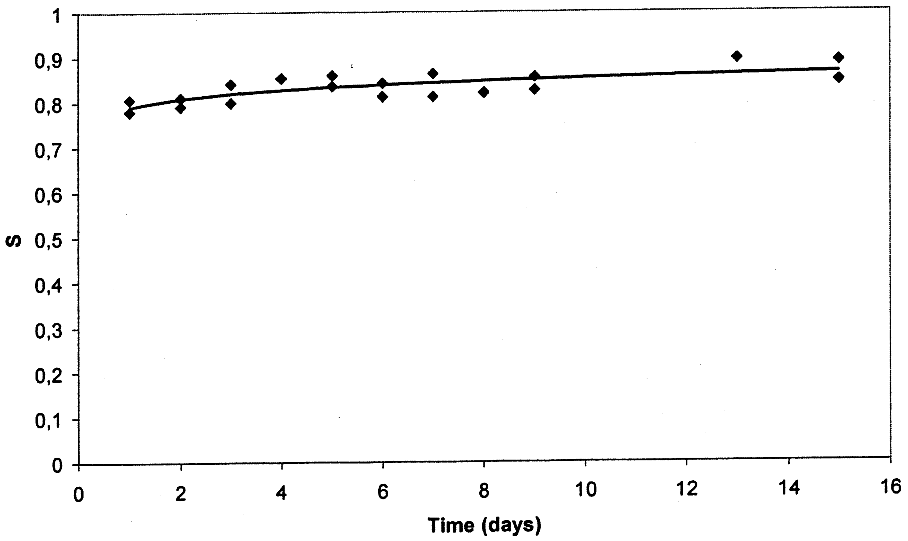

Figure 6.13: Sand-lime brick: Result of the determination of capillary absorption. The long-term absorption.

6.4.4 The frost damage risk and the potential service life

Deterministic calculation

The mean potential service life is obtained by using the mean values of the critical and actual degrees of saturation in equation (5.10).

$$t_{life,pot} = [(0.805-0.781)/0.017]^{1/0,63} = 1.7 \text{ days} \qquad (6.7)$$

Thus, there is 50% risk that the sand-lime brick can only stand 40 hours of continuous water absorption before it is hurt by frost.

Stochastic calculation

A stochastic calculation of the damage risk as function of the capillary water absorption time is made by means of equation (6.3). The result of the calculation is shown in Figure 6.14. The "potential service life" is *less than 3 hours* if only 20% damage risk is accepted. The sand lime brick therefore has lower potential service life than the under-burnt clay brick. The spread in calculated damage risk is very big and depends on the big spread in the critical and capillary degrees of saturation.

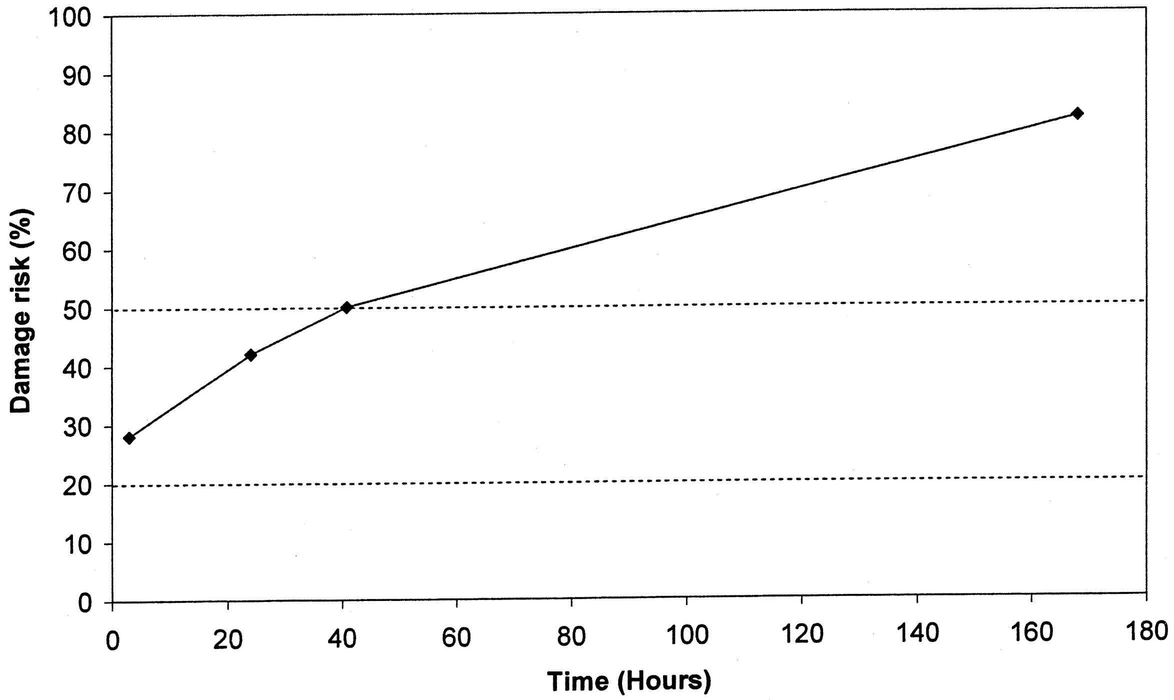

Figure 6.14: Sand lime brick. Damage risk as function of the water absorption time. (Note, the time scale is in hours)

6.5 Example 4; autoclaved cellular concrete

6.5.1 The material

The specimens 30·30·120 mm were prepared from factory-produced autoclaved cellular concrete blocks (Brand name, Ytong).

The following material data are valid:

Bulk density: 532 kg/m^3 (σ=4 kg/m^3)
Total porosity: 79.3 % (σ=0.2%)

6.5.2 The critical water content

The determination of the critical degree of saturation is shown in Figure 6.15. Damage is defined by change in the dynamic E-modulus. If a loss in E of 20% is used as criterion the following mean value and standard deviation for the critical degree of saturation are valid:

S_{CR}=0.510
$\sigma\approx$0.03

The damage level 20% is selected, since the spread in calculated E-modulus is fairly high, probably due to the fact that a slight surface spalling occurred. The dynamic E-modulus calculated from the measured fundamental frequency of vibration, is therefore afflicted with some errors, since no corrections for the weight loss and loss in moment of inertia was made. A loss in E of 20% is however not very high. The corresponding loss in strength is considerably lower.

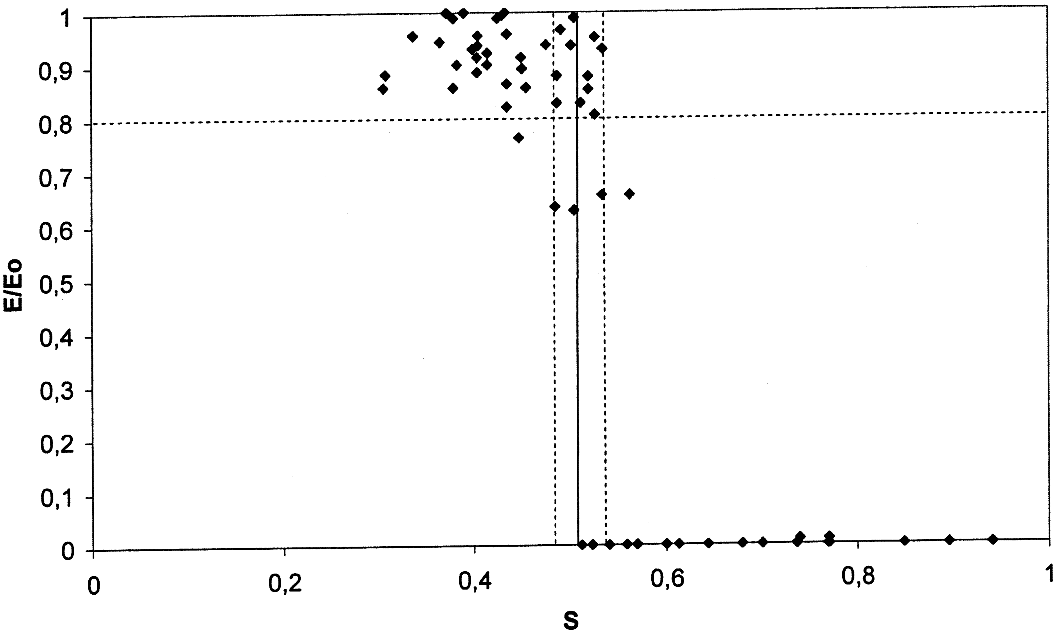

Figure 6.15: Cellular concrete: Results of a determination of the critical degree of saturation.

6.5.3 The actual water content

The actual water content is determined by a 21-week capillary water uptake by the method shown in Figure 5.11. The specimen thickness is 30 mm.

The initial absorption curve is shown in Figure 6.16. Capillary saturation is reached after 100 minutes (1.7 hours):

$S_b=0.38$ ($\sigma \approx 0.01$)
$t_b=100$ minutes

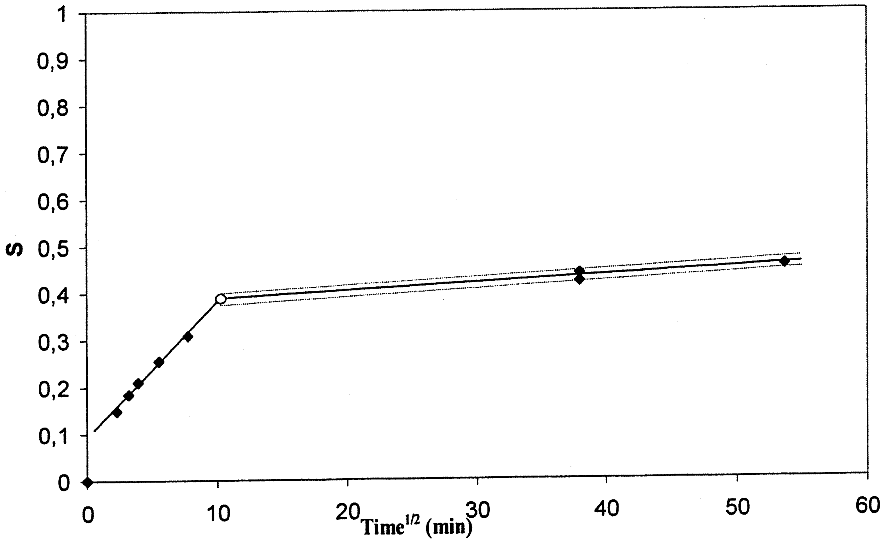

Figure 6.16: Cellular concrete: Result of the determination of capillary absorption. The initial absorption with a rising water front.

The long-term absorption is shown in Figure 6.17. For t>1 day the degree of saturation is described by:

$$S_{ACT} = 0.193+0.219 \cdot t^{0.16} \quad \text{t in days} \tag{6.8}$$
$\sigma \approx 0.03$

Inserting $t_b=100$ min (0.07 days) in equation (6.8) gives $S_b=0{,}34$ i.e. somewhat lower than the observed value. This shows that equation (6.8) can only be used down to about 1 day of absorption.

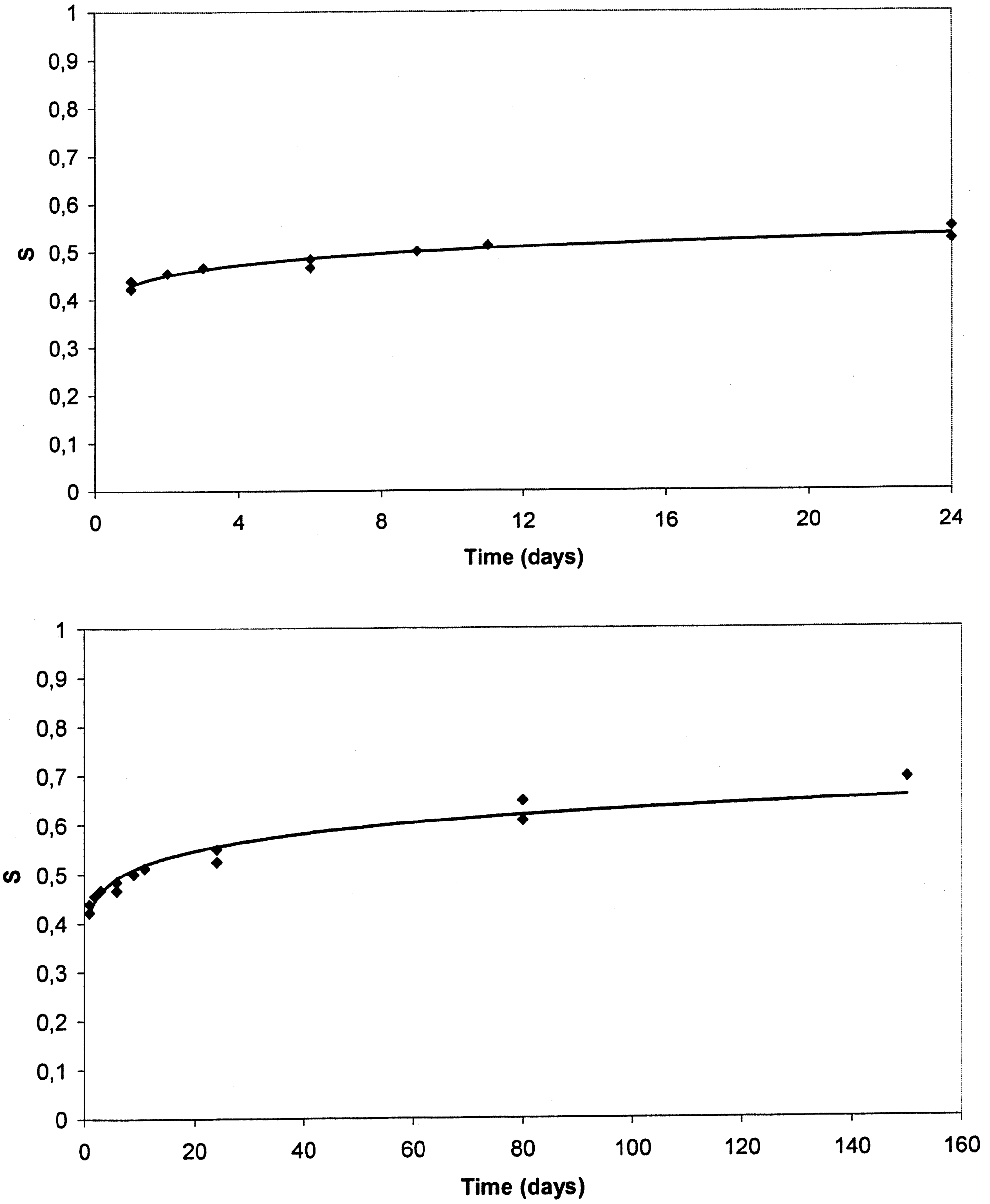

Figure 6.17: Cellular concrete: Result of the determination of capillary absorption. The long-term absorption.

Upper: Absorption between 1 day and 24 days. Lower: Absorption until 150 days.

6.5.4 The frost damage risk and the potential service life

Deterministic calculation

The mean potential service life is obtained by using the mean values of the critical and actual degrees of saturation in equation (5.10).

$$t_{life,pot} = [(0.510-0.193)/0.219]^{1/0,16} = 10 \text{ days} \qquad (6.9)$$

Thus, there is 50% chance that the cellular concrete can stand about 10 days of continuous water absorption before it can become hurt by frost.

Stochastic calculation

A stochastic calculation of the damage risk as function of the capillary water absorption time is made by means of equation (6.3). The result of the calculation is shown in Figure 6.18. The "potential service life" is about 4.5 days if only 20% damage risk is accepted.

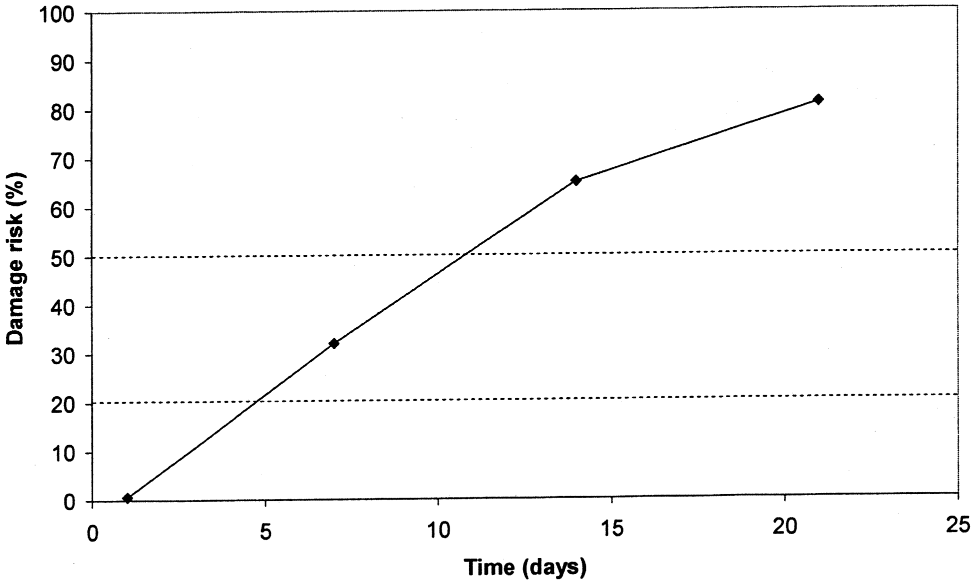

Figure 6.18: Cellular concrete. Damage risk as function of the water absorption time.

6.6 Example 5; non-air-entrained concrete (w/c 0.50, 2.1% air)

6.6.1 The material

Cylinders with diameter 10 cm and length 20 cm were cast of non-air-entrained concrete with w/c-ratio 0.50 and cement content 380 kg/m^3. The degree of hydration at start of the test was about 70%.

The following material data are valid:

Porosity:	14.6% (σ=0.01%)
Air in fresh concrete:	2.1%
28-day strength:	56.3 MPa

6.6.2 The critical water content

The determination of the critical degree of saturation was made on the cylinders. The result is shown in Figure 6.19. If a loss in E of 10 % is used as criterion the following mean value and standard deviation for the critical degree of saturation are valid:

$S_{CR,mean}$=0.905

$\sigma \approx$0.010

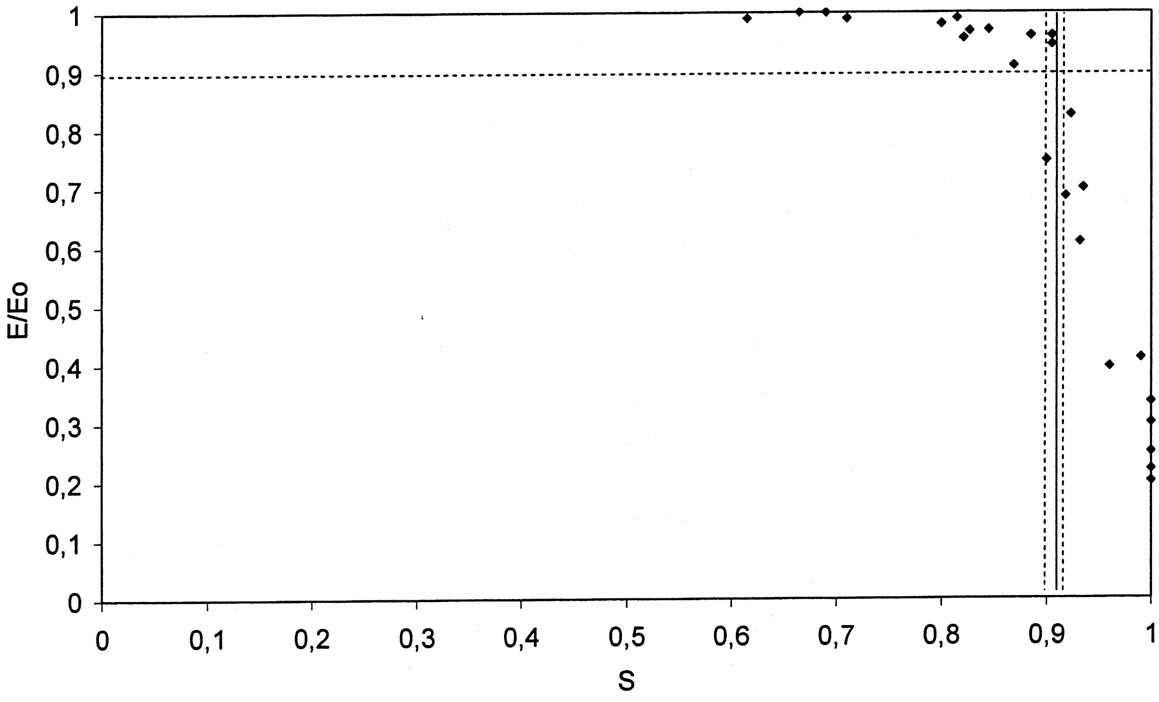

Figure 6.19: Non-air-entrained concrete (w/c 0.50, 2.1% air): Results of a determination of the critical degree of saturation.

The critical degree of saturation can be compared with the degree of saturation when all pores except the air pores are water-filled, S′:

$$S'=1-P_{air}/P_{total}=1-2.1/14.6=0.85 \qquad (6.10)$$

S_{CR} is bigger than this, which shows that a certain part of the air-pore system has to be water-filled before frost damage can occur. This fraction of air-filled pores is $S_{air,CR}$:

$$S_{air,CR} = (S_{CR}-S')/(1-S')=(0.905-0.855)/(1-0.855)=0.05/0.145=0.34 \qquad (6.11)$$

Thus, about 35% of the air-pore system has to be water-filled before frost damage can occur.

6.6.3 The actual water content

The actual water content is determined by a 4-week capillary water uptake by the method shown in Figure 5.11. The specimens were slices sawn from the cylinders. The slice thickness was about 25 mm. The initial absorption curve is shown in Figure 6.20.

Capillary saturation is reached after 4.5 hours:

$S_b=0.850$ $(\sigma\approx0.1)$
$t_b=4.5$ hours

S_b is found to be identical with S′, which is the degree of saturation when all pores except the air-pores are water-filled. *This shows that the breaking-point in the absorption curve marks the start of long-term absorption in the air-pore system.* This has been found to be valid for most concrete types

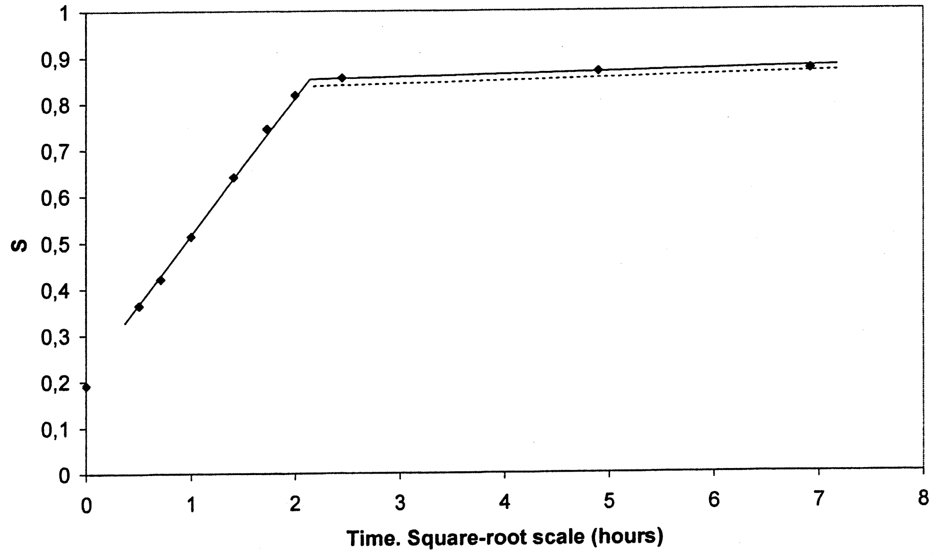

Figure 6.20: Non-air-entrained concrete (w/c 0.50, 2.1% air): Result of the determination of capillary absorption. The initial absorption with a rising water front.

The long-term absorption is shown in Figure 6.21. For t>1 day the degree of saturation is described by:

$$S_{ACT} = 0.863+0.0079\cdot t^{0.57} \quad \text{t in days} \qquad (6.12)$$
$$\sigma \approx 0.01 \text{ for all t.}$$

Inserting t_b=4.5 hours (0.187 days) in equation (6.12) gives S_b=0,86 i.e. almost the same as the observed value. This shows that equation (6.12) can be used down to the breaking-point absorption.

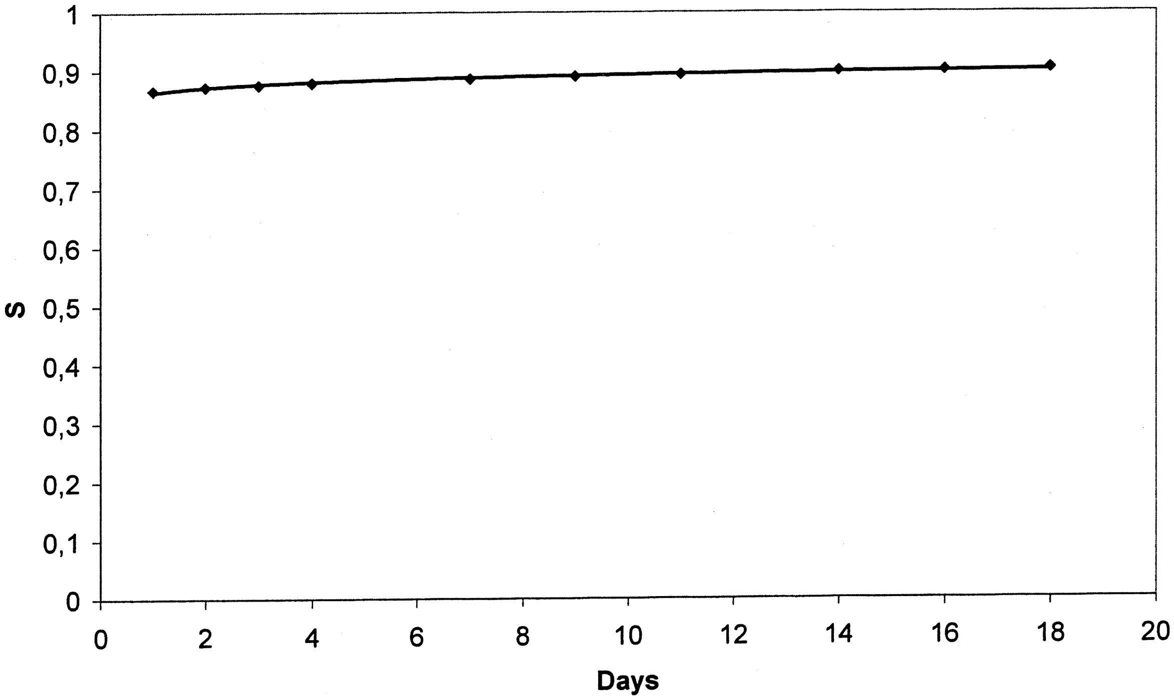

Figure 6.21: Non-air-entrained concrete (w/c 0.50 ,2.1% air): Result of the determination of capillary absorption. The long-term absorption.

6.6.4 The frost damage risk and the potential service life

Deterministic calculation

The mean potential service life is obtained by using the mean values of the critical and actual degrees of saturation in equation (5.10).

$$t_{life,pot} = [(0.905-0.863)/0.0079]^{1/0,57} = 19 \text{ days} \qquad (6.13)$$

Thus, it is about 50% risk that the non-air-entrained concrete cannot stand more than 19 days of continuous water absorption before it can become hurt by frost.

Stochastic calculation

A stochastic calculation of the damage risk as function of the capillary water absorption time is made by means of equation (6.3). The result of the calculation is shown in Figure 6.22. The "potential service life" is about 12 days if only 20% damage risk is accepted. This indicates that *non-air-entrained concrete has fairly low frost resistance in moist renvironment also when the water-cement ratio is as low as 0.50*

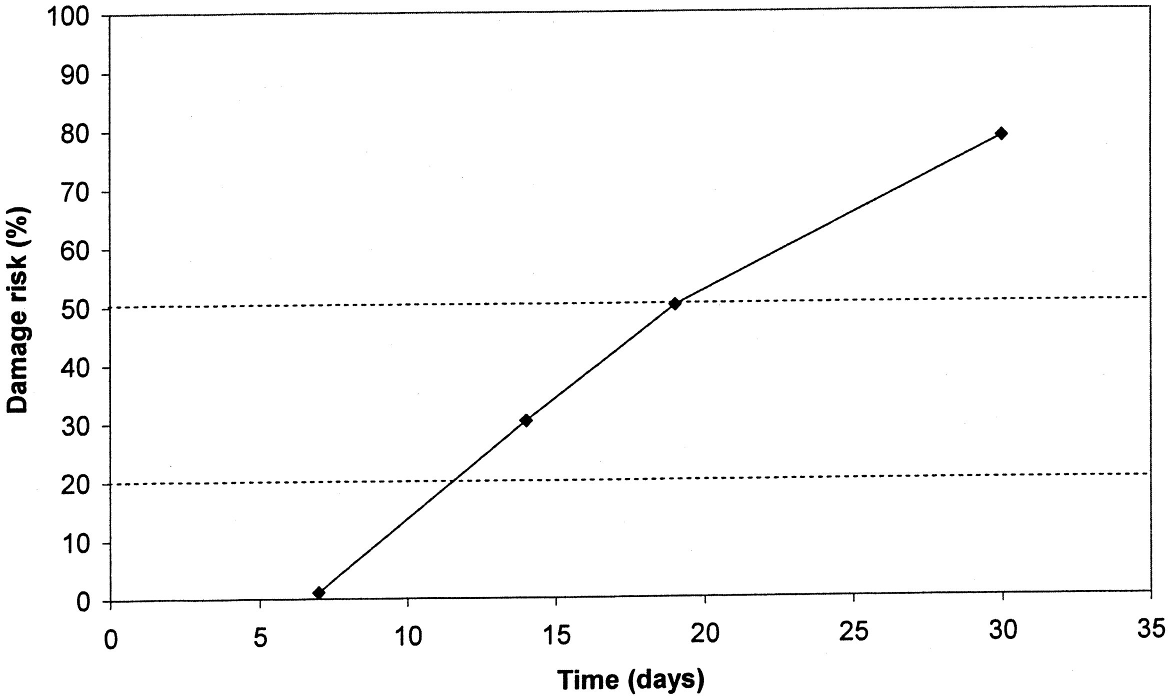

Figure 6.22: Non-air-entrained concrete (w/c 0.50 ,2.1% air). Damage risk as function of the water absorption time.

6.7 Example 6; air-entrained concrete, high w/c-ratio (w/c 0.57, 7.6% air)

6.7.1 The material

Cylinders with diameter 10 cm and length 20 cm were cast of air-entrained concrete with w/c-ratio 0.573 and cement content of 298 kg/m^3. The degree of hydration at start of the test was about 70%.

The following material data are valid:

Porosity:	20.3% (σ=0.003%)
Air in fresh concrete:	7.6%
28-day strength:	34.3 MPa

6.7.2 The critical water content

The determination of the critical degree of saturation was made on the cylinders. The result is shown in Figure 6.23. If a loss in E of 10% is used as criterion the following mean value and standard deviation for the critical degree of saturation are valid:

$S_{CR,mean}$=0.835

$\sigma \approx$0.025

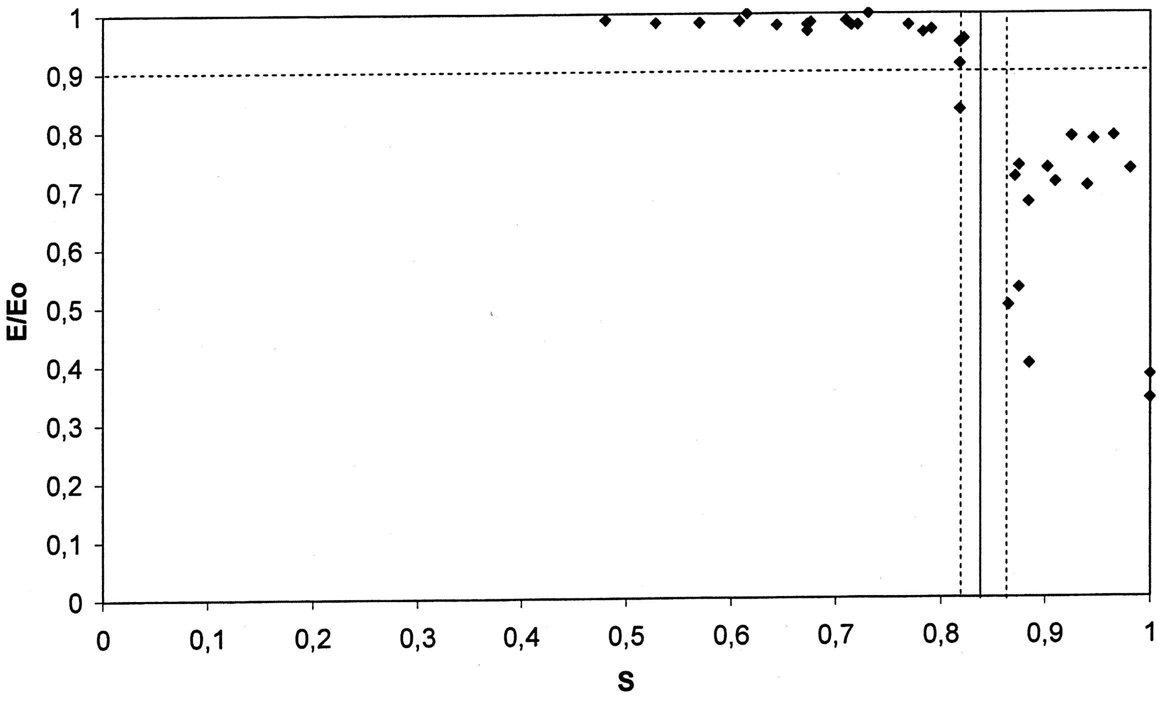

Figure 6.23: Air-entrained concrete with high water-cement ratio (w/c 0.57, 7.6% air)*:*
Results of a determination of the critical degree of saturation.

The degree of saturation when all pores except the air pores are water-filled, S′ is, see Equation (6.10):

$$S'=1-P_{air}/P_{total}=1-7.6/20.3=0.625$$

S_{CR} is bigger than this value, which shows that a certain part of the air-pore system has to be water-filled before frost damage can occur. This fraction of air-filled pores is $S_{air,CR}$ is (see equation 6.11):

$$S_{air,CR} = (S_{CR}-S')/(1-S')=(0.835-0.625)/(1-0.625)=0.21/0.375=0.56$$

Thus, more than 56% of the air-pore system has to be water-filled before frost damage can occur.

6.7.3 The actual water content

The actual water content is determined by a 4-week capillary water uptake by the method shown in Figure 5.11. The specimens were slices sawn from the cylinders. The slice thickness was 25 mm.

The initial absorption curve is shown in Figure 6.24. Capillary saturation is reached after 4.8 hours:

$S_b=0.59$ ($\sigma\approx0,02$)
$t_b=4.8$ hours

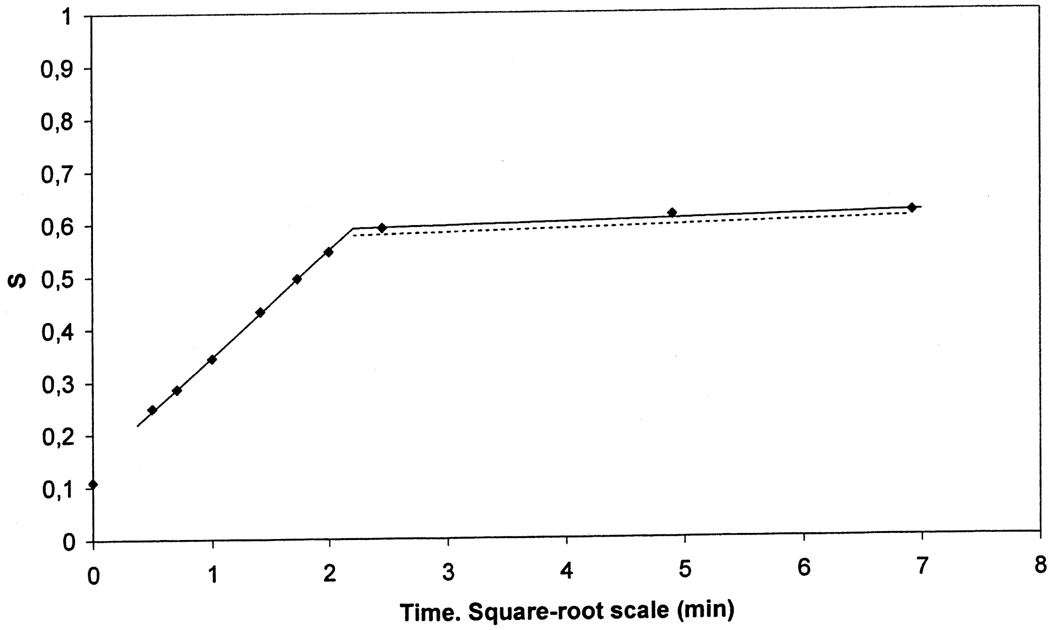

Figure 6.24: Air-entrained concrete with high water-cement ratio (w/c 0.57, 7.6% air)*: Result of the determination of capillary absorption. The initial absorption with a rising water front.*

The long-term absorption is shown in Figure 6.25. For t>1 day the degree of saturation is described by:

$$S_{ACT} = 0.612+0.0042\cdot t^{0,90} \quad \text{t in days} \tag{6.14}$$
$\sigma \approx 0.01$ for all t.

Inserting t_b=4.8 hours (0.2 days) in equation (6.14) gives S_b=0.612 i.e. somewhat higher than the observed value. This shows that equation (6.14) can only be used down to about 1 day of absorption.

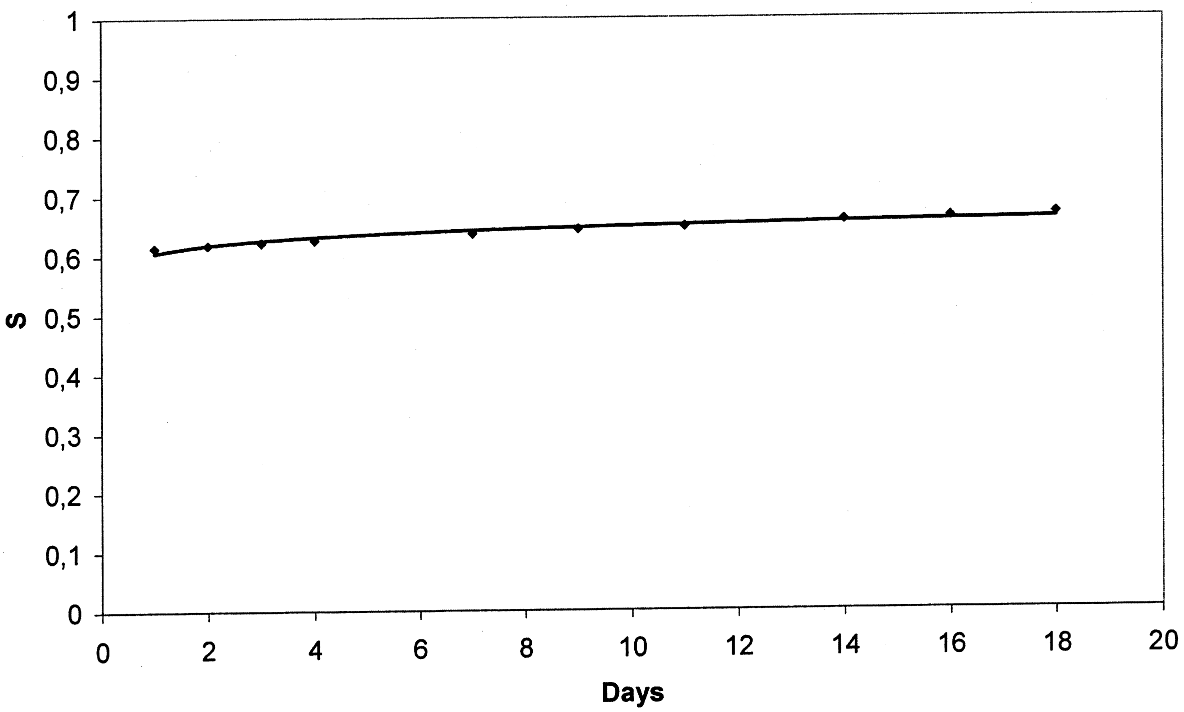

Figure 6.25: Air-entrained concrete with high water-cement ratio (w/c 0.57, 7.6% air): *Result of the determination of capillary absorption. The long-term absorption*

6.7.4 The frost damage risk and the potential service life

Deterministic calculation

The mean potential service life is obtained by using the mean values of the critical and actual degrees of saturation in equation (5.10).

$$t_{life,pot} = [(0.835-0.612)/0.0042]^{1/0,90} = 83 \text{ days} \tag{6.15}$$

Thus, the air-entrained concrete is considerably more frost resistant than the non-air-entrained. The reason is not that the critical moisture content is higher, on the contrary, it is lower. The reason is that the water uptake in the air-pores is a very slow process, and more air hast to be removed before S_{CR} is reached.

Stochastic calculation

A stochastic calculation of the damage risk as function of the capillary water absorption time is made by means of equation (6.3). The result of the calculation is shown in Figure 6.26. The "potential service life" is about 72 days if only 20% damage risk is accepted. Thus, the frost resistance is considerably higher than for the non-air-entrained concrete despite the higher water-cement ratio.

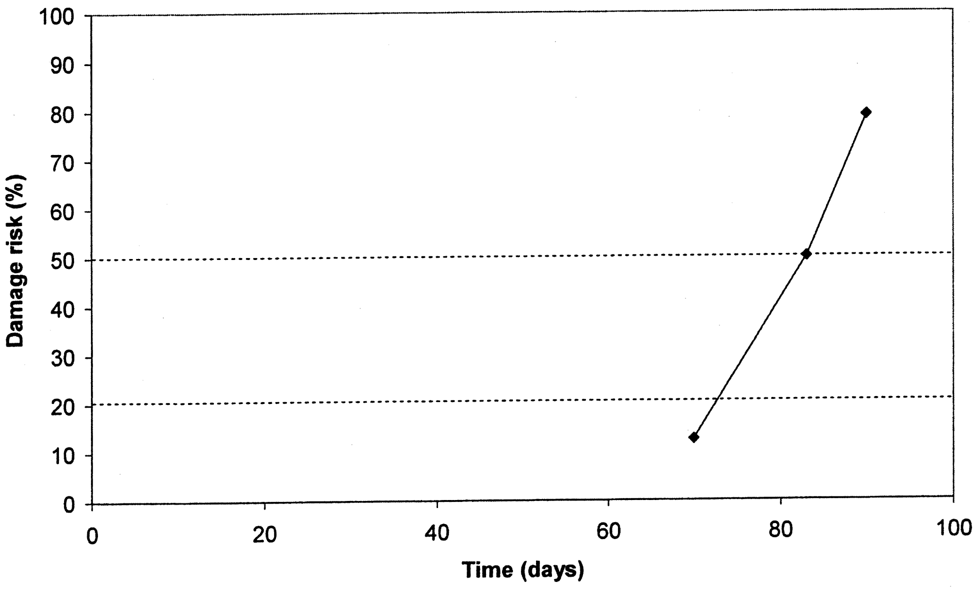

Figure 6.26: Air-entrained concrete with high water-cement ratio (w/c 0.57, 7.6% air). *Damage risk as function of the water absorption time.*

6.8 Example 7; air-entrained concrete, low w/c-ratio, "normal" air content (w/c 0.45, 4.5% air)

6.8.1 The material

Cylinders with diameter 10 cm and length 20 cm were cast of air-entrained cement concrete with w/c-ratio 0.45 and cement content 400 kg/m^3.

The following material data are valid:

Porosity:	16.6% (σ=0.004%)
Air in fresh concrete:	5.6%
Air in hardened concrete:	4.5%
Specific surface of air-pore system:	36 mm^{-1}

6.8.2 The critical water content

The determination of the critical degree of saturation was made on the cylinders. The result is shown in Figure 6.27. If a loss in E of 10% is used as criterion the following mean value and standard deviation for the critical degree of saturation are valid:

$S_{CR,mean}$=0.895
$\sigma \approx$0.005

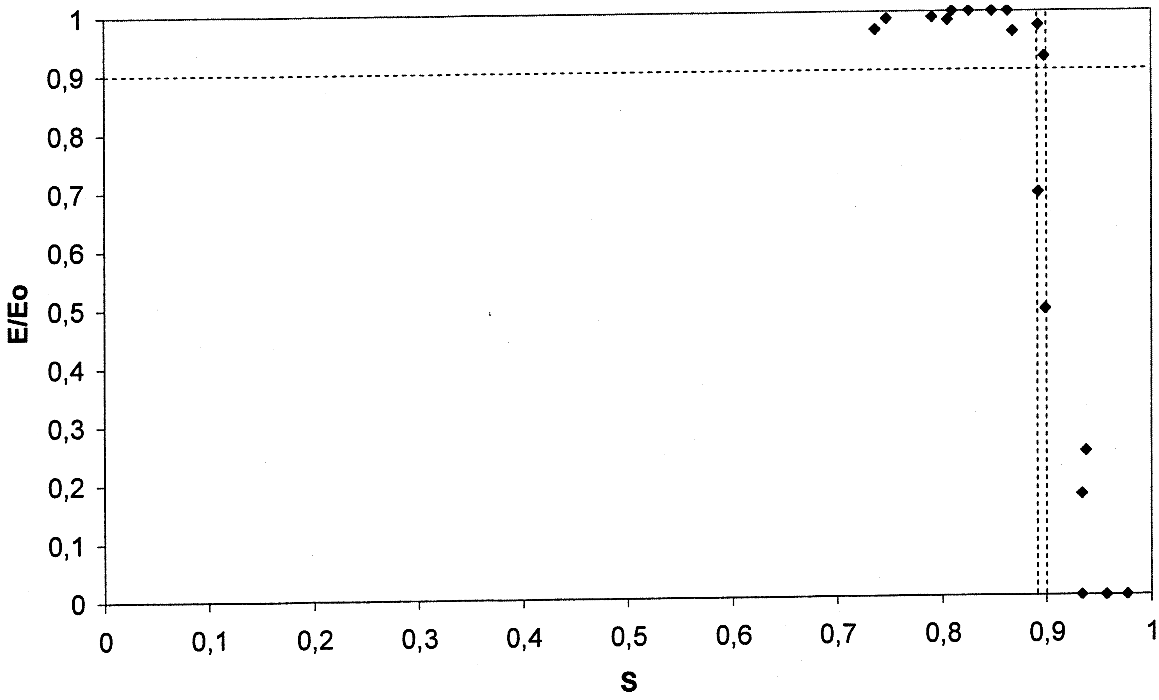

Figure 6.27: Air-entrained concrete with low water-cement ratio (w/c 0.45, 4.5% air)*:* *Results of a determination of the critical degree of saturation.*

The degree of saturation when all pores except the air pores are water-filled, S′ is (see equation (6.10)

$S'=1-P_{air}/P_{total}=1-4.5/16.6=0.67$

S_{CR} is bigger than this value, which shows that a certain part of the air-pore system has to be water-filled before frost damage can occur. This fraction of air-filled pores is $S_{air,CR}$ (see equation 6.11):

$S_{air,CR} = (S_{CR}-S')/(1-S')=(0.895-0.67)/(1-0.67)=0.225/0.33=0.68$

Thus, more than 65% of the air-pore system has to be water-filled before frost damage can occur.

6.8.3 The actual water content

The actual water content is determined by a 18 day capillary water uptake by the method shown in Figure 5.11. The specimens were slices sawn from the cylinders. The slice thickness was 25 mm.

The initial absorption curve is shown in Figure 6.28.

Capillary saturation is reached after 4.8 hours:

$S_b=0.725$ $(\sigma\approx0{,}01)$
$t_b=8.5$ hours

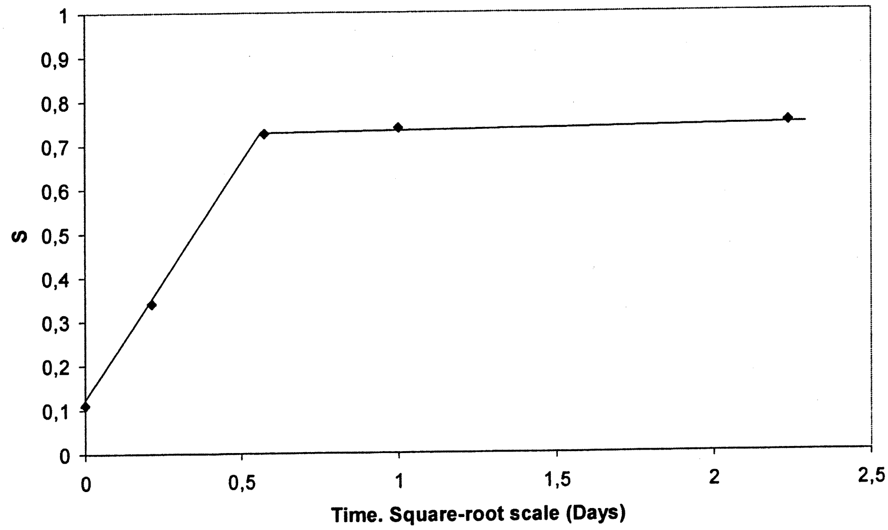

Figure 6.28: Air-entrained concrete with low water-cement ratio (w/c 0.45, 4.5% air)*: Result of the determination of capillary absorption. The initial absorption with a rising water front.*

The long-term absorption is shown in Figure 6.29. For t>1 day the degree of saturation is described by:

$$S_{ACT} = 0.726+0.0121 \cdot t^{0,40} \quad \text{t in days} \qquad (6.16)$$

$\sigma \approx 0.01$ for all t.

Inserting t_b=8.5 hours (0.35 days) in equation (6.16) gives S_b=0.734 i.e. somewhat higher than the observed value. This shows that equation (6.16) can only be used down to about 1 day of absorption.

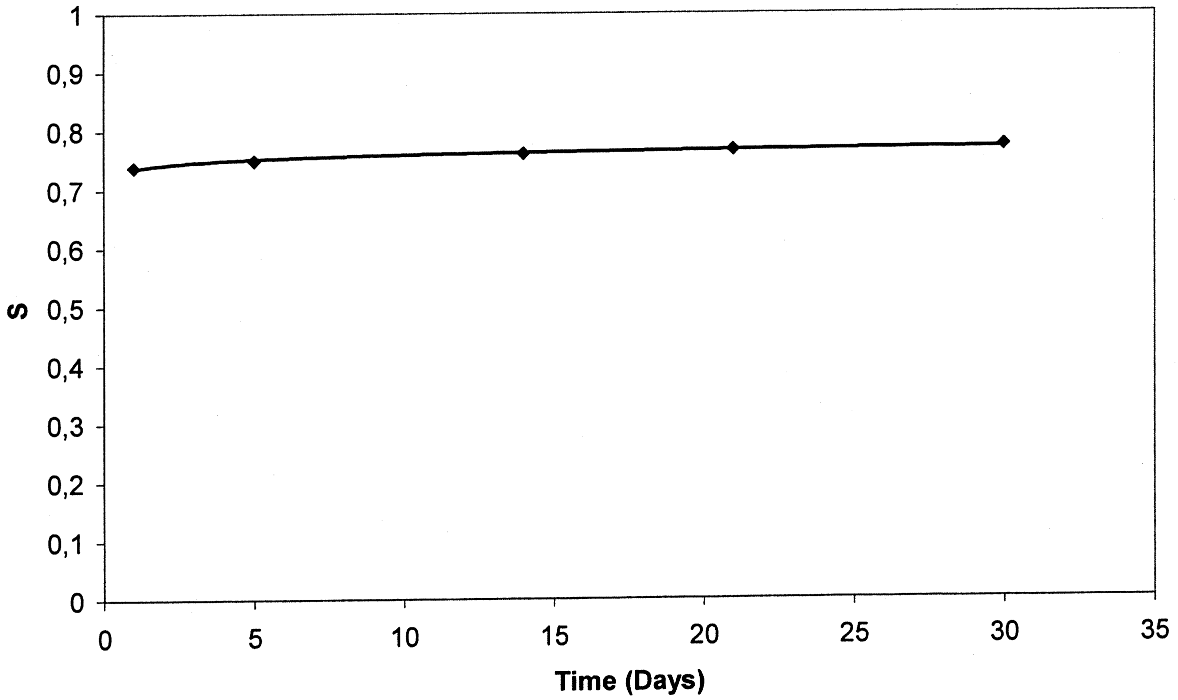

Figure 6.29: Air-entrained concrete with low water-cement ratio (w/c 0.45, 4.5% air)*: Result of the determination of capillary absorption. Long-term absorption.*

6.8.4 The frost damage risk and the potential service life

Deterministic calculation

The mean potential service life is obtained by using the mean values of the critical and actual degrees of saturation in equation (5.10).

$$t_{life,pot} = [(0.895-0.726)/0.0121]^{1/0,40} = 729 \text{ days (2years)} \qquad (6.17)$$

Thus, the air-entrained concrete with low water-cement ratio (0.45) is considerably more frost resistant than the air-entrained concrete with higher water-cement ratio (0.57).

Stochastic calculation

A stochastic calculation of the damage risk as function of the capillary water absorption time is made by means of equation (6.3). The result of the calculation is shown in Figure 6.30. The "potential service life" is about 630 days if only 20% damage risk is accepted. The very high frost resistance of concrete with low water-cement ratio and high air content is also confirmed by comprehensive and long-term experience.

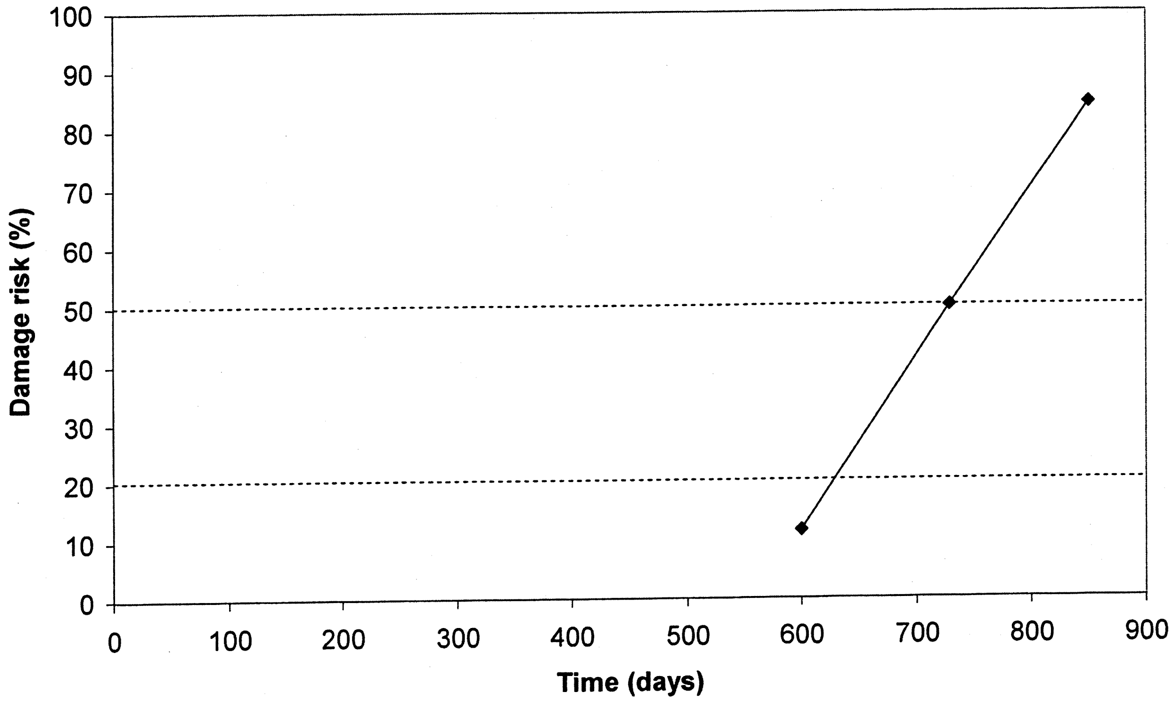

Figure 6.30: Air-entrained concrete with high water-cement ratio (w/c 0.45, 4.5% air). *Damage risk as function of the water absorption time.*

6.9 Example 8; air-entrained concrete, low w/c-ratio, high air content (w/c 0.45, 6.2% air)

6.9.1 The material

Cylinders with diameter 10 cm and length 20 cm were cast of air-entrained concrete with w/c-ratio 0.45 and cement content 383 kg/m^3. The same cement, aggregate and air-entraining agent as for the concrete in paragraph 6.8 were used.

The following material data are valid:

Porosity:	17.9% (σ=0.004%)
Air in fresh concrete:	7.4%
Air in hardened concrete:	6.2%
Specific surface of air-pore system:	45 mm^{-1}

6.9.2 The critical water content

The determination of the critical degree of saturation was made on the cylinders. The result is shown in Figure 6.31. If a loss in E of 10% is used as criterion the following mean value and standard deviation for the critical degree of saturation are valid:

$S_{CR,mean}$=0.865
$\sigma \approx$0.015

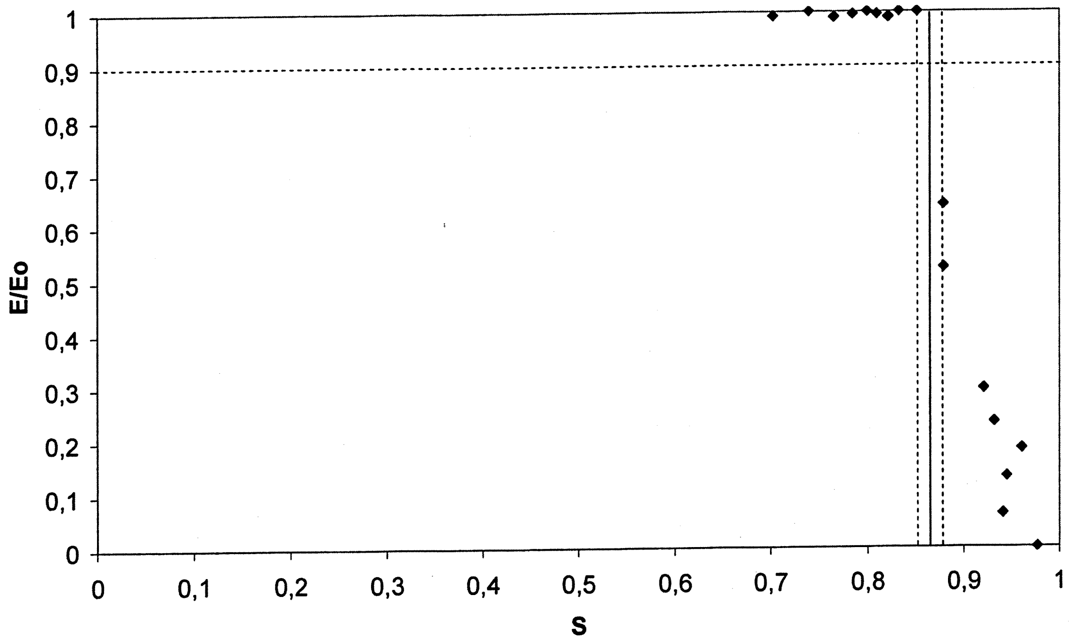

Figure 6.31: Air-entrained concrete with low water-cement ratio (w/c 0.45, 6.2% air)*: Results of a determination of the critical degree of saturation.*

The degree of saturation when all pores except the air pores are water-filled, S′ is (see equation (6.10)

$$S'=1-P_{air}/P_{total}=1-6.2/17.9=0.65$$

S_{CR} is bigger than this value, which shows that a certain part of the air-pore system has to be water-filled before frost damage can occur. This fraction of air-filled pores is $S_{air,CR}$ (see equation 6.11):

$$S_{air,CR} = (S_{CR}-S')/(1-S')=(0.865-0.65)/(1-0.65)=0.215/0.35=0.61$$

Thus, more than 60% of the air-pore system has to be water-filled before frost damage can occur.

6.9.3 The actual water content

The actual water content is determined by 18 day capillary water uptake by the method shown in Figure 5.11. The specimens were slices sawn from the cylinders. The slice thickness was 25 mm.

The initial absorption curve is shown in Figure 6.32. Capillary saturation is reached after 4.8 hours:

$S_b=0.66$ ($\sigma \approx 0,01$)
$t_b=9$ hours

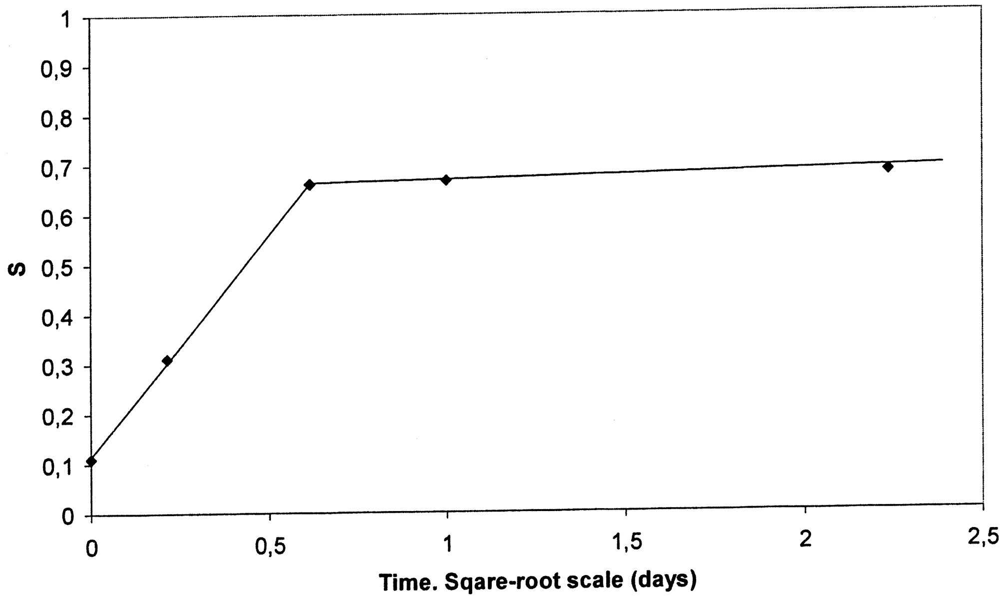

Figure 6.32: Air-entrained concrete with low water-cement ratio (w/c 0.45, 6.2% air)*: Result of the determination of capillary absorption. The initial absorption with a rising water front.*

The long-term absorption is shown in Figure 6.33. For t>1 day the degree of saturation is described by:

$$S_{ACT} = 0.66+0.0065\cdot t^{0,70} \quad \text{t in days} \tag{6.18}$$
$\sigma \approx 0.01$ for all t.

Inserting t_b=9 hours (0.38 days) in equation (6.18) gives S_b=0.663 i.e about the same as the observed value. This shows that equation (6.18) can be used from the breaking point time.

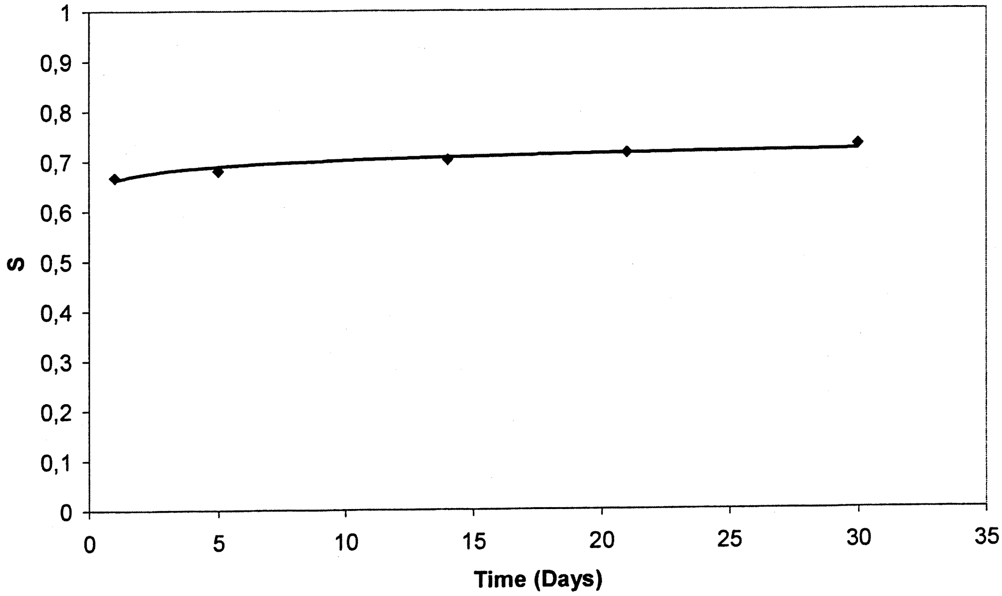

Figure 6.33: Air-entrained concrete with low water-cement ratio (w/c 0.45, 6.2% air)*: Result of the determination of capillary absorption. Long-term absorption.*

6.9.4 The frost damage risk and the potential service life

Deterministic calculation

The mean potential service life is obtained by using the mean values of the critical and actual degrees of saturation in equation (5.10).

$$t_{life,pot} = [(0.865-0.66)/0.0065]^{1/0,70} = 138 \text{ days} \tag{6.19}$$

The value is high, but it is lower than for the concrete with the lower air content (4.5%). The most plausible reason is that the air-pore system is partly continuous, due to instable air-bubbles in the fresh concrete. Therefore, more rapid water absorption can take place in the air pores.

Stochastic calculation

A stochastic calculation of the damage risk as function of the capillary water absorption time is made by means of Equation (6.3). The result of the calculation is shown in Figure 6.34. The "potential service life" is about 120 days if only 20% damage risk is accepted.

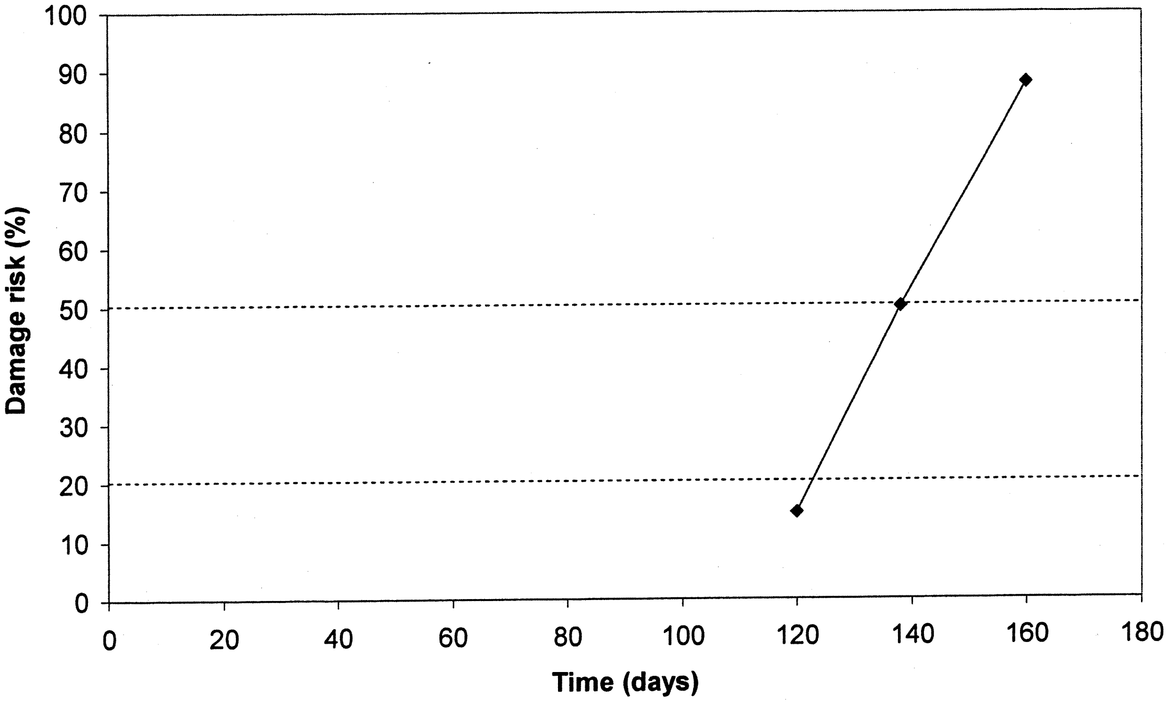

Figure 6.34: Air-entrained concrete with high water-cement ratio (w/c 0.45, 6.2% air).
Damage risk as function of the water absorption time.

6.10 Example 9; air-entrained cement mortar (w/c 0.60, 6.4% air)

6.10.1 The material

Specimens 40·40·160 mm were cast of air-entrained cement mortar with w/c-ratio 0.60 and sand/cement ratio 4.2:1. The degree of hydration at start of the test was about 60%.

The following material data are valid:

Bulk density:	2054 kg/m^3
Porosity:	22,3%
Air in fresh concrete:	6.4%

6.10.2 The critical water content

The determination of the critical degree of saturation is shown in Figure 6.35. If a loss in E of 0% is used as criterion the following mean value and standard deviation for the critical degree of saturation are valid:

$S_{CR,mean}=0.845$
$\sigma \approx 0.015$

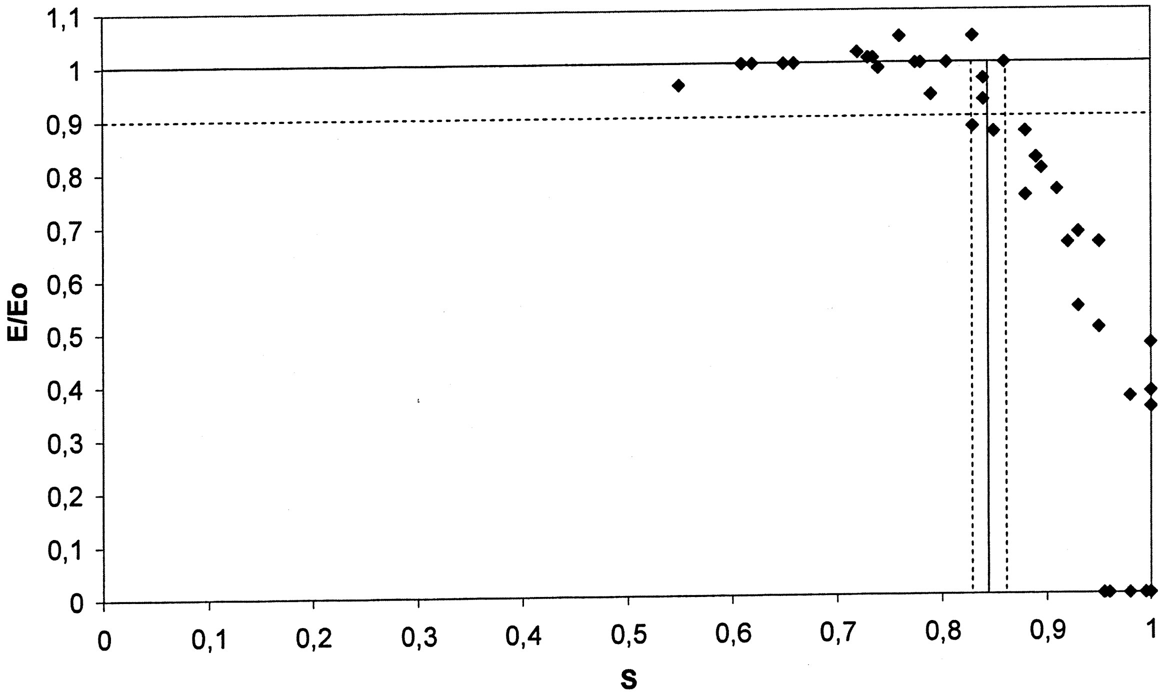

Figure 6.35: Air-entrained cement mortar (w/c 0.60, 6.4% air):
Results of a determination of the critical degree of saturation based on change in dynamic E-modulus.

The critical degree of saturation can be compared with the degree of saturation when all pores except the air pores are water-filled, S′:

$S'=1-P_{air}/P_{total}=1-6.4/22.3=0.713$

S_{CR} is bigger, which shows that a certain part of the air-pore system has to be water-filled before frost damage can occur. This fraction of air-filled pores is $S_{air,CR}$ (see equation 6.11):

$S_{air,CR} = (S_{CR}-S')/(1-S')=(0.845-0.713)/(1-0.713)=0.132/0.287=0.46$

Thus, more than 45% of the air-pore system has to be water-filled before frost damage can occur.

Damage can also be based on permanent volume change caused by freezing. Volume changes for the same specimens as in Figure 6.35 are plotted in Figure 6.36. From this, the following critical degree of saturation is obtained, provided the maximum allowed volume change is 0.5 cm^3 (This corresponds to a relative volume change of 1.9 ‰):

$S_{CR,mean}=0.885$
$\sigma \approx 0.01$

The S_{CR}-value based on change in E-modulus is lower, indicating that a fairly big reduction in E-modulus can occur before this is observed in permanent volume change. The value based on E is therefore selected in the further analysis of service life.

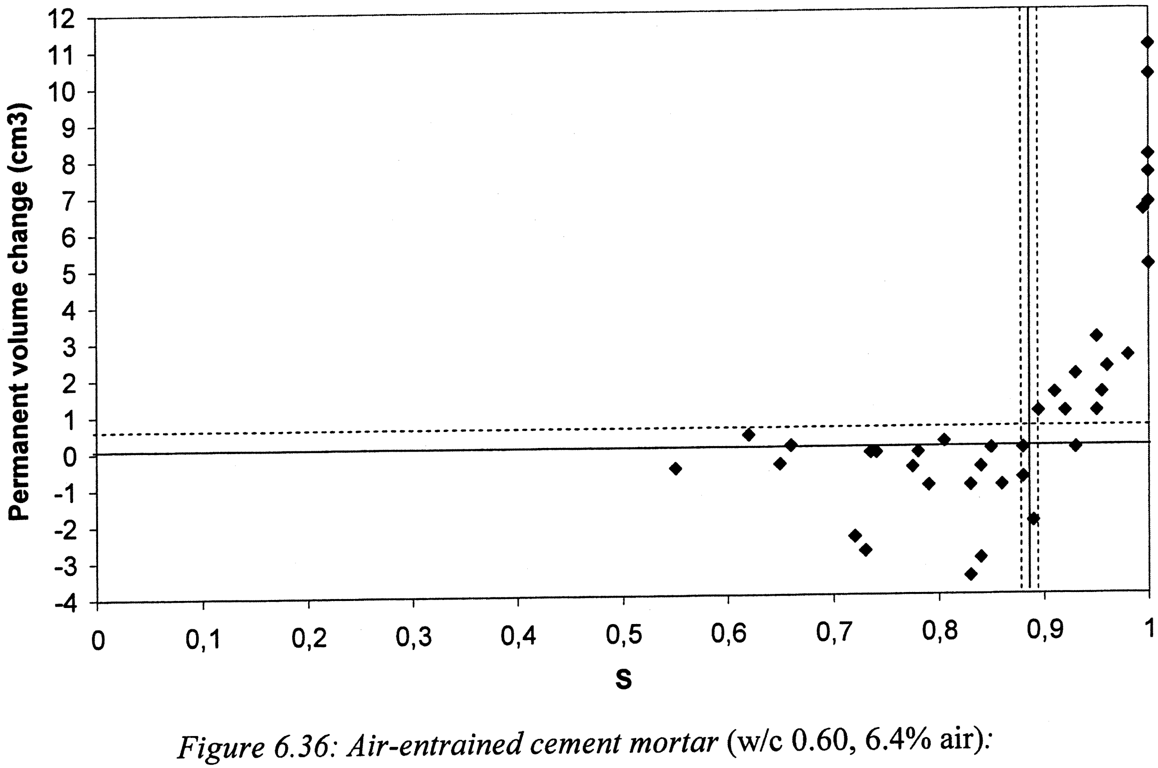

Figure 6.36: Air-entrained cement mortar (w/c 0.60, 6.4% air)*:*
Results of a determination of the critical degree of saturation based on volume change.

6.10.3 The actual water content

The actual water content is determined by a 4-week capillary water uptake by the method shown in Figure 5.11. The specimen thickness was 20 mm.

The initial absorption curve is shown in Figure 6.37.

Capillary saturation is reached after 220 minutes (3.7 hours):

$S_b=0.705$ ($\sigma \approx 0.005$)
$t_b=220$ minutes

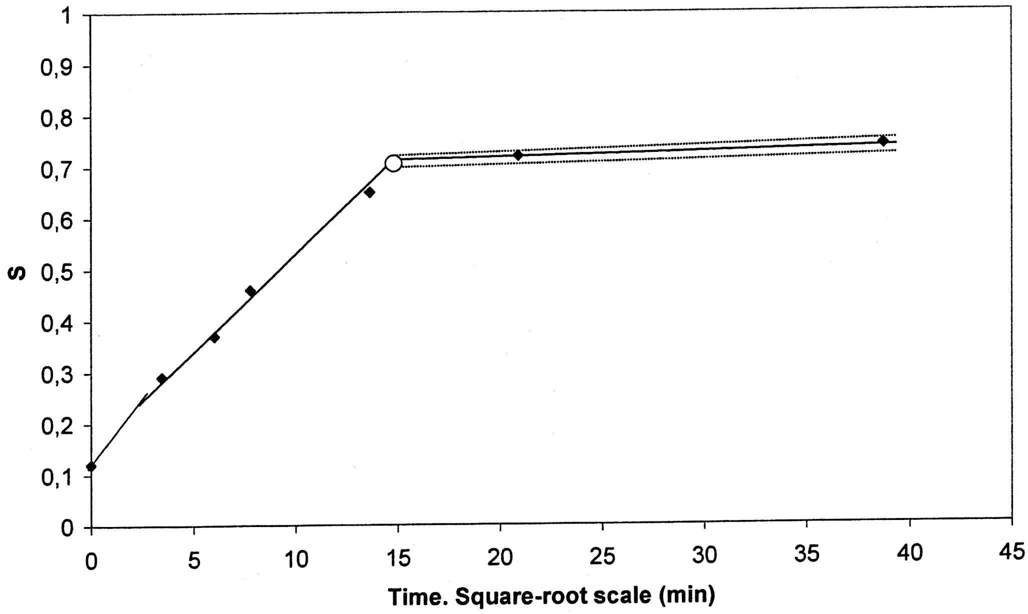

Figure 6.37: Air-entrained cement mortar (w/c 0.60, 6.4% air)*:*
Result of the determination of capillary absorption. The initial absorption with a rising water front.

The long-term absorption is shown in Figure 6.38. For t>1 day the degree of saturation is described by:

$S_{ACT} = 0.737+0.00682 \cdot t^{0.61}$ t in days (6.20)
$\sigma \approx 0.01$ for all t.

Note: Inserting $t_b=220$ min (0.153 days) in equation (6.20) gives $S_b=0{,}74$ i.e. somewhat higher than the observed value. This shows that equation (6.20) can only be used down to about 1 day of absorption.

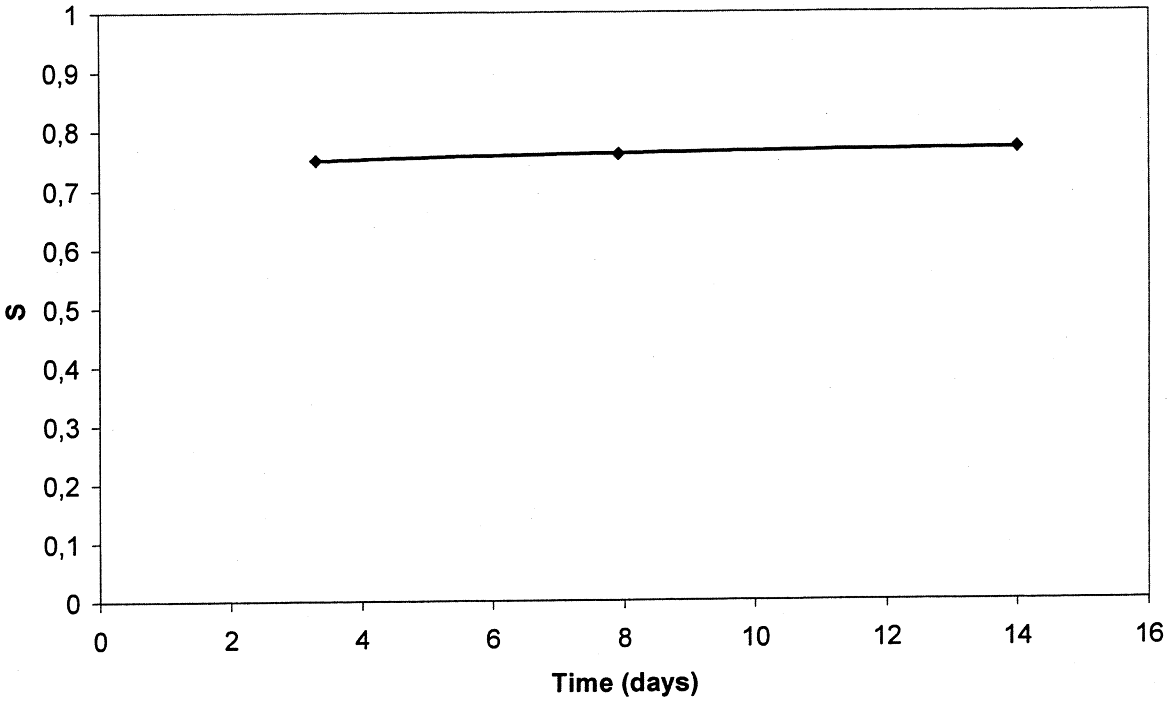

Figure 6.38: Air-entrained cement mortar (w/c 0.60, 6.4% air)*:*
Result of the determination of capillary absorption. Long-term absorption.

6.10.4 The frost damage risk and the potential service life

Deterministic calculation

The mean potential service life is obtained by using the mean values of the critical and actual degrees of saturation in equation (5.10).

$$t_{life,pot} = [(0.845-0.737)/0.0068]^{1/0,61} = 93 \text{ days} \qquad (6.21)$$

Thus, it is 50% chance that the cellular concrete can stand more than 3 months of continuous water absorption before it can become hurt by frost.

Stochastic calculation

A stochastic calculation of the damage risk as function of the capillary water absorption time is made by means of equation (6.3). The result of the calculation is shown in Figure 6.39. The "potential service life" is about 70 days if only 20% damage risk is accepted.

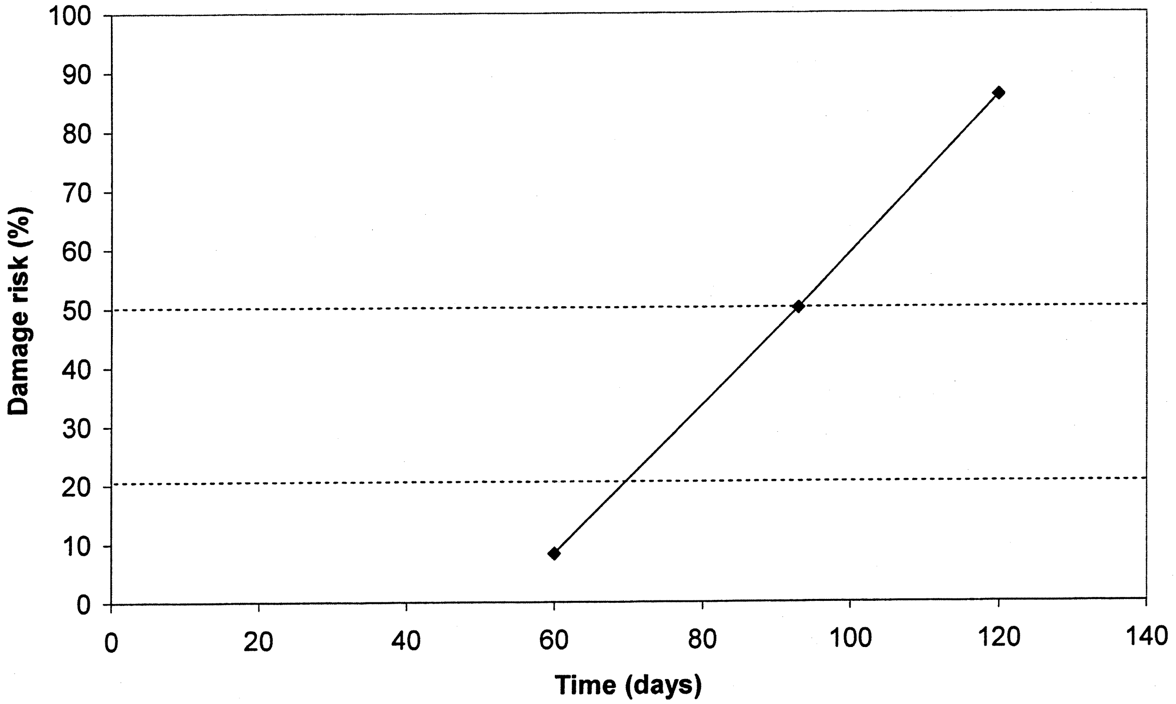

Figure 6.39: Air-entrained cement mortar (w/c 0.60, 6.4% air)*:*
Damage risk as function of the water absorption time.

6.11 Example 10; sandstone

6.11.1 The material

Specimens were prepared from blocks of natural sandstone from the Swedish island of Gotland. The data in this paragraph are taken from (Wessman 1997).

The following material data are valid:

Bulk density:	2069 kg/m^3
Total porosity:	22.7 %

6.11.2 The critical water content

The determination of the critical degree of saturation is shown in Figure 6.40. Damage is defined by permanent change in volume after thawing. If no volume change is accepted the following mean value and standard deviation for the critical degree of saturation are valid:

$S_{CR,mean}$=0.745
$\sigma \approx 0$

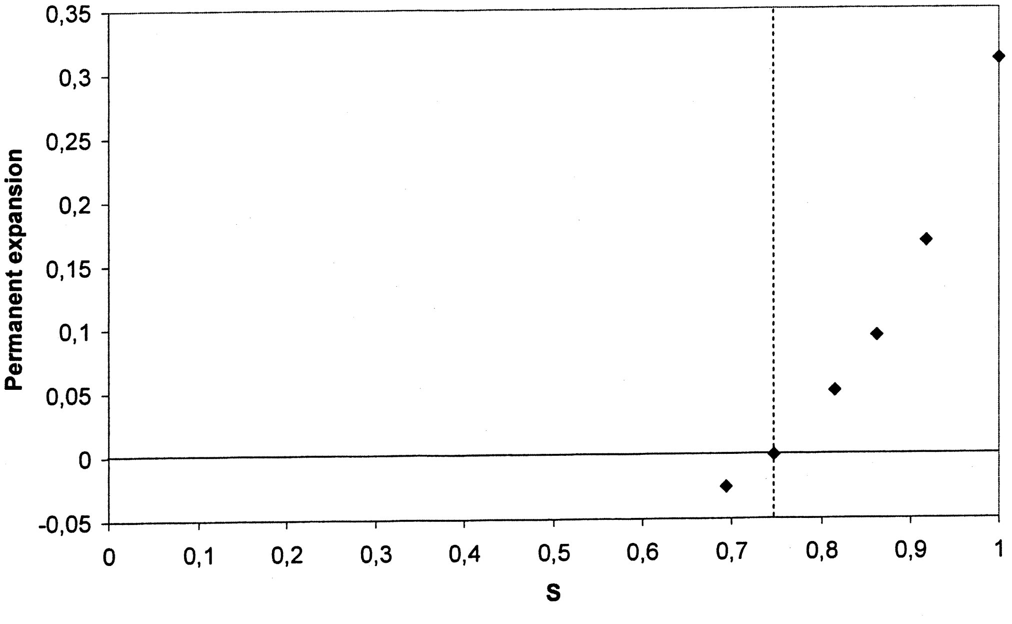

Figure 6.40: Sandstone: Results of a determination of the critical degree of saturation. (expansion in ‰)

6.11.3 The actual water content

The actual water content is determined by a 5-week capillary water uptake by the method shown in Figure 5.11. The specimen thickness was 20 mm.

Capillary saturation (the "breaking point" S_b) corresponds to S=0.67. It occurs after an absorption time of only a few minutes. Thus, the capillarity is extremely high.

The long-term absorption for t>1 day is shown in Figure 6.41. For t>1 day the degree of saturation can be described by:

$$S_{ACT} = 0.70+0.0055\cdot t^{0.97} \quad \text{t in days} \qquad (6.22)$$

$\sigma\approx0.01$ for all t.

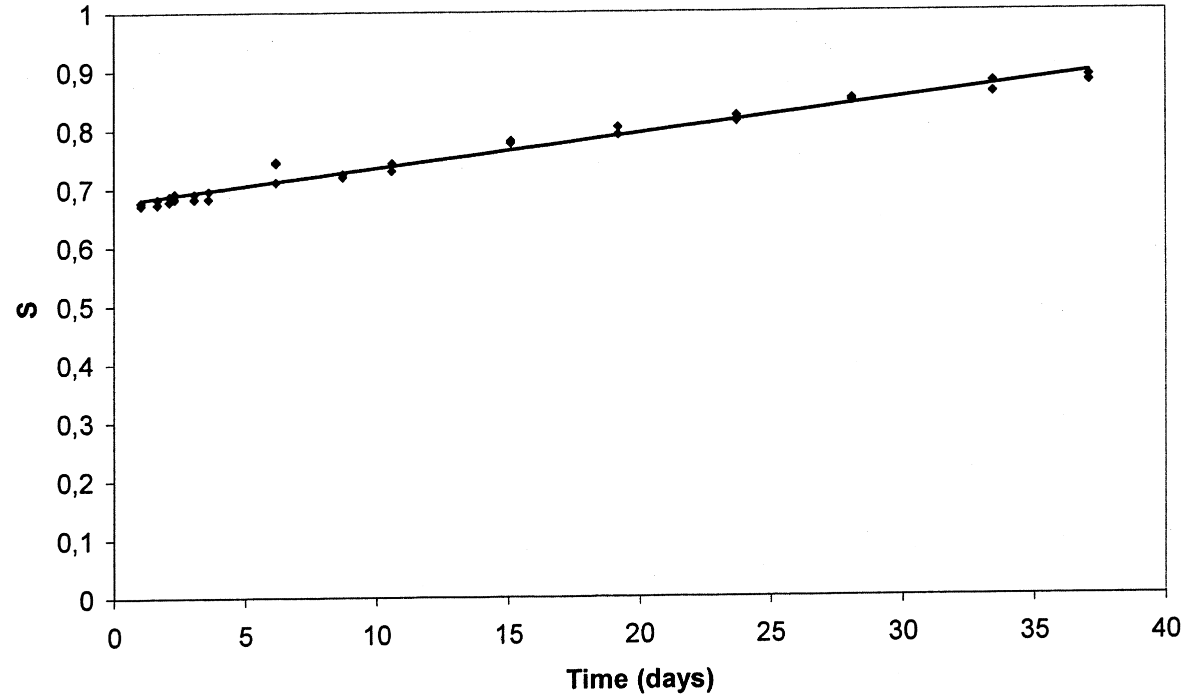

Figure 6.41: Sandstone: Result of the determination of capillary absorption. The long-term absorption.

6.11.4 The frost damage risk and the potential service life

Deterministic calculation

The mean potential service life is obtained by using the mean values of the critical and actual degrees of saturation in equation (5.10).

$$t_{life,pot} = [(0.745-0.70)/0.0055]^{1/0.97} = 9 \text{ days} \qquad (6.23)$$

Thus, there is 50% risk that the sandstone cannot stand no more than 8 days of continuous water absorption before it can become hurt by frost.

Stochastic calculation

A stochastic calculation of the damage risk as function of the capillary water absorption time is made by means of equation (4.1). The result of the calculation is shown in Figure 6.42. The "potential service life" is about 6 days if only 20% damage risk is accepted. Thus, the sandstone has low frost resistance. This is also confirmed by practical experience. The stone was frequently used in Sweden during the 17th and 18th centuries. Many of these structures and outdoor ornaments made by the stone have become severely frost damaged over the years.

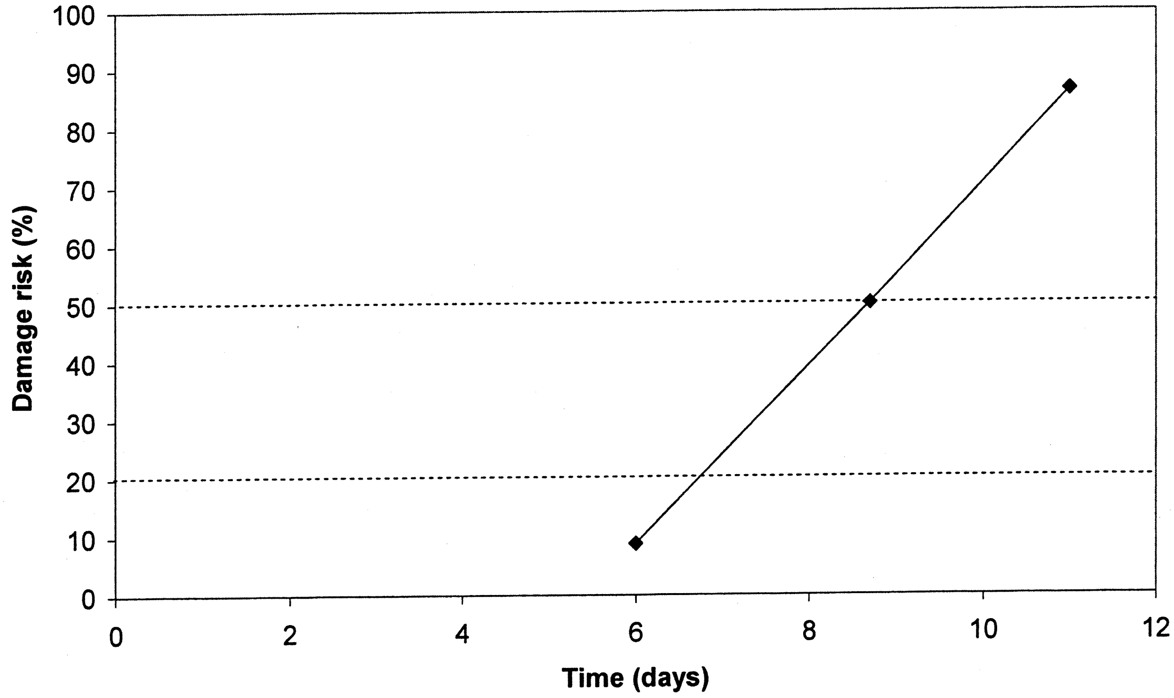

Figure 6.42: Sandstone. Damage risk as function of the water absorption time.

6.12 Discussion of experimental results

6.12.1 Critical water absorption in coarse pores

The breaking-point in the capillary absorption test, i.e. *capillary saturation*, corresponds to complete water-filling of all pores with diameter smaller than about 1 μm (Fagerlund 2004). Also coarser pores are filled at the breaking point, provided the shape of the pore system is such that no air-bubble can be enclosed during the water absorption process; see Figure 5.8 Non-permeable pores of the type shown in Figure 5.7, bigger than about 1 μm, will always contain enclosed air-bubbles at the breaking-point absorption.

If the material is continuously stored in water after the breaking-point, enclosed air will gradually dissolve. All experiments presented above show that the critical degree of saturation is above the breaking-point. This is the case for all types of materials. Therefore, certain dissolution of air in non-permeable open pores is required before the material can be harmed by frost. This also means that the critical degree of saturation is always located to moisture range 3 as defined by Figures 1.1 and 1.2.

The critical water absorption in the coarse pore system is described by equation (6.11), which in the general case can be written:

$$S_{coarse,CR} = (S_{CR}-S_b)/(1-S_b) \qquad 0\leq S_{coarse}\leq 1 \tag{6.11'}$$

Where S_b is the degree of saturation at the breaking-point.

All coarse pores are empty when $S_{coarse}=0$, and the coarse pore system is completely filled when $S_{coarse}=1$.

The critical air volume a_{CR} is:

$$a_{CR}=P_{total}(1-S_{CR}) \ (\%) \tag{6.23}$$

Where P_{total} is the total open porosity (%).

Data for all materials are presented in Table 6.1. Mean values of S_{CR} and S_b are shown.

Table 6.1: The critical absorption in the coarse pore system, and the critical air volume.

Material	**P_{total} (%)**	**S_{CR}**	**S_b**	**$S_{coarse,CR}$**	**Critical air volume (%)**	**Min air volume $0.09 \cdot W_{CR}$ [1)] (%)**
Under-burnt brick	39.5	0.850	0.700	0.50	5.9	3.0
Hard-burnt brick	31.1	0.755	0.510	0.50	7.6	2.1
Sand-lime brick	30.9	0.805	0.770	0.15	6.0	2.2
Cellular concrete	79.3	0.510	0.380	0.21	38.9	3.6
Non-air-entrained concrete w/c 0.50. 2.1% air	14.6	0.905	0.850	0.37	1.4	1.2
Air-entrained concrete w/c 0.57. 7.6% air	20.3	0.835	0.590	0.60	3.3	1.5
Air-entrained concrete w/c 0.45. 4.5% air	16.6	0.895	0.725	0.62	1.7	1.3
Air-entrained concrete w/c 0.46. 6.2% air	17.9	0.865	0.660	0.60	2.4	1.4
Air-entrained cement mortar w/c 0.60. 6.4% air	22.3	0.845	0.705	0.47	3.5	1.8
Sandstone	22.7	0.745	0.670	0.22	5.8	1.5

1) W_{CR} is the total water content at S_{CR} ($W_{CR}=P_{tot} \cdot S_{CR}$)

The following observations are made:

1. For all materials the critical degree of saturation is higher than the capillary saturation at the breaking-point; see also Figure 6.43. Therefore, a certain portion of the coarse air-pore system has to be water-filled before frost damage can occur.

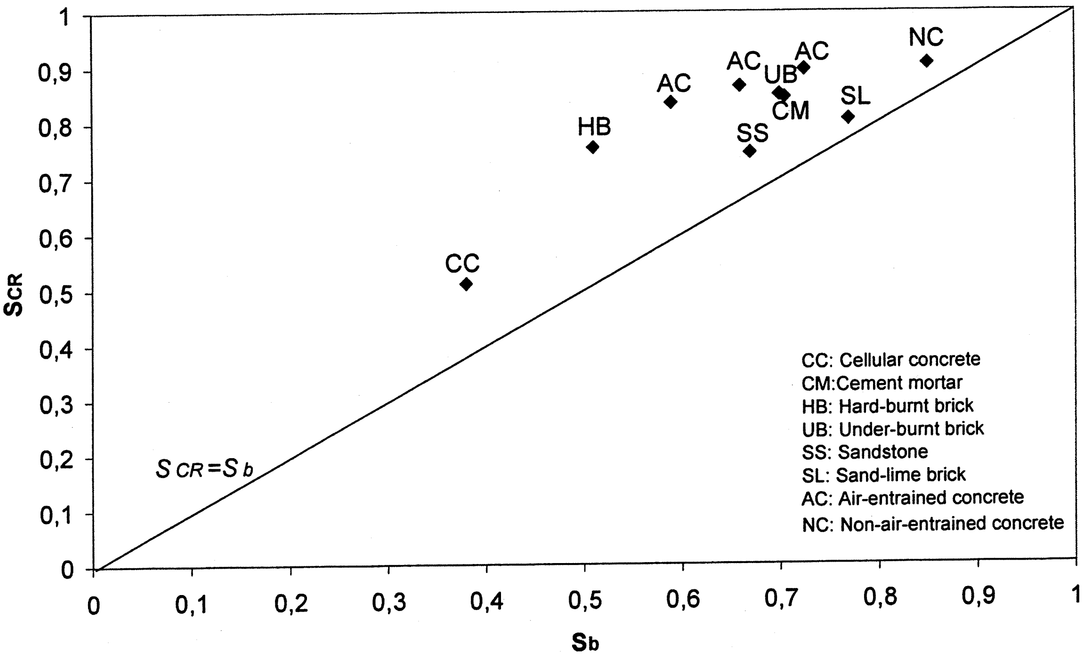

Figure 6.43: Relation between the capillary degree of saturation (breaking-point absorption, S_b) and the critical degree of saturation.

2. A higher total porosity tends to give higher critical air volume; see Figure 6.44. This might seem reasonable since a higher porosity normally means a higher amount of freezable water. Thus, the 9% increase in volume when water freezes has to be taken care of in a bigger air-filled pore volume. This is not the correct explanation, however, since in fact rather small air volume is required to take care of the water expansion at freezing; see paragraph 6.12. 4.

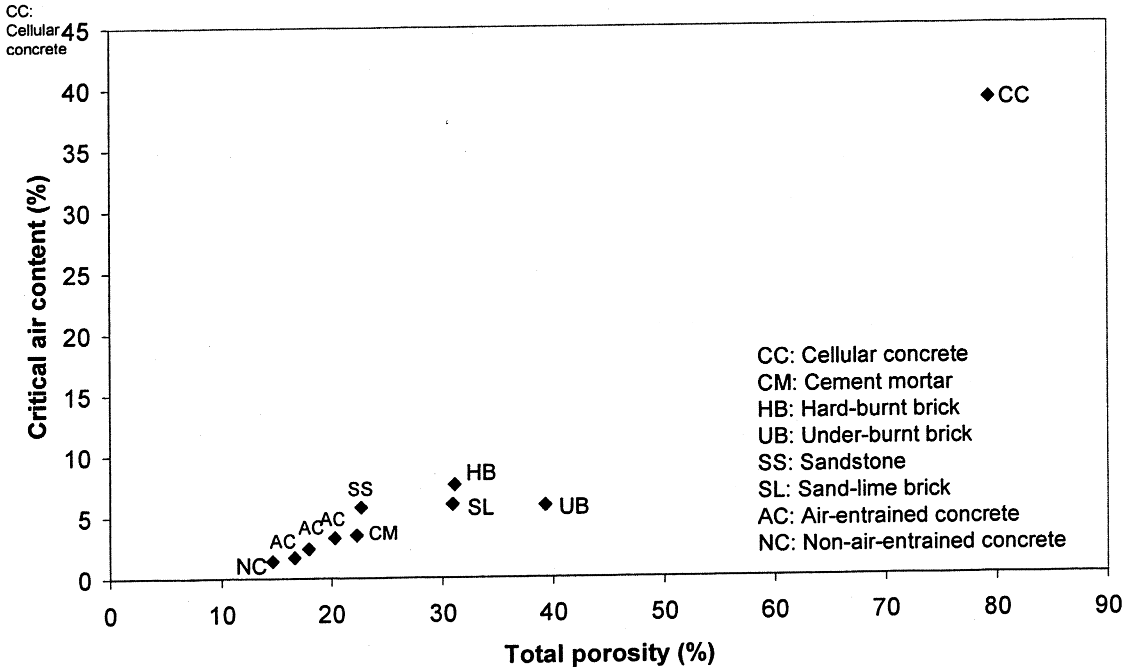

Figure 6.44: Relation between total porosity and critical porosity.

3. The last column in Table 6.1 gives the minimum air content needed if all water at S_{CR} is supposed to be freezable (min. air=9% of total water). The critical air content is always considerably higher then the minimum value, which shows that "surplus" air is needed if the material shall be frost resistant. This is also illustrated by Figure 6.45 where the critical air is plotted versus the minimum air for all materials except the cellular concrete. The difference is still higher if only the actually freezable water is regarded. For concrete, this is of the order 50% of the total water content. For clay brick, cellular concrete and sandstone the freezable water is almost the same as the total water content.

   One reason why more air than minimum is needed is that water has to be forced away from the freezing site to the nearest air-filled space, and this water transport causes internal tension in the material also when the air volume is above the minimum 9% of the freezable water. The 9% increase in volume is not the only cause of destruction.

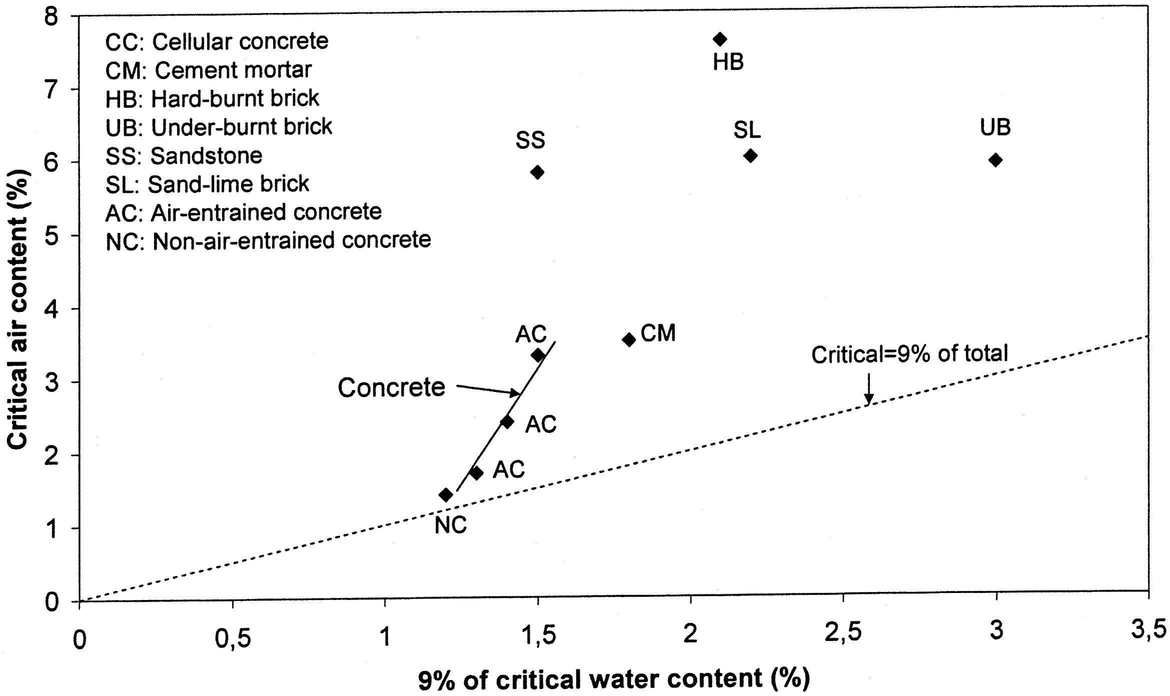

Figure 6.45: Relation between the minimum required air content for taking care of the 9% increase in volume when water freezes, and the observed critical air content (all materials except the cellular concrete).

6.12.2 Theoretical calculation of the critical degree of saturation

The most plausible destruction mechanisms, the hydraulic pressure mechanism (Powers 1949), and the ice lens growth mechanism (Powers & Helmuth 1953), both predict the existence of a maximum (critical) average distance between pores that have to be air-filled if the material shall be frost resistant. This distance can be called D_{CR}.

As shown by the experiments, these air-filled pores are so coarse that they cannot become water filled during the short-term capillary absorption process; see Table 6.1. The coarse pore system has a certain size distribution f(r) where r is the pore radius. At the breaking-point in capillary absorption, the average distance between the coarse pores is D_0. By long-term absorption more and more pores are water-filled. Thereby, the average distance increases as illustrated by Figure 6.46. It is assumed that a smaller pore is filled before a coarse; c.f. Table 5.1, which gives examples of the time needed to fill a pore of different size.

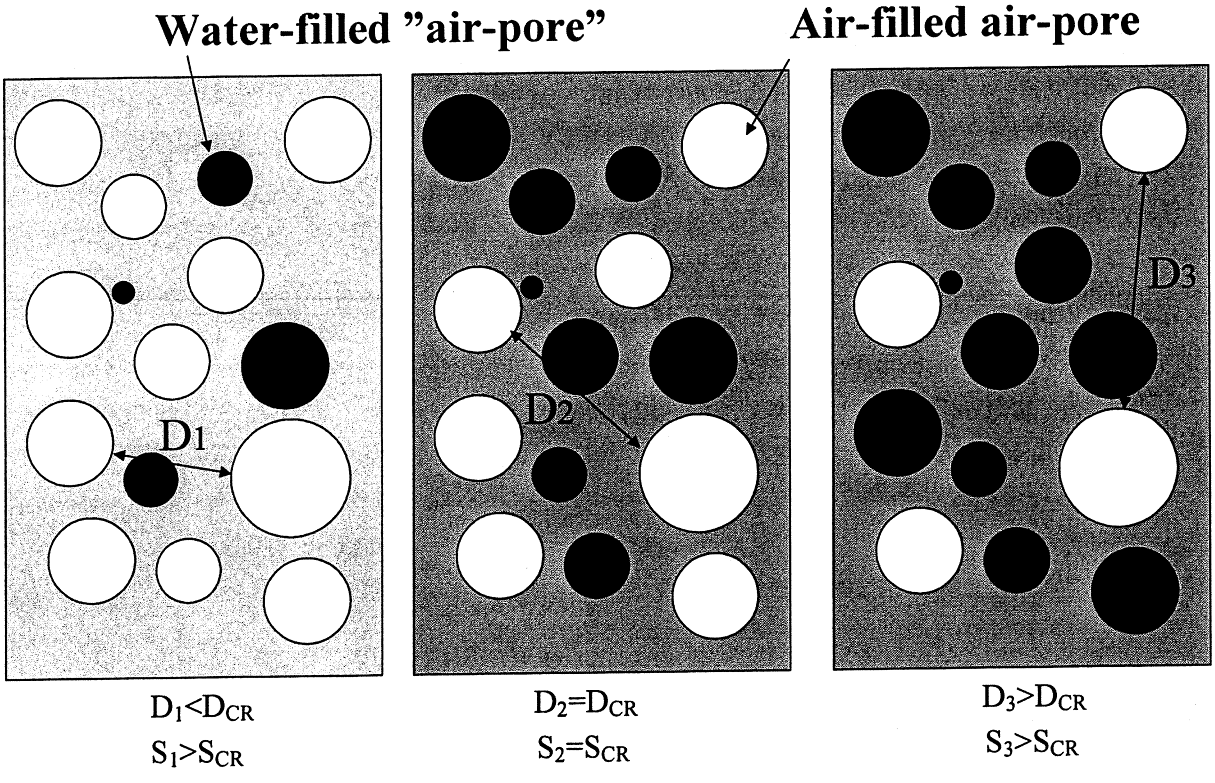

Figure 6.46: By gradual absorption in the coarse pore system the average maximum distance between a place where water freezes and the nearest air-filled pore increases. The critical degree of saturation is reached when the distance is critical.

At a certain critical absorption the average pore distance is equal to the critical distance. Then, critical saturation is reached, as illustrated by Figure 6.47. This means that the critical degree of saturation can be calculated theoretically when the pore size distribution and the critical distance are known. The method is described in detail in (Fagerlund 2004) where also examples of calculated values of S_{CR} are presented.

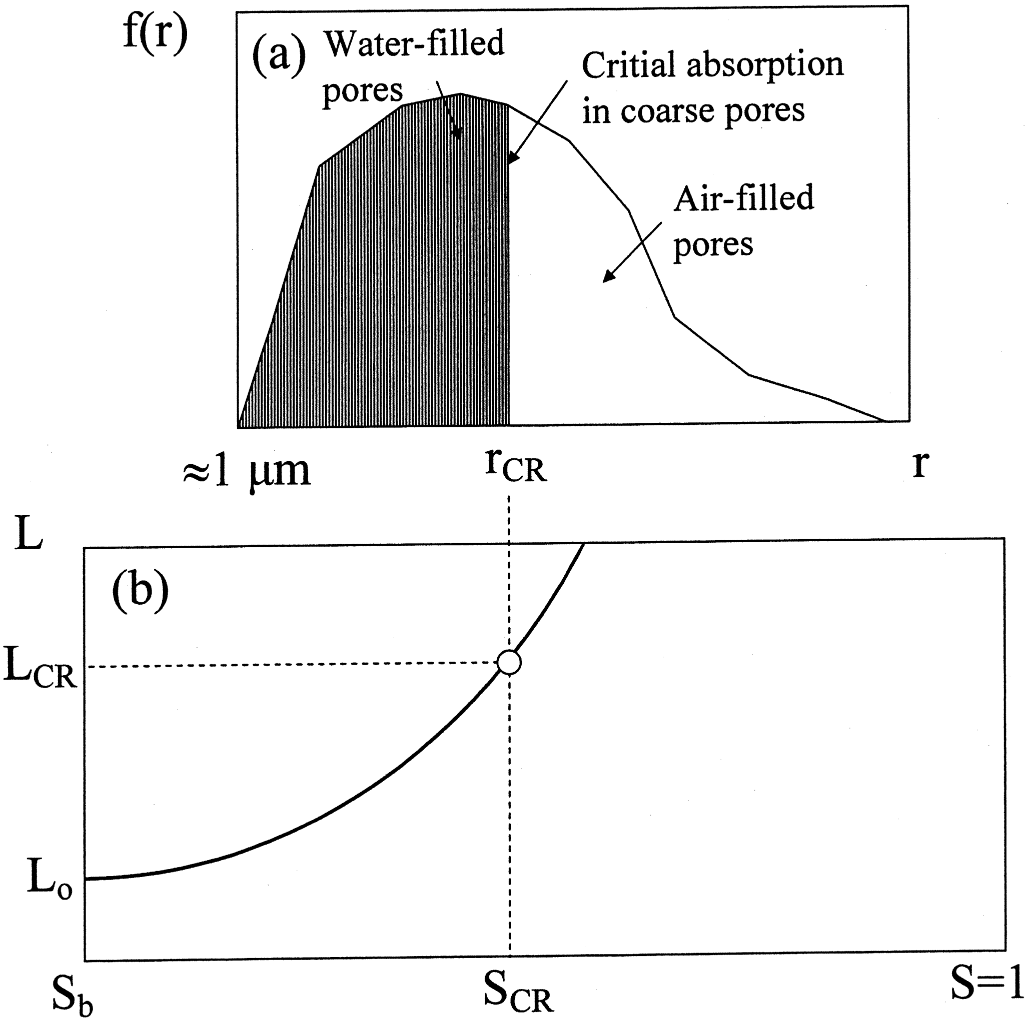

Figure 6.47: *Gradual water absorption in the coarse pore system (a) causes a gradual increase in the average distance between pores that are still air-filled (b).*

6.12.3 The lowest possible critical degree of saturation

(a) General expression

When $S_{CR} = S_b$ the entire coarse pore system must be empty if frost damage shall be avoided. This value of S_{CR} is lower than has been observed in experiments. Theoretically there is a possibility, however, that S_{CR} is even lower than S_b. Since $S<S_b$ means that air-filled pores are smaller than about 1 µm, the distance between a place where water freezes and the closed air space is very small. Therefore, an empty pore space in the fine pore system of only 9% of the freezable water is required for the material to be frost resistant. This is illustrated by Figure 6.49. Consequently, the lowest possible value of S_{CR} is:

$$S_{CR,min}=S_b-0.09\cdot W_f/P_{total} = (S_b + 0.09\cdot K)/1.09 \qquad (6.24)$$

Where K is the ratio between the amount of non-freezable water (w_{nf} m^3/m^3) and total porosity:

$$K=w_{nf}/P_{total} \tag{6.25}$$

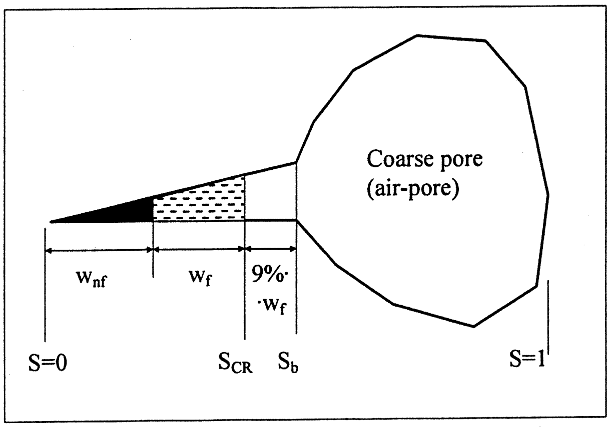

Figure 6.49: Model pore system. The minimum possible critical degree of saturation. w_{nf} is non-freezable water. w_f is freezable water.

Example

A material with total porosity 200 litres/m^3; $P_{total}=0.20$.

The capillary saturation $S_b=0.80$

The amount of non-freezable water 60 litres/m^3; $w_{nf}=0.06$.

Then, $K=0.06/0.20=0.30$

$S_{CR,min}=(0.80+0.09\cdot0.30)/1.09=\mathbf{0.76}$

Thus, $S_{CR;min}<S_b$

(b) Hardened concrete

The total porosity of concrete is

$$P_{total}=10^{-3}\cdot C(w/c-0.19\cdot\alpha)+a \tag{6.26}$$

where C is the cement content (kg/m^3 concrete), a is the air porosity (m^3/m^3) and α is the degree of hydration.

S_b corresponds to water absorption in all pores except the air pores; i.e.

$$S_b=10^{-3}\cdot C(w/c-0.19\cdot\alpha)/P_{total}=(w/c-0.19\cdot\alpha)/[(w/c-0.19\cdot\alpha)+a/10^{-3}\cdot C] \tag{6.27}$$

The minimum amount of non freezable water content corresponds to the gel porosity, and therefore is about

$$w_{nf}=10^{-3}\cdot C\cdot 0.20\cdot\alpha \qquad (6.28)$$

The ratio K becomes

$$K=10^{-3}\cdot C\cdot 0.20\cdot\alpha/P_{total}=0.20\cdot\alpha/[(w/c-0.19\cdot\alpha)+a/10^{-3}\cdot C] \qquad (6.29)$$

Finally, equation (6.24) gives

$$S_{CR,min}=[(w/c-0.19\cdot\alpha+0.09\cdot 0.20\cdot\alpha]/[(w/c-0.19\cdot\alpha)+a/10^{-3}\cdot C]\}\cdot(1/1.09) \qquad (6.30)$$

or

$$S_{CR,min}=[(w/c-0.172\cdot\alpha]/[(w/c-0.19\cdot\alpha)+a/10^{-3}\cdot C]\}\cdot(1/1.09) \qquad (6.30')$$

A typical value of α for concrete that is at least a few months old is 0.8. Thus

$$S_{CR,min}=[(w/c-0.138]/[(w/c-0.152)+a/10^{-3}\cdot C]\cdot(1/1.09) \qquad (6.31)$$

The cement content increases with decreased w/c-ratio. An approximate expression is:

$$C\approx 180/(w/c) \qquad (6.32)$$

Inserting this in equation (6.31) gives

$$S_{CR,min}=[(w/c-0.138]/[(w/c-0.152)+5.56\cdot a\cdot w/c]\cdot(1/1.09) \qquad (6.33)$$

The corresponding expression for S_b is

$$S_b=(w/c-0.152)/[(w/c-0.152)+5.56\cdot a\cdot w/c] \qquad (6.34)$$

In Figure 6.50 S_{CR} and S_b according to equations (6.33) and (6.34) are plotted for two air contents, 2% and 6%. The S_{CR}-values are somewhat below capillary saturation. Such low values have never been experimentally observed for mature concrete.

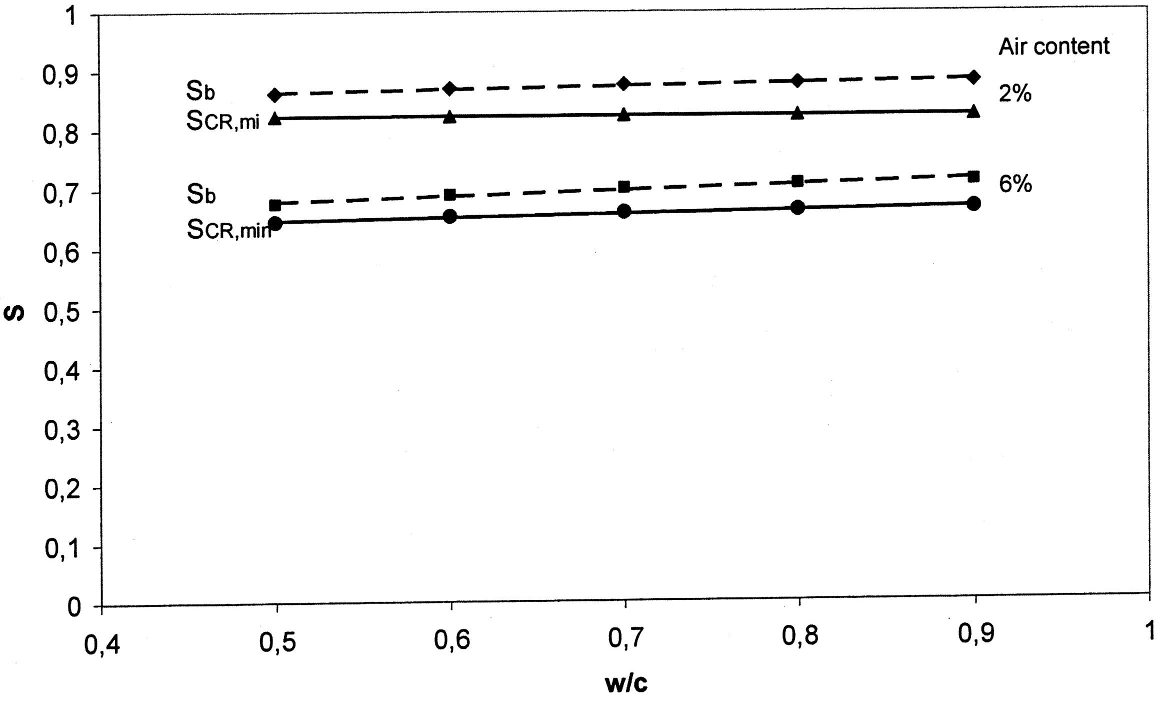

Figure 6.50: Calculated values of capillary degree of saturation and minimum critical degree of saturation for hardened concrete with 80% degree of hydration; equations (6.33) and (6.34).

(c) Young concrete

Minimum S_b- and S_{CR}-values for concrete with other degrees of hydration than 80% can be calculated by the general equations (6.27) and (6.30). In Figure 6.51 the effect of the degree of hydration has been calculated for non-air-entrained concrete with 2% compaction pores and air-entrained concrete with 6% entrained air. The relation (6.32) between cement content and w/c-ratio is used.

For non-air-entrained concrete the minimum critical degree of saturation is almost independent of the degree of hydration while the capillary saturation decreases with increased hydration, which depends on a gradual decrease in the amount of “capillary pores”.

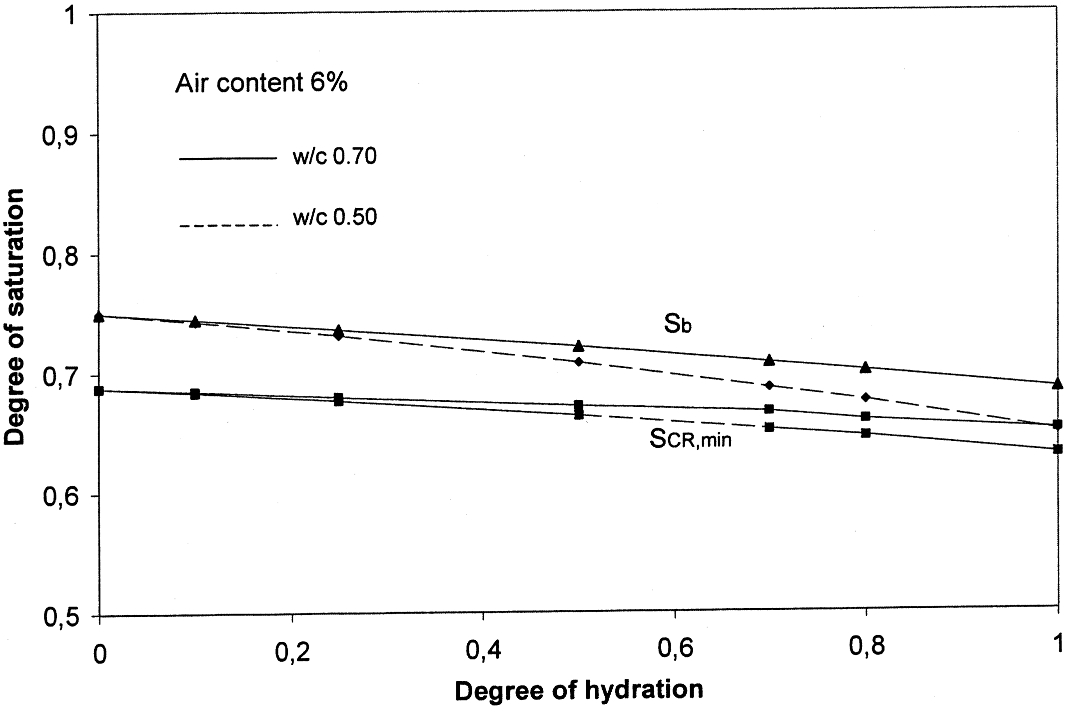

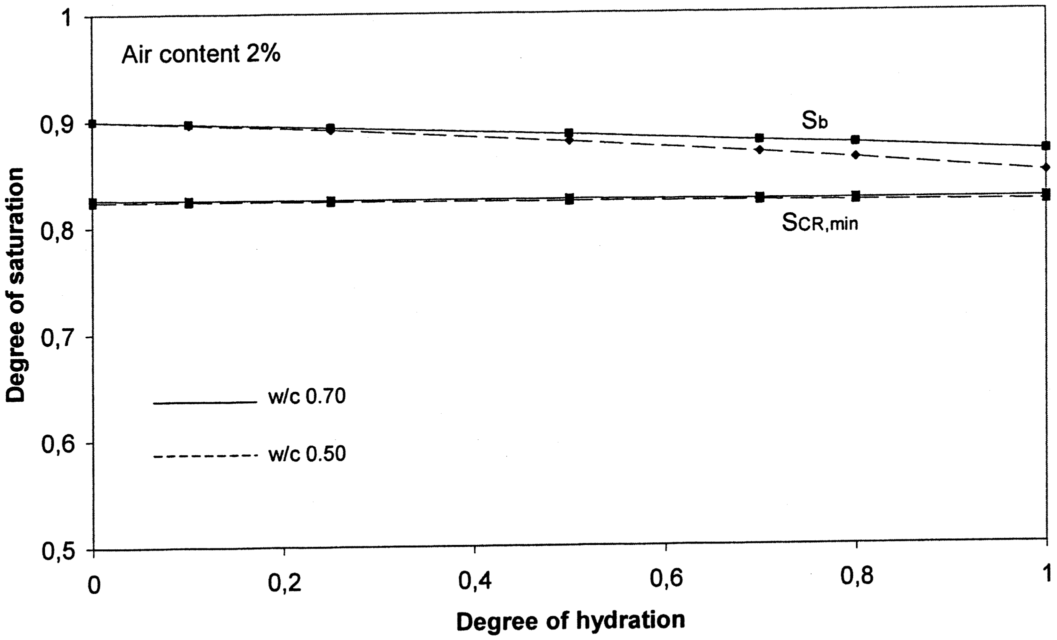

Figure 6.51: Capillary degree of saturation and minimum critical degree of saturation as function of the degree of hydration. Upper figure: air-entrained concrete with 6% air. Lower figure: non-air-entrained concrete with 2% compaction pores.

6.12.4 The highest possible critical degree of saturation

(a) General expression

The highest possible critical degree of saturation is given by the following condition

$$0.09 \cdot w_f = a_{CR} \tag{6.35}$$

Where w_f is the amount of freezable water (m^3/m^3), and a_{CR} is the critical volume of air-filled pores (m^3/m^3). When this condition is fulfilled, all the 9% increase in water volume when it freezes, can be taken care of within the air-filled pore system.

The maximum critical degree of saturation becomes

$$S_{CR,max} = (P_{total} - a_{CR})/P_{total} = 1 - 0.09 \cdot w_f / P_{total} \tag{6.36}$$

But

$$S = w_{total}/P_{total} = (w_f + w_{nf})P_{total} \tag{6.37}$$

Using this equation and equation (6.25) for the non-freezable water (w_{nf}) in equation (6.36) the following expression is obtained

$$S_{CR,max} = (1 + 0.09 \cdot K)/1.09 = 0.917 + 0.083 \cdot K \tag{6.38}$$

When all water is freezable, maximum S_{CR} is 0.917. When no water is freezable, maximum S_{CR} is 1. Thus, $0.917 \leq S_{CR,max} \leq 1$

Example

A certain material has total porosity 38%. The non-freezable water is 120 litres/m^3.
Hence, $K = 0.12/0.38 = 0.316$.
$S_{CR,max} = 0.917 + 0.083 \cdot 0.316 = \mathbf{0.943}$

(b) Hardened concrete

The factor K is given by equation (6.29). Inserting this in equation (6.38) gives

$$S_{CR,max} = 0.917 + 0.0166 \cdot \alpha/[(w/c - 0.19 \cdot \alpha) + a/10^{-3} \cdot C] \tag{6.39}$$

Inserting equation (6.32) for the relation between water-cement ratio and cement content and assuming 80% degree of hydration gives

$$S_{CR,max} = 0.917 + 0.0133/[(w/c - 0.152) + 5.56 \cdot a \cdot w/c] \tag{6.40}$$

Values of $S_{CR,max}$ for the air contents 2% and 6% are plotted in Figure 6.52.

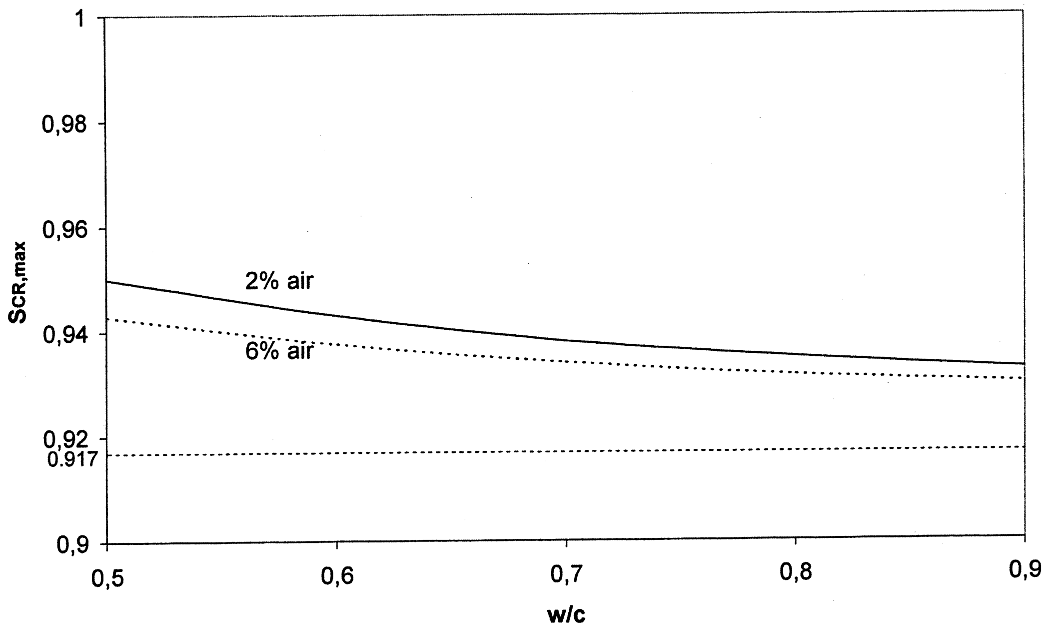

Figure 6.52: The maximum value of S_{CR} for non-air-entrained concrete (2% air) and air-entrained concrete (6% air).

6.12.5 Experimental S_{CR} of concrete versus theoretical minimum and maximum values

The observed critical degrees of saturation are plotted in Figure 6.53 together with the limiting values expressed by equations (6.33) and (6.40). The observed value lies always between the two limiting values. Normally it is closest to the maximum value.

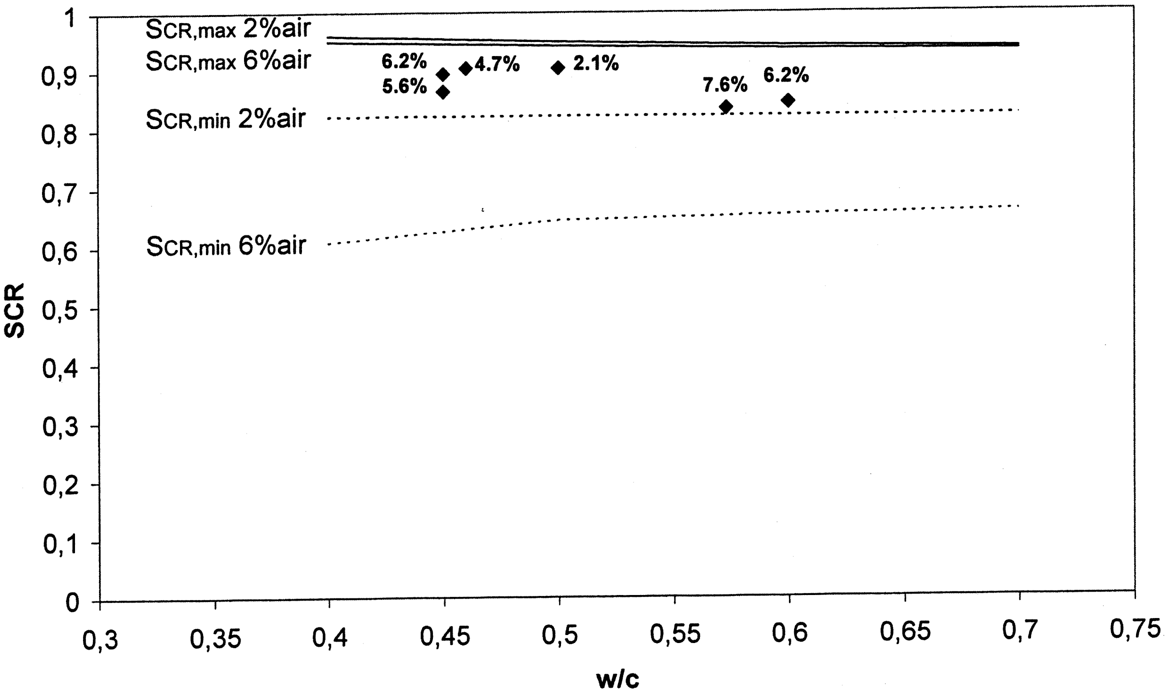

Figure 6.53: Observed values of S_{CR}.
Curves for the maximum and minimum possible values of S_{CR}.

6.12.6 Capillary absorption

Long-term capillary absorption can be described by two coefficients B and C in equation (5.8′). Water content W is exchanged for degree of saturation S:

$$S=A+B\cdot t^{C} \tag{5.8''}$$

The coefficients B and C for the tested materials are listed in Table 6.2.

Table 6.2: Coefficients B and C in equation (5.8′′).

Material	**Total porosity (%)**	**Total volume of coarse pores $(1-S_b)\cdot 100$ (%)**	**B**	**C**
Under-burnt brick	39.5	11.9	0.0290	0.55
Hard-burnt brick	31.1	15.2	0.1990	0.17
Sand-lime brick	30.9	7.1	0.0170	0.63
Cellular concrete	79.3	49.2	0.2190	0.16
Non-air-entrained concrete w/c 0.50. 2.1% air	14.6	2.1	0.0079	0.57
Air-entrained concrete w/c 0.57. 7.6% air	20.3	7.6	0.0042	0.90
Air-entrained concrete w/c 0.45. 4.5% air	16.6	4.5	0.0121	0.40
Air-entrained concrete w/c 0.45. 6.2% air	17.9	6.2	0.0065	0.70
Air-entrained cement mortar w/c 0.60. 6.4% air	22.3	6.4	0.0068	0.61
Sandstone	22.7	7.5	0.0055	0.97

The coefficient B is a function of the diffusivity of dissolved air, which is a function of the fineness and continuity of the pore system. It also ought to increase with increased volume of coarse pores. The relation between the porosity of coarse pores and the coefficient B is plotted in Figure 6.54. The two most coarse-porous materials -hard-burnt brick and cellular concrete- have the highest B-value, as expected. The materials in Figure 6.54 are of quite different character. Therefore, one cannot expect a well-defined relation. Also the 5 concretes/cement mortar differ in w/c-ratio, cement type and age, which makes it unlikely to find a unique relation. It is clear, however, that for the two concretes with the same w/c-ratio (0.45) but different air content, the concrete with the highest air content has the lowest B-value, which is unexpected.

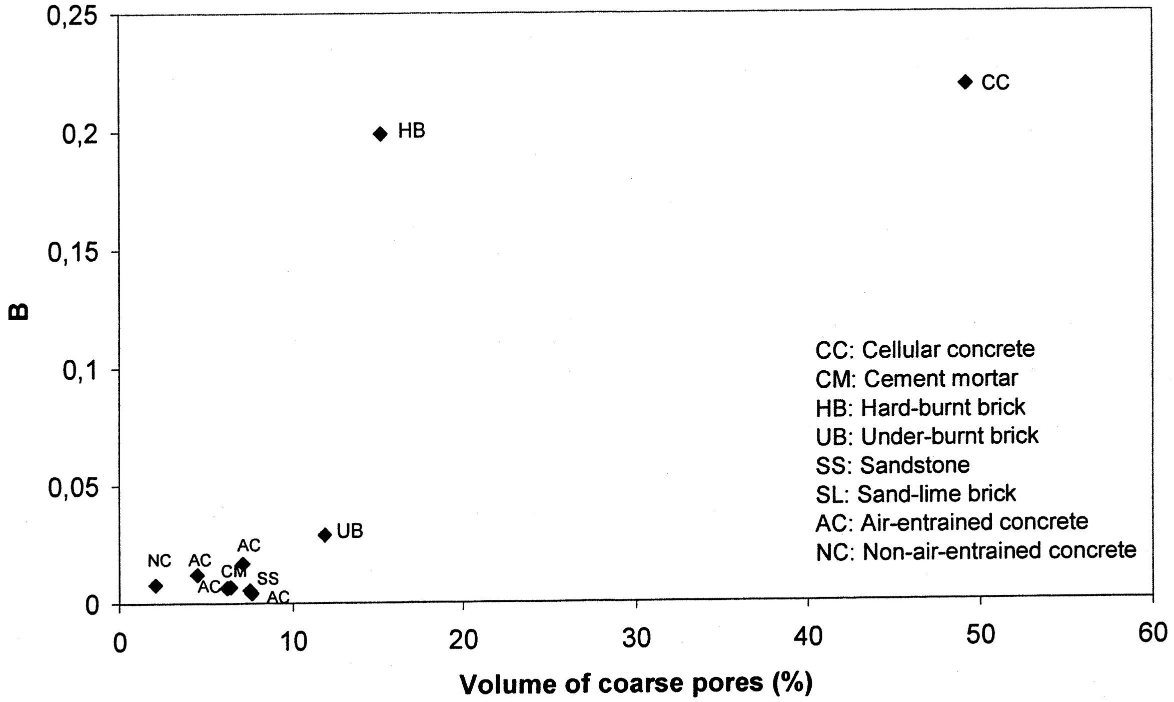

Figure 6.54: Relation between the porosity of coarse pores and the coefficient B.

The coefficient C is primarily a function of the shape of the coarse pore system. No analysis of the pore system was made. Therefore, it cannot be compared with the C-values. Instead the relation between the total amount of coarse pores and C is made in Figure 6.55. All values are below 1 indicating a gradual retarding long-term absorption.

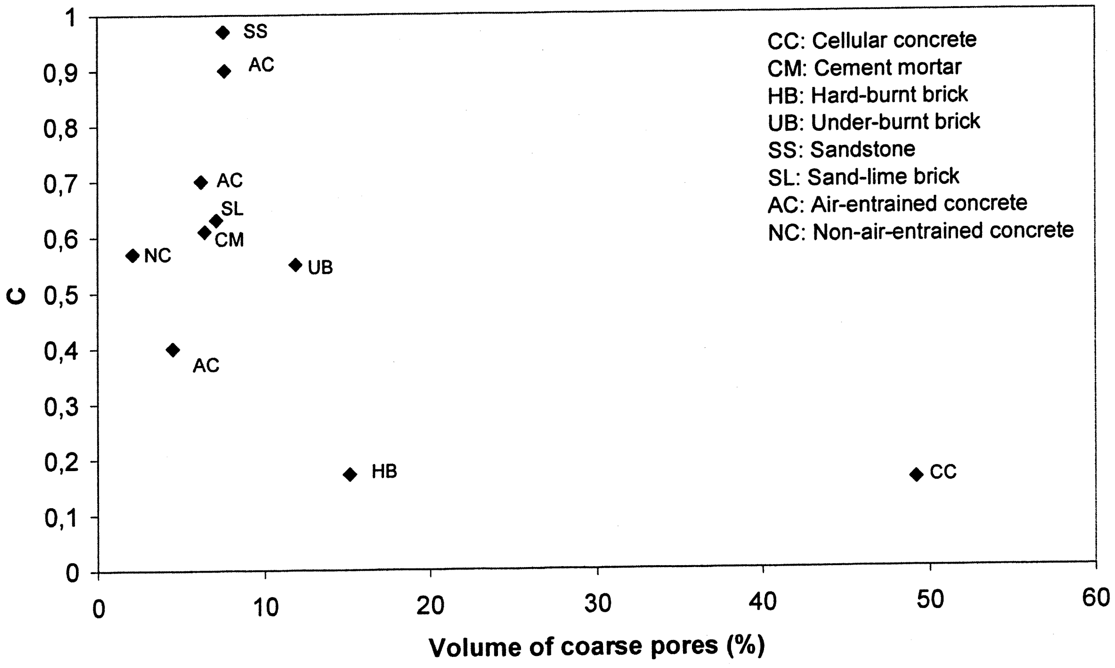

Figure 6.55: Relation between the porosity of coarse pores and the coefficient B.

6.12.7 The frost damage risk

A comparison between the calculated frost damage risk for all materials (except one concrete) is shown in Figure 6.56. A comparison between all cement-bound materials is shown in Figure 6.57. It is quite clear that, by using the parameters S_{CR} and S_{ACT}, a quantitative comparison can be made also between quite different types of materials. For some materials, like sandstone, under-burnt brick, cellular concrete and non-air-entrained concrete, the potential service life is only a few days. For air-entrained concrete it varies between some months and many years. These results agree with practical experience.

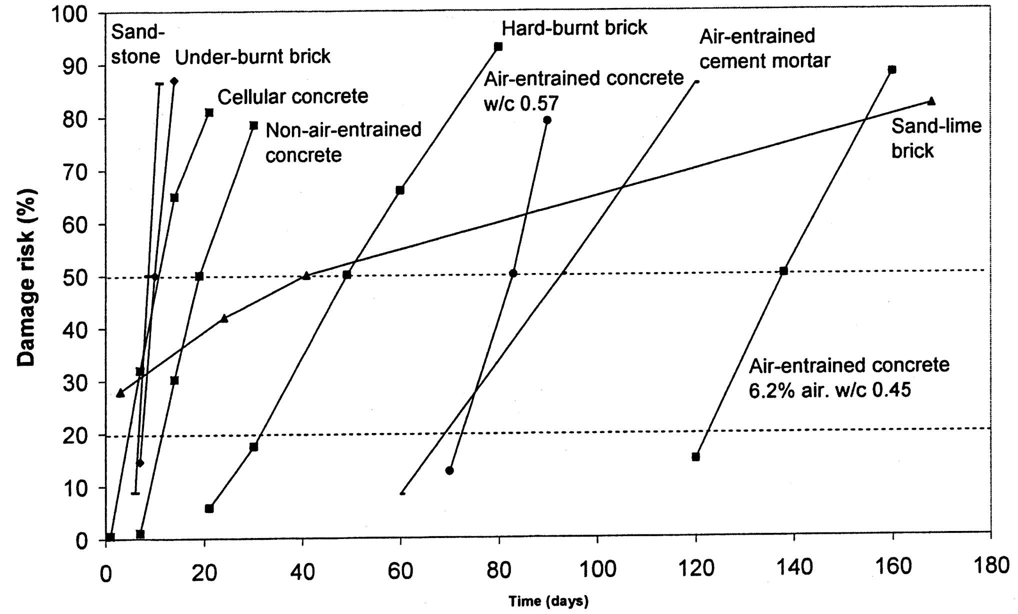

Figure 6.56: The potential service life for all materials besides one concrete.

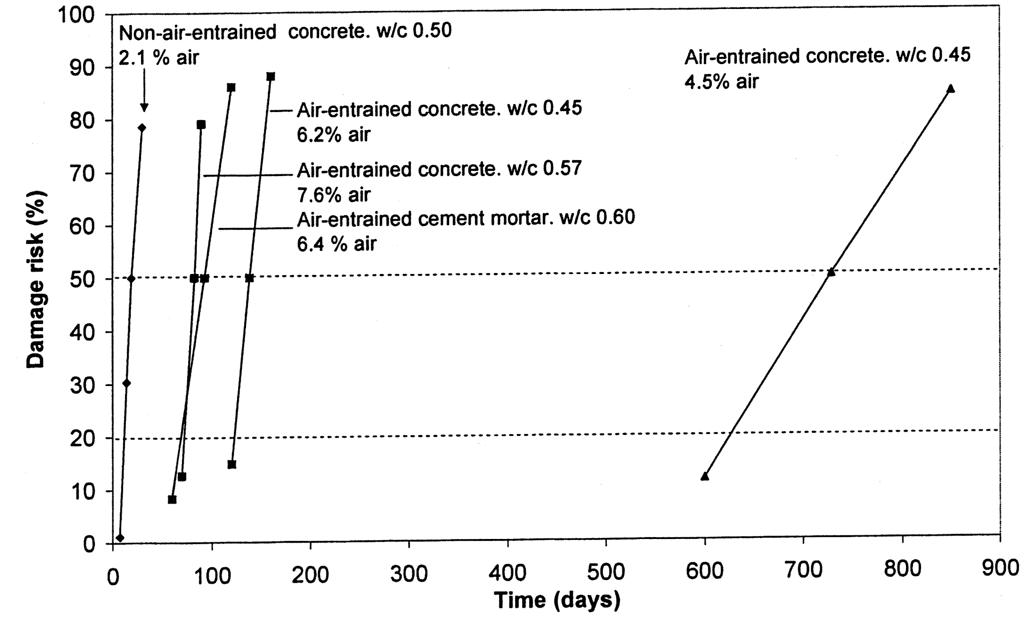

Figure 6.57: The potential service life for all concretes and one cement mortar.

REFERENCES

Adan, O.C.G. (1994). *On the fungal defacement of interior finishes*. University of Eindhoven.

Ahlgren, L. (1972). *Fuktfixering I porösa byggnadsmaterial. (Moisture fixation in porous building materials).* Division of Building Technology. Lund Institute of Technology. Report 34. (In Swedish).

Elfving, P. (1994). *Aspects on the air pollution induced deterioration of calcareous stone material.* Department of Inorganic Chemistry. Chalmers Technical University. Gothenburg.

Everett, D.H.. (1961). *The thermodynamics of frost damage to porous solids.* Transactions of the Faraday Society, No 57.

Fagerlund, G. (1972). *Kritiska vattenmättnadsgrader i samband med frysning av porösa och spröda material. (Critical degrees of saturation at freezing of porous and brittle materials).* Division of Building Technology. Lund Institute of Technology. Report 34. (In Swedish).

Fagerlund, G. (1977). *The critical degree of saturation method of assessing the freeze/thaw resistance of concrete.* Materials and Structures, Vol. 10.

Fagerlund, G. (2000A). *Leaching of concrete. The leaching process. Extrapolation of deterioration. Effect on the structural stability.* Division of Building Materials, Lund Institute of Technology. Report TVBM-3091.

Fagerlund, G. (2004). *A service life model for internal frost damage in concrete.* Division of Building Materials, Lund Institute of Technology. Report TVBM-3119.

Fagerlund, G., Hedenblad, G. (1993). *Calculation of the moisture-time fields in concrete .* Division of Building Materials, Lund Institute of Technology. Report TVBM-3052.

Fridh, K. (2005). *Internal frost damage in concrete. Experimental studies of destruction mechanisms.* Division of Building Materials, Lund Institute of Technology. Report TVBM-1023.

Halvorsen, U.A. (1966). *Corrosion and leaching of lime in cracked concrete structures.* Division of Building Technology, Lund Institute of Technology. Bulletin No 1.

Hedenblad, G. (1993). *Moisture permeability of mature concrete, cement mortar and cement paste.* Division of Building Materials, Lund Institute of Technology. Report TVBM-1014.

Hedenblad, G. (1996). *Materialdata för fukttransportberäkningar, (Material data for calculation of moisture transport.)* Division of Building Technology. Lund Institute of Technology. Report 34. (In Swedish).

Hedenblad, G., Nilsson, L-O.(1987). *Kritiska fukttillstånd för några byggnadsmaterial. Preliminär undersökning.(Critical moisture conditions for some building materials. Preliminary investigation).* Division of Building Materials, Lund Institute of Technology. Report TVBM-3028. (In Swedish).

Houst, Y.F. (1993). *Influence of moisture on carbonation shrinkage kinetics of hydrated cement paste.* Proceedings of the 5th International RILEM Symposium on Creep and Shrinkage, Barcelona. EFN Spon.

Gustafsson, H. (1990). *Kemisk emission från byggnadsmaterial – beskrivning av skadefall, mätteknik och åtgärder. (Chemical emission from building materials – account of damage cases, measuring technique and measures).* Swedish National Testing and Research Institute. Report 1990:25. (In Swedish).

Gustafsson, H. (1992). *Building materials identified as major sources for indoor air pollutants.* Swedish Council for Building Research, Document D10:1992.

Janz, M. (2000). *Moisture transport and fixation in porous materials at high moisture levels.* Division of Building Materials, Lund Institute of Technology. Report TVBM-1018.

Johansson, P. (2005). *Water absorption in two-layer masonry systems. Properties, profiles and predictions.* Division of Building Materials, Lund Institute of Technology. Report TVBM-1024.

Lindmark, S. (1995). *Influence of testing conditions on salt scaling resistance of concrete.* Div. of Building Materials, Lund Institute of Technology. Report "High Performance Concrete", M2:05.

Lindmark, S. (1998). *Mechanisms of salt frost scaling of portland cement-bound materials. Studies and hypothesis.* Division of Building Materials, Lund Institute of Technology. Report TVBM-1017.

Locher, F.W., Sprung, S. (1975). *Die Beständigkeit von Beton gegenüber kalklösender Kohlensäure.* Beton 7/75.

Long Phan. (1966). *High strength concrete at high temperature.* Symposium on the Utilization of High Performance Concrete. Paris (Editors de Larrard, F., Lacroix, R.).

Nilsson, L-O. (1977). *Fuktproblem vid betonggolv. (Moisture problems at concrete floors).* Division of Building Materials, Lund Institute of Technology. Report TVBM-3002. (In Swedish).

Nilsson, L-O. (2004). *Fuktpåverkan på material - en informationsskrift (Moisture effects on materials - an information booklet).* Division of Building Materials, Lund Institute of Technology. Report TVBM-7178. (In Swedish).

Powers, T.C. (1945). *A working hypothesis for further studies of frost resistance of concrete.* Journal of the American Concrete Institute. Vol. 16, No4.

Powers, T.C. (1949). *The air-requirement of frost resistant concrete.* Proceedings Highway Research Board, No 29.

Powers, T.C. (1956). *Resistance to frost at early ages.* Proceedings, RILEM Congress Winter Concreting. Copenhagen, 1956.

Powers, T.C. (1965). *The mechanism of frost action in concrete* .Stanton Walker Lecture No 3, University of Maryland. National Ready Mixed Concrete Association.

Powers. T.C., Helmuth, R.A. (1953). *Theory of volume changes in hardened Portland cement paste during freezing*. Proceedings Highway Research Board. No 32.

Setzer, M.J. (1998). *Micro ice-lens formation.* 5th Bolomey Conference, Essen 1998.

Tange Jepsen, M. (2002). *Salt frost scaling –Interaction of transport mechanisms and ice formation in concrete*. Danish Technological Institute. Building Technology, Taastrup.

Tuutti, K. (1982). *Corrosion of steel in concrete.* Swedish Cement and Concrete Research Institute. Research Fo 4.82.

Viitanen, H. (1996). *Factors affecting the development of mould and brown rot decay of wooden materials and wooden structures. Effect of humidity, temperature and exposure time.* The Swedish University of Agricultural Sciences. Department of Forest Products. Uppsala.

Wengholt-Jonsson, H. (1995). *Kemisk emission från golvsystem – effekt av olika betongkvalitet och fuktbelastning. (Chemical emission from flooring systems – effect of different concrete qualities and moisture loads).* Division of Building Materials, Chalmers University of Technology. Publication P95:4. Gothenburg. (In Swedish).

Wessman, L. (1997). *Studies of the frost resistance of natural stone.* Division of Building Materials, Lund Institute of Technology. Report TVBM-3077.

LUNDS TEKNISKA
HÖGSKOLA
Lunds universitet